



Configuration, Performance, and Commissioning of the ATLAS b -jet Triggers for the 2022 and 2023 LHC data-taking periods

The ATLAS Collaboration

In 2022 and 2023, the Large Hadron Collider produced approximately two billion hadronic interactions each second from bunches of protons that collide at a rate of 40 MHz. The ATLAS trigger system is used to reduce this rate to a few kHz for recording. Selections based on hadronic jets, their energy, and event topology reduce the rate to $\mathcal{O}(10)$ kHz while maintaining high efficiencies for important signatures resulting in b -quarks, but to reach the desired recording rate of hundreds of Hz, additional real-time selections based on the identification of jets containing b -hadrons (b -jets) are employed to achieve low thresholds on the jet transverse momentum at the High-Level Trigger. The configuration, commissioning, and performance of the real-time ATLAS b -jet identification algorithms for the early LHC Run 3 collision data are presented. These recent developments provide substantial gains in signal efficiency for critical signatures; for the Standard Model production of Higgs boson pairs, a 50% improvement in selection efficiency is observed in final states with four b -quarks or two b -quarks and two hadronically decaying τ -leptons.

Contents

| | | |
|----------|---|-----------|
| 1 | Introduction | 2 |
| 2 | ATLAS detector | 3 |
| 3 | Datasets and simulated events | 4 |
| 4 | The ATLAS trigger system | 5 |
| 5 | Algorithms | 6 |
| 5.1 | Level 1 trigger selections | 6 |
| 5.2 | Key inputs to HLT b -jet identification | 6 |
| 5.3 | Low-level identification algorithms | 9 |
| 5.4 | High-level taggers: DL1d and GN1 | 10 |
| 5.5 | Classifier training procedure | 10 |
| 5.6 | Performance in simulation | 11 |
| 6 | The b-jet trigger menu | 12 |
| 6.1 | Estimated rates for b -jet chains | 12 |
| 6.2 | List of b -jet chains | 13 |
| 6.3 | Performance in $t\bar{t}$ enriched data | 15 |
| 6.4 | Efficiency improvements for $HH \rightarrow bbbb$ and $HH \rightarrow b\bar{b}\tau\tau$ compared with Run 2 | 18 |
| 7 | Offline and online b-jet trigger monitoring | 21 |
| 8 | Conclusion | 24 |

1 Introduction

In its third proton–proton (pp) run (Run 3), the Large Hadron Collider (LHC) [1] produces collisions at $\sqrt{s} = 13.6$ TeV every 25 ns. The average number of pp collisions per bunch crossing, $\langle\mu\rangle$, delivered to the ATLAS experiment [2, 3] in the 2022 and 2023 data-taking has ranged from about 30 to about 70. To contend with this 40 MHz event rate, the ATLAS experiment utilises a two-staged triggering system [4]. The first stage, composed of hardware-based selection algorithms that run at the full 40 MHz rate, reduces this to a 100 kHz stream of events. Software-based algorithms impose further selections to bring this rate down to about 3 kHz for the event streams used in most analyses of the ATLAS data. The hardware stage is known as the Level 1 (L1) trigger system, and the software stage is called the High-Level Trigger (HLT) system.

Collimated final-state hadrons from the fragmentation of quarks and gluons (“jets”) are produced at a high rate at the LHC, but jets containing b -hadrons (b -jets) provide striking signatures in collider detectors that can be used to identify them [5]. The identification of b -jets (b -tagging) is a key component of a broad range of ATLAS analyses of the LHC data and is used for example to probe properties of the Higgs boson [6–8] and the top quark [9, 10] and to search for a wide variety of possible processes beyond the Standard Model (SM) [11–13].

At a hadron collider experiment, the cross-section of multijet events is substantial compared with electroweak or Higgs boson production processes [14]; analyzing hadronic final states therefore poses a significant experimental challenge already at the trigger stage. For fully hadronic final-states including b -quarks, b -tagging is a strong tool for reducing the trigger rate to the point of being manageable with the available hardware and computing resources while maintaining a high signal efficiency. Several analyses of the LHC data probe processes with fully hadronic final states that involve at least one b -jet. These include Higgs boson and top-quark pair production events in the fully hadronic channels [8, 15] and the production of new resonances decaying preferentially to b -quarks [12].

This article describes the real-time b -jet identification algorithms developed by the ATLAS Collaboration for the LHC Run 3 pp collision data, highlighting differences relative to Run 2 ATLAS triggering strategy for b -jets [16]. First, an overview of the ATLAS detector and trigger systems is given. The real-time b -tagging algorithms utilised in the HLT are then introduced; their optimisation and expected performance in simulation is also presented. Comparisons between detector simulation and observed data collected during the LHC 2022 and 2023 data-taking are shown, and triggering rates from this period are reported.

2 ATLAS detector

The ATLAS detector at the LHC covers nearly the entire solid angle around the collision point. It consists of an inner tracking detector surrounded by a thin superconducting solenoid, electromagnetic and hadron calorimeters, and a muon spectrometer incorporating three large superconducting air-core toroidal magnets.

The inner-detector system (ID) is immersed in a 2 T axial magnetic field and provides charged-particle tracking in the range of $|\eta| < 2.5$.¹ The high-granularity silicon pixel detector covers the interaction region and typically provides four measurements per track, the first hit normally being in the insertable B-layer (IBL). It is followed by the silicon microstrip tracker (SCT), which usually provides eight measurements per track. These silicon detectors are complemented by the transition radiation tracker (TRT), which enables radially extended track reconstruction up to $|\eta| = 2.0$. The TRT also provides electron identification information based on the fraction of hits (typically 30 in total) above a higher energy-deposit threshold corresponding to transition radiation.

The calorimeter system covers the pseudorapidity range $|\eta| < 4.9$. Within the region $|\eta| < 3.2$, electromagnetic calorimetry is provided by barrel and endcap high-granularity lead/liquid-argon (LAr) calorimeters, with an additional thin LAr presampler covering $|\eta| < 1.8$ to correct for energy loss in material upstream of the calorimeters. Hadron calorimetry is provided by the steel/scintillator-tile calorimeter (Tile calorimeter), segmented into three barrel structures within $|\eta| < 1.7$, and two copper/LAr hadron endcap calorimeters. The solid angle coverage is completed with forward copper/LAr and tungsten/LAr calorimeter modules optimised for electromagnetic and hadronic energy measurements respectively.

The muon spectrometer (MS) comprises separate trigger and high-precision tracking chambers measuring the deflection of muons in a magnetic field generated by the superconducting air-core toroidal magnets. The field integral of the toroids ranges between 2.0 and 6.0 Tm across most of the detector. Three layers of

¹ ATLAS uses a right-handed coordinate system with its origin at the nominal interaction point (IP) in the centre of the detector and the z -axis along the beam pipe. The x -axis points from the IP to the centre of the LHC ring, and the y -axis points upwards. Polar coordinates (r, ϕ) are used in the transverse plane, ϕ being the azimuthal angle around the z -axis. The pseudorapidity is defined in terms of the polar angle θ as $\eta = -\ln \tan(\theta/2)$. Angular distance is measured in units of $\Delta R \equiv \sqrt{(\Delta\eta)^2 + (\Delta\phi)^2}$.

precision chambers, each consisting of layers of monitored drift tubes, cover the region $|\eta| < 2.7$, except in the innermost layer of the endcap region, where layers of small-strip thin-gap chambers and Micromegas chambers both provide precision tracking in the region $1.3 < |\eta| < 2.7$. The muon trigger system covers the range $|\eta| < 2.4$ with resistive-plate chambers in the barrel, and thin-gap chambers in the endcap regions, and with these small-strip thin-gap chambers and Micromegas chambers in the innermost layer of the endcap.

The Run 3 detector configuration benefits from several upgrades compared with that for Run 2 to maintain high detector performance at the higher pile-up levels of Run 3. The improvements include a new innermost layer of the muon spectrometer in the endcap region, which provides higher redundancy and a strong reduction in fake-muon triggers. Other updates and further details are provided in Ref. [3]

An extensive software suite [17] is used in data simulation, in the reconstruction and analysis of real and simulated data, in detector operations, and in the trigger and data acquisition systems of the experiment.

3 Datasets and simulated events

The results presented in this paper use data from pp collisions with a centre-of-mass energy $\sqrt{s} = 13.6$ TeV, collected during the first two years of the Run 3 of the LHC, in 2022 and 2023.

Monte Carlo (MC) simulations of top-quark pairs ($t\bar{t}$) produced in pp collisions are used throughout this paper to provide a sample of simulated jets resulting from b -, c -, and light-flavour quarks. These simulated events are used for the optimisation of online b -tagging algorithms and to compare the simulated performance of said algorithms to observed performance in collision data. The production of $t\bar{t}$ events was modelled using the POWHEG Box v2 [18–21] generator at next-to-leading-order (NLO) with the NNPDF3.0NLO [22] parton distribution function (PDF) set and the h_{damp} parameter² set to $1.5 m_{\text{top}}$ [23]. The events were interfaced to PYTHIA 8.230 [24] to model the parton shower, hadronisation, and underlying event, with parameters set according to the A14 set of tuned parameters (“tune”) [25] and using the NNPDF2.3LO set of PDFs [26]. This combination of calculations and tune parameters was found to provide the best agreement to collision data in measurements of b -tagging efficiency [27] and b -quark fragmentation in top-quark decays [28].

Samples of simulated Higgs boson pair production (“di-Higgs boson production”) via gluon–gluon fusion in the fully hadronic $b\bar{b}b\bar{b}$ and $b\bar{b}\tau\tau$ final states are used to assess the expected performance of the trigger chains that make use of b -tagging algorithms at the HLT. These samples are generated with POWHEG Box v2, the PDF4LHC15NLO PDF set [29], and PYTHIA 8.244 to model the parton shower hadronisation and underlying event, with parameters set according to the A14 tune.

The decays of bottom and charm hadrons were performed by EVTGEN 1.6.0 [30]. All simulated events have additional overlaid minimum-bias interactions generated with PYTHIA 8.160 [31] with the A3 set of tuned parameters [32] and NNPDF2.3LO parton distribution functions to simulate pile-up background.³ The simulated events were processed through the full ATLAS detector simulation [33] based on GEANT4 [34].

²The h_{damp} parameter is a resummation damping factor and one of the parameters that controls the matching of POWHEG matrix elements to the parton shower and thus effectively regulates the high- p_T radiation against which the $t\bar{t}$ system recoils.

³Pile-up interactions correspond to additional pp collisions accompanying the hard-scatter pp interaction in proton bunch collisions at the LHC.

4 The ATLAS trigger system

ATLAS records data from LHC collisions using a two-stage triggering system; the first-level, L1, is custom hardware-based while the second-level, HLT, is software-based. The Data Acquisition (DAQ) system [4] transports data from custom subdetector electronics through to offline processing, according to the decisions made by the trigger.

The L1 trigger uses custom electronics to trigger on reduced-granularity information from the calorimeter and muon detectors. The L1 calorimeter (L1Calo) trigger takes signals from the calorimeter detectors as input. The Run-2 L1Calo system was operated in parallel to the upgraded L1Calo system during the start of Run 3. While the upgraded system was in operation during this time, it was not used for jet selections at Level 1; rather the “legacy” Run-2 system was used. In the legacy system, analogue detector signals are digitised and calibrated by the preprocessor and sent in parallel to the cluster processors (CP) and the jet/energy-sum processors (JEP). The CP system identifies electron, photon, and τ -lepton candidates above a programmable threshold, and the JEP system identifies jet candidates and produces global sums of total and missing transverse energy.

The L1 muon (L1Muon) trigger uses hits from resistive-plate chambers (RPCs) in the barrel and thin-gap chambers (TGCs) in the endcap to coarsely determine the muon candidate momentum [35]. To reduce the rate in the endcap regions of particles not originating from the interaction point, the L1Muon trigger in Run 2 applied coincidence requirements between the outer TGC station and either the inner TGC stations or the Tile calorimeter. In Run 3, the replacement of the original small wheels by the new small wheels allow for a further rate reduction from good rate tolerance and improved resolution.

The L1 topological processor (L1Topo) system takes input Trigger OBjects (TOBs) containing kinematic information from the L1Calo and L1Muon systems and applies topological selections. New modules were designed for Run 3 to accommodate input from the new L1Calo and L1Muon systems. During 2022 and 2023, the Run 2 (legacy) L1Topo system ran in parallel with the upgraded L1Topo system, although the legacy system did not process inputs from the L1Muon system.

The L1 trigger decision is formed by the central trigger processor (CTP); in the legacy system this is done combining information mainly from the L1Calo and muon trigger processors, while the upgraded system receives the information from the L1Muon trigger system through the muon-to-central Trigger Processor Interface [36], which was also upgraded for Run 3. The muon information is then processed together with L1Topo and L1Calo systems’ outputs. The total L1 trigger rate of accepting collision events has an upper limit of about 100 kHz, determined by the rate at which the detector can be read out.

If accepted by the L1 trigger, events are then sent to the HLT. Here, algorithms reconstruct the event at progressively higher levels of detail than at L1, either in restricted regions-of-interest (RoIs), which are regions of the detector in which candidate trigger objects are identified by the L1 trigger, or in the full event. The ATLAS jet, b -jet, and missing-transverse-energy trigger algorithms run in the full-event context, while electron, muon, τ -lepton, and photon identification usually run in RoIs defined by the L1 system.

A typical real-time (“online”) reconstruction sequence makes use of dedicated fast trigger algorithms to provide early rejection, followed by more precise and more CPU-intensive algorithms that are similar or identical to those used for offline reconstruction to make the final selection. The HLT software is incorporated in the same software framework used offline to reconstruct recorded events but runs on a dedicated computing farm composed of about 90k multi-processor units. Events accepted by the HLT selection are distributed to a server cluster, where they are compressed and written to disk or tape for

storage. The physics output rate of the HLT during an ATLAS data-taking run with the nominal Run-3 physics menu and LHC conditions is on average 3 kHz, excluding streams used for detector calibrations, trigger-level analyses [37] and other specialised applications. Most physics b -jet trigger chains are part of the *Main Stream*, and promptly undergo offline reconstruction right after data-taking, while some HH -dedicated chains are instead part of the *Delayed Stream*, and are reconstructed only when resources are available [4]. The pipeline can maintain about an 8 GB/s rate of data to offline storage.

5 Algorithms

After a brief description of the pertinent L1 trigger selection and the main inputs to HLT b -jet identification, this paper focuses on the optimisation and performance of the b -tagging algorithms used in the HLT.

5.1 Level 1 trigger selections

Since track finding requires reading out the ATLAS ID subsystems, which is only possible at a frequency much lower than the 40 MHz LHC maximum bunch-crossing rate, the L1 selection for b -jets is based exclusively on information from the ATLAS calorimeter and muon systems [4]. In 2022 and 2023, the legacy L1 system introduced in Section 4 was used for the hardware jet selection. Hadronic jets are reconstructed in the L1Calo systems as clusters of energy in the grid of trigger towers (0.2×0.2 in η and ϕ) presenting hadronic and electromagnetic transverse energy sum substantially above the expectation from noise [38]. Suppression of backgrounds from different bunch crossings (“out-of-time backgrounds”) and pile-up from the same bunch crossing is improved through noise thresholds that are η dependent and through an energy pedestal subtraction that varies based on the LHC bunch crossing being analysed. Jets reconstructed in the calorimeter systems are used to select events that are likely to contain high-momentum jets and to reject the large background of diffractive and soft-QCD processes.

Since b -hadron decay chains include muons about 20% of the time [39], selecting events with muon candidates in addition to calorimeter jets greatly reduces the rate of non- b -jet backgrounds with a non-negligible b -jet selection efficiency, especially in the case of multi- b -jet final states where the combinatorial probability of having at least one muon from b -hadron decays grows quickly with the number of b -jets. Some ATLAS trigger selections take advantage of this, either at L1 alone (through the L1Topo system) or in both the L1 and HLT selections; specifically, muon triggers are used for signatures targeting four or more b -jets and for single-jet triggers used in b -tagging calibrations.

5.2 Key inputs to HLT b -jet identification

Real-time software b -tagging depends on three main reconstructed inputs: hadronic jets, charged-particle tracks (tracks), and primary interaction vertices (PVs). A more detailed description of each of these ingredients is given in Section 4 of Ref. [5] for the ATLAS offline b -tagging algorithms; here the focus is on the primary differences between the inputs to offline and online b -tagging.

5.2.1 Charged-particle tracking

Charged-particle tracks are reconstructed in the ID [40], and several track reconstruction strategies are used, depending on the rate at which they run. Here is presented an overview of these strategies as pertains to the selection of b -jets in the HLT, but a more complete description can be found in Ref. [41] and in Section 5.1 of Ref. [4].

A *fast track finder* (FTF) – less CPU intensive than alternative strategies – performs track pattern recognition and a fast track fit. To reduce CPU consumption, TRT hits are not included in the track fit in the FTF stage. A *precision track finder*, also referred to as “precision tracking,” is optionally run after the FTF stage. The precision tracking strategy uses the output of FTF tracking, namely the spacepoints assigned to tracks, and later runs the full offline track fit on these spacepoints [42]. This achieves higher CPU efficiency than using the full offline track reconstruction algorithm. Using the offline track fit in the precision tracking strategy provides well-measured tracks with high purity after quality requirements and good resolution relative to the full offline tracks [4, 42].

Tracking may be run over the entire detector (full-scan tracking), in regions of interest of a defined geometry around some seeding object (RoI tracking), or by combining several RoIs into a single larger RoI (super-RoI tracking). Performing tracking in a limited subset of the detector reduces the computing time required. The choice of full-scan tracking, RoI tracking, or super-RoI tracking depends on the event rate at which tracking is required and the performance needs of selections that depend on these tracks. In HLT selections involving b -tagging, an instance of full-scan tracking using the FTF strategy is used for primary-vertex reconstruction and jet finding; tracking parameters are chosen to enable it to run very quickly over the full detector but at the expense of the tracking efficiency. Charged-particle tracks that are input to the b -tagging algorithms themselves are the result of FTF and precision tracking steps that run in jet RoIs. For some signatures involving multiple b -jets, the FTF full-scan tracking is unaffordable at the input rate required; in such cases, a b -tagging “preselection” is imposed based on a separate FTF reconstruction instance operating in a super-RoI built from calorimeter jets. In events with at least four calorimeter jets with transverse momentum $p_T > 20$ GeV, full-scan tracking requires about 1 second per event, super-RoI tracking about 250 ms per event, and RoI precision tracking for b -tagging about 350 ms per event.

The precision and FTF tracking efficiencies for charged pions with $p_T > 4$ GeV ranges from 90% for $|\eta| < 1$ to 70% in the forward region ($2.3 < |\eta| < 2.5$) of the detector; the efficiency for both tracking algorithms falls very quickly for charged particles with $p_T < 1$ GeV [4]. Additional selection criteria for reconstructed tracks are applied in the b -tagging algorithms to maintain a high efficiency for charged particles from heavy-flavour hadron decays while rejecting tracks originating from pile-up interactions. For example, tracks with poor fit quality are discarded. These additional selections are detailed in Sections 4 and 5 of Ref. [5].

5.2.2 Primary vertex reconstruction

The reconstruction of primary vertices for each event is crucial for high-performance b -tagging, since the measured location of the hard-scatter collision (i.e. the collision in a bunch crossing resulting in the process of interest) is used as a reference point for calculating track and vertex displacements [43]. For use in b -tagging algorithms, a track’s transverse and longitudinal impact parameters relative to the reconstructed PV, d_0 and z_0 , are respectively defined as the track’s distance of closest approach to the PV in the transverse plane and the longitudinal separation between the PV and the point on the track where d_0 is measured; this

d_0 measuring point is called the “perigee”. The impact parameters d_0 and z_0 tend to be larger for tracks from b -hadron decays than for those originating directly from the hard-scatter interaction.

During LHC Run 3, PV finding in the HLT is performed using a Gaussian distribution track-density seed finder, which seeds vertex-finding locations based on reconstructed tracks, followed by an adaptive multi-vertex finder algorithm [43] that associates tracks to vertex candidates via association weights optimised through an annealing process. For pp collisions with a high track multiplicity, the vertex z position resolution is about $30\text{ }\mu\text{m}$, while the transverse position resolution in the core of the distribution is 10 to $12\text{ }\mu\text{m}$. For comparison, the luminous region typically is of the order of tens of millimeters in z and less than $10\text{ }\mu\text{m}$ in the transverse plane.

5.2.3 Jet reconstruction algorithms

Two different types of hadronic jets are reconstructed in the HLT for the purpose of b -jet identification; these differ primarily in their input constituents, and the choice of constituent depends on the event rate at which they can be constructed given computing constraints. The first type of jet is built from topological clusters of calorimeter cells with significant energy, calibrated to the electromagnetic energy scale [44]; these are called EMTopo jets. The second is known as “particle-flow” jets, since their constituents are particle-flow objects (PFOs) inferred from information from both the ATLAS calorimeters and ID. In particular, particle-flow jet reconstruction can take advantage of the superior resolution of particle tracking when low- p_T charged hadrons yield both calorimeter deposits and a charged-particle track; the calibration of the PFO candidates considers both calorimetry and tracking information [45]. PFO candidates that are not matched to the hard-scatter vertex are omitted from jet finding, reducing the impact of pile-up interactions on the jet response. However, particle-flow jet reconstruction comes at a much higher computational cost due to its reliance on event-wide ID track finding to construct constituents and to determine the hard-scatter vertex.

The anti- k_t algorithm with radius parameter $R = 0.4$ [46], implemented in FASTJET [47], is used for both collections of jets. Jets with $p_T < 20\text{ GeV}$ or $|\eta| \geq 2.5$ are not considered for b -tagging for several reasons: (1) jets outside this η range are beyond the fiducial volume of the ATLAS ID, (2) the number of jets that must be considered at low- p_T quickly becomes computationally prohibitive, and (3) the efficiency calibration of low- p_T jets is extremely challenging [48].

To reduce the number of jets with large energy fractions from pile-up collision vertices before b -tagging algorithms are run, the “jet vertex tagger” (JVT) algorithm is used [49] for particle-flow jets. The JVT procedure is based on a multivariate discriminant for each jet within $|\eta| < 2.4$ built from the ID tracks ghost-associated⁴ with the jet; in particular, jets with a large fraction of high-momentum tracks from pile-up vertices are less likely to satisfy the JVT requirement. The JVT efficiency for jets originating from the hard pp scattering is above 90% in the simulation across this p_T range and grows with jet p_T . Since the rate of pile-up jets with $p_T \geq 60\text{ GeV}$ is sufficiently small, the JVT requirement is removed above this threshold.

⁴The ghost-association algorithm collects tracks within a jet’s geometric catchment area, taking into account possibly overlapping jet areas and is detailed in Ref [46].

5.2.4 Track-to-jet matching and jet labeling

Tracks are matched to jets by setting a maximum allowed angular separation ΔR between the track momenta, defined at the perigee, and the jet axis, which is defined as the direction of the four-momentum sum of the jet constituents. Given that the decay products from higher- p_T b -hadrons are more collimated, the ΔR requirement varies as a function of jet p_T , being wider for low- p_T jets (0.45 for jet $p_T = 20$ GeV) and narrower for high- p_T jets (0.26 for jet $p_T = 150$ GeV); if more than one jet fulfils the matching criteria, the closest jet is preferred [5]. The jet axis is also used to assign signed impact parameters to tracks, where the sign is defined to be positive if the track intersects the jet axis in the transverse plane in front of the primary vertex, and negative if the intersection lies behind the primary vertex [50].

The flavour of a jet in simulation is determined by the nature of the hadrons it contains. Jets are labelled as b -jets if at least one weakly decaying b -hadron having $p_T \geq 5$ GeV is found within a cone of size $\Delta R = 0.3$ around the jet axis. If no b -hadrons are found, c -hadrons and then τ -leptons are searched for, based on the same selection criteria. The jets matched to a c -hadron (τ -lepton) are labelled as c -jets (τ -lepton jets). The remaining jets are labelled as light-flavour jets. For jets with more than one heavy-flavour hadron, e.g. from gluon splitting into $b\bar{b}$ or $c\bar{c}$, the procedure above is still followed, and $b\bar{b}$ ($c\bar{c}$) jets will receive a b (c) label.

5.3 Low-level identification algorithms

The outputs of three “low-level” b -jet identification algorithms are used as inputs to the full “high-level” HLT discriminants used for the trigger decision. These can be broadly categorised as secondary-vertex (SV) finders and neural-network-based discriminators with tracks as their inputs.

Two secondary-vertex finders were used in the HLT in 2022 data-taking, the `JetFitter` and `SSVF` algorithms; each algorithm attempts to reconstruct the b -hadron decay vertex and, in the case of `JetFitter`, the subsequent c -hadron decay as a tertiary vertex. The `SSVF` vertexing algorithm finds at most one displaced vertex consistent with a heavy-flavour hadron decay based on charged-particle tracks within a jet [51]. `JetFitter` is a topological multi-vertex finding algorithm that attempts to reconstruct the full b -hadron decay chain, employing a modified Kalman filter to fit the b -hadron decay hypothesis [52]. Many observables from `SSVF` and `JetFitter` vertex finding, including the track multiplicity, invariant mass, and three-dimensional decay length significance of the vertex candidates, are constructed for use as inputs to high-level b -tagging algorithms.

Features from a neural-network discriminator taking ID tracks as input are also constructed for HLT b -tagging. This discriminator is based on the `DeepSet` architecture [53], which is a universal approximator of permutation-invariant functions with variable-length input sets. The Deep Impact Parameter Sets (DIPS) discriminator uses ten quantities for individual tracks to determine the probability that a given jet is a b -jet, c -jet, or light-flavour jet. This follows the algorithm originally designed for offline flavour-tagging [54, 55], but a subset of the input variables used in the offline case are included: the transverse and longitudinal impact parameters of the track relative to the primary vertex, the corresponding signed impact parameter significances⁵, the number of hits in the IBL, the number of hits in the first pixel layer beyond the IBL, the total number of hits in the pixel system, the total number of hits in the SCT, the ΔR between the track and the jet axis, and the ratio of the track p_T to the jet p_T . Using the notation of Ref. [54], the per-track embedding network ϕ comprises three layers containing 100, 100, and 128 nodes each; the jet-wide network

⁵The impact parameter significance of a track is defined as the ratio of the track impact parameter to its uncertainty.

F has four internal layers with 100, 100, 100, and 30 nodes each. The resulting flavour probabilities are used as low-level inputs to high-level b -tagging algorithms.

5.4 High-level taggers: DL1d and GN1

Two high-level b -tagging algorithms are used for HLT b -jet identification: DL1d and GN1. Both are constructed from neural networks and optimised using the categorical cross-entropy loss to derive an optimal discriminant between b -, c -, and light-flavour jets.

DL1d is a multi-layer perceptron (MLP) classifier that takes as inputs the jet p_T and $|\eta|$ and several outputs from low-level taggers and emits approximate probabilities that a jet has a given flavour, denoted p_u , p_c , and p_b for light-flavour, c -, and b -jet probabilities. From SSVF, key inputs are the invariant mass of the SV (m_{SV}), the energy fraction of SV tracks (E_{frac}), the SV track multiplicity (n_{trk}^{SV}), the 3D and transverse distances (L_{xyz} and L_{xy}) between the PV and SV, the significance of the 3D distance between PV and SV (S_{xyz}), and the ΔR between the jet axis and the displacement of the SV relative to the PV. Similarly, for JetFitter the most important inputs are the b -hadron SV m_{SV} , E_{frac} , L_{xy} , L_{xyz} , S_{xyz} , ΔR to the jet axis, and additionally the invariant mass and energy fraction of the possible tertiary vertex. Finally, the DIPS classification scores, p_u^{DIPS} , p_c^{DIPS} , and p_b^{DIPS} , are used as inputs to DL1d. The network architecture comprises eight dense layers of [256, 128, 60, 48, 36, 24, 12, 6] nodes per layer and the ReLU activation function [56]. For a complete list of inputs and network architectural details, see Ref. [5]. The DL1d algorithm was used for real-time b -jet identification in the HLT during the 2022 data-taking.

During the 2023 LHC pp collision run, a new flavour-tagging algorithm based on graph neural networks, GN1, was used [57]. In addition to the jet transverse momentum and pseudorapidity, GN1 directly uses about 20 quantities for each track associated with a jet rather than the outputs of low-level taggers to discriminate between jet flavours. Only tracks with $p_T > 500$ MeV and satisfying loose requirements on the number of associated silicon hits in the pixel and SCT systems are considered. Among the 20 quantities, important input features include the track q/p , its angular distance to the jet axis, its impact parameters relative to the primary vertex, the corresponding impact parameter significances, and summary quality criteria; Ref. [57] provides a detailed description of all tracking quantities used.

In this article, the DL1r tagging algorithm, based on the same architecture as DL1d, but utilizing a low-level algorithm based on Recurrent Neural Networks [58] instead of DIPS, and used in a wide array of physics results as an offline tagging algorithm [5], is shown for performance comparisons only. While DL1r was not deployed as part of the ATLAS trigger system in LHC Run 3, its performance is shown in what follows to provide a perspective on the algorithm evolution leading to the DL1d and GN1 algorithms.

5.5 Classifier training procedure

Following the prescription detailed in Ref. [5], a training sample is built of jets taken from simulated $t\bar{t}$ production with at least one leptonically decaying W boson in the final state. This yields a good mixture of b -, c -, and light-flavour jets with which to train the neural-network classifiers. This population of jets is resampled such that all flavours have the same distribution in the two-dimensional $p_T \times |\eta|$ space to ensure that these jet kinematic quantities are not used for discrimination; the b -jet distribution is used as the resampling target. The classifiers are trained using the ADAM optimizer [59] within the KERAS [60] and PYTORCH [61] frameworks. The categorical cross-entropy loss is minimized to derive the optimal classifier of b -, c -, and light-flavour jets.

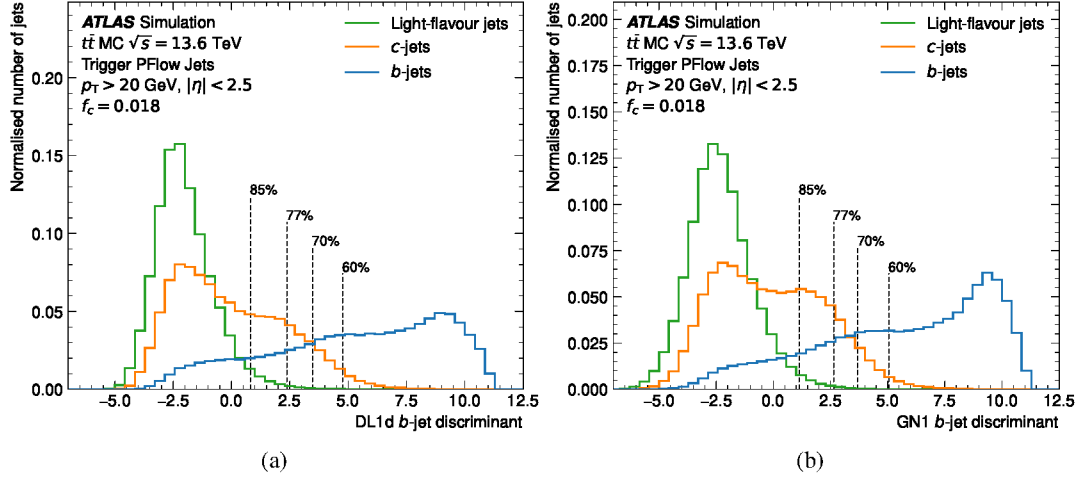


Figure 1: The (a) DL1d and (b) GN1 discriminant scores for b -, c -, and light-flavour jets in $t\bar{t}$ events with $p_T > 20$ GeV and $|\eta| < 2.5$. Dashed vertical lines indicate the discriminant selections for operating points that are commonly used in the HLT.

In the online environment, the performance of flavour-tagging for relatively low- p_T jets is particularly important: the cross-section of multijet production falls quickly with the energy scale of the event, to the point that above ~ 400 GeV, flavour-tagging is not needed to reduce HLT rates to a tractable level. As such, the online b -tagging algorithms are trained only using jets from $t\bar{t}$ production without additional jets from high- Q^2 processes, which were included in previous studies for offline flavour-tagging [5].

5.6 Performance in simulation

After training, a discriminant for b -jet identification is constructed from the outputs of the DL1d and GN1 classifiers, which are the probabilities that a jet belongs to the b -, c -, or light-jet categories. For b -jet identification, this is defined as

$$D_b = \log \frac{p_b}{f_c p_b + (1 - f_c) p_u}, \quad (1)$$

where f_c is a hyperparameter denoting the c -jet fraction of the background population of jets. For both DL1d and GN1, the choice of $f_c = 0.018$ is made, following the optimisation over many measurements and searches [5], in order to maximize the overlap between online and offline b -tagging selections. From these discriminants, operating points (OPs) are defined; e.g. the “70% b -tagging operating point” is the value of D_b for which 70% of b -jets with $p_T > 20$ GeV in a SM $t\bar{t}$ sample have a higher discriminant score. Figure 1 shows the real-time b -tagging discriminant output for b -, c -, and light-jets in a simulated sample of $t\bar{t}$ events; clear discrimination among the jet flavour classes is observed.

The receiver operating characteristic (ROC) curves for the b -jet vs light-jet classification task are shown in Figure 2 (a) for DIPs and DL1d compared with the Run 2 baseline b -jet identification algorithm, DL1r; here, the rejection of background jets for a selection is defined as $1/\varepsilon$, where ε is the probability of a background jet to satisfy the selection. The focus in the trigger system is on light-jet discrimination, as opposed to c -jet discrimination, as most multijet events at the LHC do not produce a high-momentum charm hadron. The simulated performance of GN1 is compared with DL1d in Figure 2 (a): the GN1 classifier

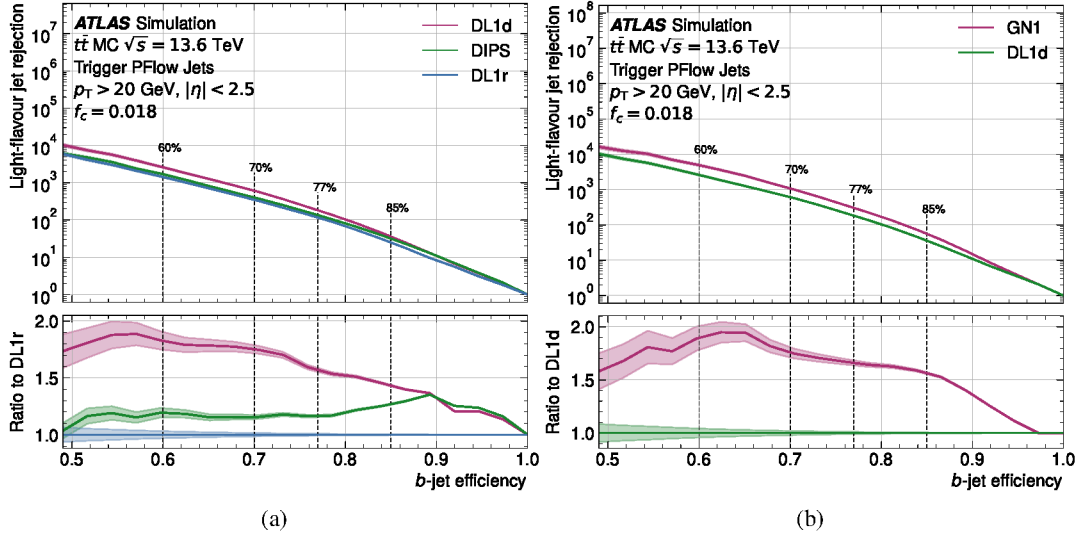


Figure 2: The ROC curves for various flavour-tagging discriminants using light-flavour jets and b -jets from $t\bar{t}$ events with $p_T > 20$ GeV and $|\eta| < 2.5$. The DL1d and DIPS discriminants are compared with the (a) DL1r tagger used for b -tagging with the ATLAS detector in the LHC Run 2, and (b) the GN1 classifier is compared with the DL1d classifier. The lower panels show the ratio of the light-jet rejection factors to DL1r (a) and DL1d (b). The shaded area represents the statistical uncertainty.

outperforms DL1d for all b -jet efficiency OPs, providing up to a factor two improvement in light-flavour jet rejection at a fixed b -tagging selection efficiency.

6 The b -jet trigger menu

To record events, the objects defined in Section 5 are used in combination according to a set of sequential rules named *trigger chains*. A chain consists of an L1 trigger item and a series of HLT algorithms organised into distinct steps that reconstruct physics objects and apply kinematic selections to them [4]. The list of trigger chains is referred to as the *trigger menu*. A large variety of b -jet trigger chains were deployed since the start of Run 3 and were optimised using simulated events and validated using the first data recorded at the beginning of the Run 3 data-taking.

6.1 Estimated rates for b -jet chains

Before data taking, rates for the proposed chains are evaluated with a data-driven technique that uses a sample of collision events selected by the L1 system during previous runs to produce a compact data sample, referred to as *enhanced bias* [62]. Enhanced bias data have the statistical power to assess the trigger rate of algorithmic selections performed by the HLT. This is a crucial asset when designing low- p_T b -jet trigger chains, where the rates express a trade-off between requiring tighter b -tagging working points or higher jet p_T thresholds at HLT to reject the overwhelming multijet production. Figure 3 shows the estimated rate for a four-jet trigger with at least three b -tagged jets ($3b1j^{asym}$), which is described in more detail in Section 6.2) as a function of the working point used for DL1d and for GN1. With an estimated

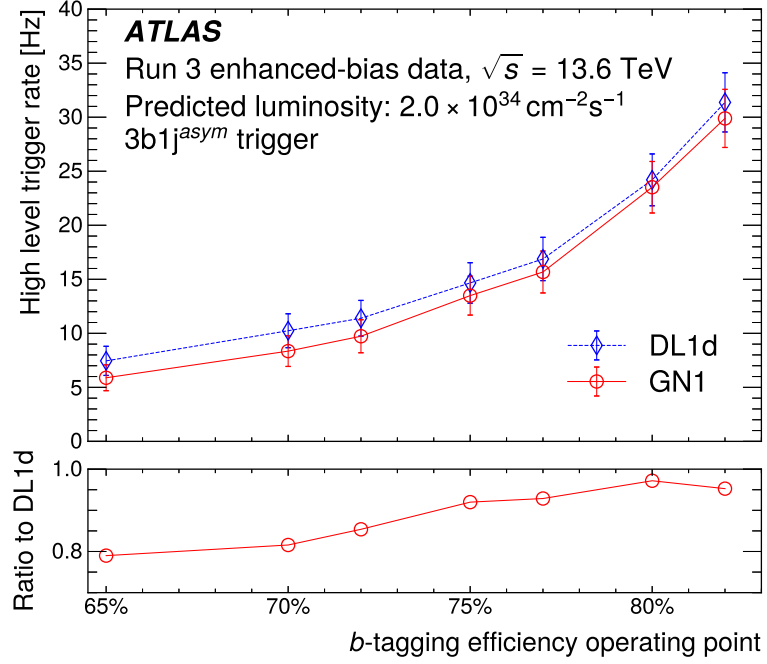


Figure 3: Estimated trigger rates by applying the trigger decision to enhanced bias data for the multi- b -jet selection ($3b1j^{asym}$) using different DL1d and GN1 HLT b -tagging working points.

$3b1j^{asym}$ trigger rate of approximately 30 Hz, the $\epsilon = 82\%$ operating point was deployed online; GN1 outperforms DL1d by about a 5% relative rate at this particular operating point.

6.2 List of b -jet chains

The list of b -jet trigger chains used in Run 3, itemized according to the requirements used at each level, from L1 to HLT preselection to HLT is summarised in Table 1 for the general-purpose chains, and in Tables 2, 3 and 4 for the chains specialized for analyses such as di-Higgs boson [8], supersymmetric searches [13] and Vector Boson Fusion (VBF) measurements. Starting from Run 3, most b -jet trigger chains use a preselection step, to reduce the rate at which the precision tracking is performed. This consists of loose EMTopo jet p_T requirements combined with a loose b -tagging preselection, based on the DIPS algorithm which uses FTF as input [55], referred to as FASTDIPS. The loose FASTDIPS working points deployed at preselection level present a b -tagging efficiency of 85%, 90% and 95% when estimated on $t\bar{t}$ simulated events, and a light-jet rejection of 10, 5 and 2.5 respectively [55]. Figure 4 shows the linear dependency of the output rates for the high- p_T threshold 1b, 2b1j and for the $2b2j^{asym}$ (seeded by three low- p_T jets at L1) b -jet triggers, as a function of the instantaneous luminosity for a collision run taken in 2022.

Table 1: Details of the lowest-threshold b -jet triggers chains included in the Main Stream. For L1 (HLT preselection and selection), $n \times E_T$ (p_T) indicates that n trigger objects must satisfy the listed requirements, the L1 energy scale corresponds to an uncorrected EM scale [63]. In the b -tag column, $n \times b$ indicates that n jets with $p_T > 20$ GeV must satisfy the specified b -tagging operating point; these b -jet candidates need not be a subset of the jets satisfying the p_T -threshold requirements. L1 and HLT jets are required to be within $|\eta| < 3.2$ and $|\eta| < 2.9$ respectively. Unless otherwise specified, the preselection follows the $|\eta|$ requirements of the HLT. Jets with $|\eta| > 2.5$ are not considered for b -tagging. At HLT the value associated with the b -tagging efficiency (ε) is the DL1d (GN1) working point deployed in 2022 (2023) at HLT, while, for the HLT preselection level, it is the FastDIPS working point. For each trigger chain, the requirements listed in a given column must be satisfied independently. The trigger thresholds denoted by the asterisk (*) were moved down by $\sim 6\%$ from May 2023, thanks to an updated jet calibration at the HLT which improved the p_T response. Jets in the HLT preselection are built from calorimeter inputs alone (EMTopo), while those in the HLT selection include charged-particle tracking (particle-flow).

| Type | L1 threshold E_T [GeV] | HLT preselection threshold | | HLT selection threshold | |
|----------------------|----------------------------------|----------------------------------|----------------------------------|--|----------------------------------|
| | | p_T [GeV] | b -tag | p_T [GeV] | b -tag |
| 1b | 1×100 | 1×180 | - | $1 \times 255^*$ | $1 \times b, \varepsilon = 70\%$ |
| | | 1×225 | - | $1 \times 300^*$ | $1 \times b, \varepsilon = 77\%$ |
| | | 1×225 | - | $1 \times 360^*$ | $1 \times b, \varepsilon = 85\%$ |
| 2b | 1×100 | $1 \times 140,$ 1×45 | $2 \times b, \varepsilon = 85\%$ | $1 \times 175,$ 1×60 | $2 \times b, \varepsilon = 60\%$ |
| 2b1j | $1 \times 85,$ 2×30 | $1 \times 80,$ 2×45 | $2 \times b, \varepsilon = 90\%$ | $1 \times 150^*,$ $2 \times 55^*$ | $2 \times b, \varepsilon = 70\%$ |
| 3b | $3 \times 35,$ $ \eta < 2.3$ | 3×45 | $2 \times b, \varepsilon = 95\%$ | $3 \times 65^*$ | $3 \times b, \varepsilon = 77\%$ |
| 1b3j | 4×20 | 4×50 | $1 \times b, \varepsilon = 85\%$ | $1 \times 75^*$ $3 \times 75^*, \eta < 3.2$ | $1 \times b, \varepsilon = 60\%$ |
| 2b2j _{cent} | $4 \times 15,$ $ \eta < 2.5$ | 4×25 | $2 \times b, \varepsilon = 85\%$ | $4 \times 35, \eta < 2.5$ | $2 \times b, \varepsilon = 60\%$ |
| 2b2j | $4 \times 15,$ $ \eta < 2.5$ | 4×25 | $2 \times b, \varepsilon = 85\%$ | 2×45 $2 \times 45, \eta < 3.2$ | $2 \times b, \varepsilon = 60\%$ |
| 2b+H _T | $H_T > 150,$ $M_{jj} > 400$ | | | 2×45 $M_{jj} > 700, H_T > 300^*$ | $2 \times b, \varepsilon = 70\%$ |
| 3b1j | $4 \times 15,$ $ \eta < 2.5$ | 4×25 | $2 \times b, \varepsilon = 85\%$ | 3×35 $1 \times 35, \eta < 3.2$ | $3 \times b, \varepsilon = 70\%$ |
| 4b | $4 \times 15,$ $ \eta < 2.5$ | 4×25 | $4 \times b, \varepsilon = 95\%$ | 4×35 | $2 \times b, \varepsilon = 85\%$ |
| | | | | | $2 \times b, \varepsilon = 70\%$ |
| | | | | | $4 \times b, \varepsilon = 77\%$ |
| 2b3j | $5 \times 15,$ $ \eta < 2.5$ | 5×25 | $2 \times b, \varepsilon = 85\%$ | 3×35 $2 \times 35, \eta < 3.2$ | $2 \times b, \varepsilon = 60\%$ |

Table 2: Details of the asymmetric b -jet triggers dedicated for Higgs boson physics included in the Main and Delayed (*) Streams. For L1 (HLT preselection and selection), $n \times E_T$ (p_T) indicates that n trigger objects must satisfy the listed requirements, the L1 energy scale corresponds to an uncorrected EM scale [63]. In the b -tag column, $n \times b$ indicates that n jets with $p_T > 20$ GeV must satisfy the specified b -tagging operating point; these b -jet candidates need not be a subset of the jets satisfying the p_T -threshold requirements. L1 (j) and HLT jets are required to be within $|\eta| < 3.2$ and $|\eta| < 2.4$ respectively. Unless otherwise specified, the preselection follows the $|\eta|$ requirements of the HLT. Jets with $|\eta| > 2.5$ are not considered for b -tagging. At HLT the value associated with the b -tagging efficiency (ε) is the DL1d (GN1) working point deployed in 2022 (2023) at HLT, while, for the HLT preselection level, it is the FASTDIPS working point. For each trigger chain, the requirements listed in a given column must be satisfied independently. Jets in the HLT preselection are built from calorimeter inputs alone (EMTopo), while those in the HLT selection include charged-particle tracking (particle-flow). L1 muons require two- and three-stations coincidence respectively for the barrel ($|\eta| < 1.05$) and the endcap $1.05 < |\eta| < 2.4$.

| Type | L1 threshold | HLT preselection | | HLT selection | |
|----------------------|-----------------------------|------------------|----------------------------------|---------------|----------------------------------|
| | E_T [GeV] | p_T [GeV] | b -tag | p_T [GeV] | b -tag |
| $3b1j^{asym}$ | j: 1×45 , | | | 1×80 | |
| | $ \eta < 2.1$ | 4×20 | $2 \times b, \varepsilon = 85\%$ | 1×55 | $3 \times b, \varepsilon = 82\%$ |
| | 2×15 , | | | 1×28 | |
| | $ \eta < 2.5$ | | | 1×20 | |
| $2b2j^{asym(*)}$ | j: 1×45 , | | | 1×80 | |
| | $ \eta < 2.1$ | 4×20 | $2 \times b, \varepsilon = 85\%$ | 1×55 | $2 \times b, \varepsilon = 77\%$ |
| | 2×15 , | | | 1×28 | |
| | $ \eta < 2.5$ | | | 1×20 | |
| $\mu+2b2j^{asym(*)}$ | j: 1×20 | | | 1×80 | |
| | 1×15 | 4×20 | $2 \times b, \varepsilon = 85\%$ | 1×55 | $2 \times b, \varepsilon = 77\%$ |
| | $\mu: 1 \times 8$ (p_T) | | | 1×28 | |
| | | | | 1×20 | |

6.3 Performance in $t\bar{t}$ enriched data

Top quark pairs are copiously produced at the LHC and can be used as a control sample to compare data and simulations. Since the branching fraction of the top-quark decay into a W boson and a b -quark is nearly 100%, identifying these events can provide a large sample of relatively pure b -jets, an important asset when assessing b -tagging performance for both offline [27] and online [16] algorithms. Moreover, MC simulated $t\bar{t}$ events are used, before data-taking, to optimise the algorithm working points which are later deployed online. Once collected using lepton triggers, top quark pairs decay into final state with at least one lepton approximately 56% of the time [64]; data enriched in $t\bar{t}$ events provide an unbiased sample in which the b -jet trigger performance for b -jets in data can be compared with MC. This comparison is performed once data is processed through the offline reconstruction algorithms. These algorithms benefit from the better knowledge of detector conditions, obtained during the offline processing, and are therefore more precise than their online equivalent. Moreover, the amount of CPU time per event is less of a constraint for offline reconstruction, whereas the online performance is largely affected by the limitations on the CPU

Table 3: Details of the missing transverse energy plus b -jet triggers dedicated for supersymmetric searches included in the Main Stream. For L1 (HLT preselection and selection), $n \times E_T$ (p_T) indicates that n trigger objects must satisfy the listed requirements, the L1 energy scale corresponds to an uncorrected EM scale [63]. In the b -tag column, $n \times b$ indicates that n jets with $p_T > 20$ GeV must satisfy the specified b -tagging operating point; these b -jet candidates need not be a subset of the jets satisfying the p_T -threshold requirements. L1 (j) and HLT jets are required to be within $|\eta| < 3.2$ and $|\eta| < 2.9$ respectively. Unless otherwise specified, the preselection follows the $|\eta|$ requirements of the HLT. Jets with $|\eta| > 2.5$ are not considered for b -tagging. At HLT the value associated with the b -tagging efficiency (ε) is the DL1d (GN1) working point deployed in 2022 (2023) at HLT, while, for the HLT preselection level, it is the FASTDIPS working point. Cell-based missing transverse energy (E_T^{miss}) [4] is used for early reduction, whereas the final E_T^{miss} selection at HLT is based on PFOs. For each trigger chain, the requirements listed in a given column must be satisfied independently. Jets in the HLT preselection are built from calorimeter inputs alone (EMTopo), while those in the HLT selection include charged-particle tracking (particle-flow).

| Type | L1 threshold | HLT preselection | HLT selection | |
|---------------------------|---|---|---|-------------------------------------|
| | E_T [GeV] | $E_{T,\text{cell}}^{\text{miss}}$ [GeV] | p_T [GeV] | b -tag |
| 1b1j+E $_T^{\text{miss}}$ | $E_T^{\text{miss}} > 40$ j: 2×50 | 60 | j: 1×80 | $1 \times b$, $\varepsilon = 60\%$ |
| 1b+E $_T^{\text{miss}}$ | $E_T^{\text{miss}} > 55$ | 50 | $E_T^{\text{miss}} > 85$ j: 1×100 | $1 \times b$, $\varepsilon = 60\%$ |
| 2b+E $_T^{\text{miss}}$ | $E_T^{\text{miss}} > 55$ j: 2×15 | 50 | $E_T^{\text{miss}} > 85$ j: 2×45 | $2 \times b$, $\varepsilon = 60\%$ |
| 3b+E $_T^{\text{miss}}$ | $E_T^{\text{miss}} > 40$ j: 3×15 , $ \eta < 2.5$ | 50 | $E_T^{\text{miss}} > 70$ j: 3×35 | $3 \times b$, $\varepsilon = 60\%$ |

consumption imposed to the FTF seed finding, a major source of inefficiency for online tracking [65]. This has a direct impact on the better performance of the offline b -tagging algorithms relative to their online equivalent.

6.3.1 Offline reconstruction

Electron candidates are reconstructed from an isolated electromagnetic calorimeter energy deposit with $|\eta_{\text{cluster}}| < 2.47$, which is matched to a track in the ID [66]. The electron track must satisfy $|z_0 \sin \theta| < 0.5$ mm, where θ is the track polar angle, and $|d_0|/\sigma_{d_0} < 5$, where σ_{d_0} is the uncertainty in d_0 . For the tight likelihood identification working point [66] used in this work, the isolation criteria, defined as an upper requirement on the sum of the transverse energy or momentum reconstructed in a cone of size around the electron, excluding the energy of the electron itself, depends on the electron's p_T . Furthermore, electrons are required to have $p_T > 4.5$ GeV.

Particle-flow jets are constructed from offline PFOs analogously to online particle-flow jets introduced in Section 5. These jets are then calibrated to the particle level by applying a jet energy scale derived from simulation with in situ corrections based on collected data [44]. A cleaning procedure is used to identify and remove jets arising from calorimeter noise or non-collision backgrounds. To suppress pile-up jets within $|\eta| < 2.4$, a discriminant called the ‘jet vertex tagger’ (nnJVT) is constructed using a neural network

Table 4: Details of the forward jets plus b -jet trigger chains dedicated to VBF measurements included in the Main Stream. For L1 (HLT preselection and selection), $n \times E_T$ (p_T) indicates that n trigger objects must satisfy the listed requirements, the L1 energy scale corresponds to an uncorrected EM scale [63]. In the b -tag column, $n \times b$ indicates that n jets with $p_T > 20$ GeV must satisfy the specified b -tagging operating point; these b -jet candidates need not be a subset of the jets satisfying the p_T -threshold requirements. L1 (j) and HLT jets are required to be within $|\eta| < 3.2$ and $|\eta| < 2.9$ respectively, while forward jets (f) are required to have $3.1 < |\eta| < 4.9$ both at L1 and HLT. Unless otherwise specified, the preselection follows the $|\eta|$ requirements of the HLT. Jets with $|\eta| > 2.5$ are not considered for b -tagging. At HLT the value associated with the b -tagging efficiency (ε) is the DL1d (GN1) working point deployed in 2022 (2023) at HLT, while, for the HLT preselection level, it is the FASTDIPS working point. For each trigger chain, the requirements listed in a given column must be satisfied independently. Jets in the HLT preselection are built from calorimeter inputs alone (EMTopo), while those in the HLT selection include charged-particle tracking (particle-flow).

| Type | L1 threshold E_T [GeV] | HLT preselection p_T [GeV] | HLT selection p_T [GeV] | b -tag |
|--------|-----------------------------------|---------------------------------|-----------------------------------|----------------------------------|
| 1b2f | $1 \times 25, \eta < 2.3$ | 1×45 | 1×55 | $1 \times b, \varepsilon = 70\%$ |
| | $2 \times 15, 3.1 < \eta < 4.9$ | 1×40 | $2 \times 45, 3.1 < \eta < 4.9$ | |
| 2b1f | $1 \times 40, \eta < 2.5$ | 1×60 | 1×80 | $1 \times b, \varepsilon = 70\%$ |
| | 1×25 | 1×45 | 1×60 | $1 \times b, \varepsilon = 85\%$ |
| | $1 \times 20, 3.1 < \eta < 4.9$ | 1×40 | $1 \times 45, 3.1 < \eta < 4.9$ | |
| 1b1j1f | $1 \times 40, \eta < 2.5$ | 1×60 | $1 \times 80, \eta < 2.4$ | $1 \times b, \varepsilon = 60\%$ |
| | 1×25 | 1×45 | 1×60 | |
| | $1 \times 20, 3.1 < \eta < 4.9$ | 1×40 | $1 \times 45, 3.1 < \eta < 4.9$ | |

method [49]. Jets within $|\eta| < 2.5$ are b -tagged using the DL1d b -tagging algorithm [5, 27] with a working point corresponding to a b -tagging efficiency of 77%, measured in a sample of simulated $t\bar{t}$ events. The corresponding rejection factors are approximately 200 and 6 for light- and c -jets, respectively.

6.3.2 Data Monte-Carlo comparison in $t\bar{t}$ enriched events

Data enriched in $t\bar{t}$ events are selected with the following requirements:

- Satisfy the isolated single-electron-plus-jets trigger, corresponding to an E_T requirement of 26 GeV for the electron and $p_T \geq 20$ GeV for the two jets at the HLT.
- Contain an offline electron with $E_T \geq 28$ GeV, $|\eta| < 2.47$, excluding the transition region between the barrel and endcap cryostats ($1.37 \leq |\eta| < 1.52$), satisfying the tight identification and isolation requirements.
- Exactly one electron satisfying the trigger selection.
- At least four offline jets with $|\eta| < 2.5$ and with $p_T > 120$ GeV, for the leading jet, $p_T > 70$ GeV, for the subleading jet and $p_T > 30$ GeV, for any extra jet in the event.
- At least two offline jets must satisfy the offline b -tagging DL1d algorithm criteria for the 77% efficiency working point.

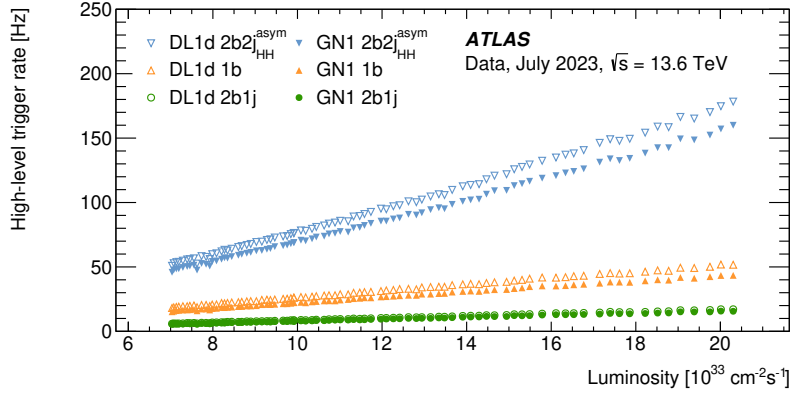


Figure 4: Output rates of selected ATLAS b -jet triggers as a function of the instantaneous luminosity during 2023 proton–proton data taking with a centre-of-mass energy of 13.6 TeV and an LHC bunch-crossing interval of 25 ns for DL1d (empty markers) and GN1 (solid markers). The trigger chains represented, $2b2j^{asym}$ (inverted triangles), $1b$ (triangles) and $2b1j$ (circles) are defined in Tables 1 and 2.

After this selection, the data sample contains at least 90% $t\bar{t}$ events, and it is used to compare data and MC simulation [67].

Figure 5 shows the percentage of the selected lepton-triggered events satisfying the $2b2j^{asym}$ b -jet trigger defined in Table 2, for both DL1d and GN1 algorithms. This $2b2j^{asym}$ event-level trigger efficiency is shown independently as a function of the first-, second-, third- and fourth-leading offline jet p_T . The offline jet p_T requirements are chosen such that at least 95% of the events passing the $t\bar{t}$ offline selection satisfy the L1 and HLT jet requirements of the $2b2j^{asym}$ trigger chain; this condition is referred to as “above the plateau of the jet trigger turn-on”. The jet p_T requirements depend on the presence of the isolated electron from the top-quark decay which can participate as a reconstructed jet in the $2b2j^{asym}$ decision. After the offline jet requirements, the $2b2j^{asym}$ efficiency shown in Figure 5 is only sensitive to residual difference between the performance of the b -jet trigger in data and MC $t\bar{t}$ events. Finally, Figure 5 shows an overall good agreement for the correlation of the offline and online b -tagging between data and MC simulation.

6.4 Efficiency improvements for $HH \rightarrow bbbb$ and $HH \rightarrow bb\tau\tau$ compared with Run 2

The trigger menu described in Section 6.2 yields substantial improvements in the data recording efficiency relative to Run 2 for two of dominant final states of Higgs boson pair production: $HH \rightarrow bbbb$ and $HH \rightarrow bb\tau\tau$. The gain in efficiency is driven by improvements in the b -jet identification algorithms, described in Section 5, that consequently allows loosening jet transverse momentum thresholds.

An inclusive efficiency gain of about 50% is achieved compared with the Run 2 trigger strategy for the SM $HH \rightarrow bbbb$ signal. The efficiency improvements are especially large ($\sim 75\%$) in the low HH invariant mass (m_{HH}) region close to the $2m_H$ threshold, which is known to have particular sensitivity to the Higgs boson self-interaction strength [68]. Figure 6 compares the $HH \rightarrow bbbb$ signal efficiency of the Run 2 ATLAS trigger strategy with the new menu deployed in Run 3 as a function of m_{HH} .

The $2b2j^{asym}$ trigger chain also efficiently selects events from the $HH \rightarrow bb\tau\tau$ process in which both τ -leptons decay hadronically; for SM $HH \rightarrow bb\tau\tau$ production, an efficiency above 50% is predicted, in simulation, for events passing the $HH \rightarrow bb\tau\tau$ fiducial selection: two b -jets having $p_T > 20$ GeV and two

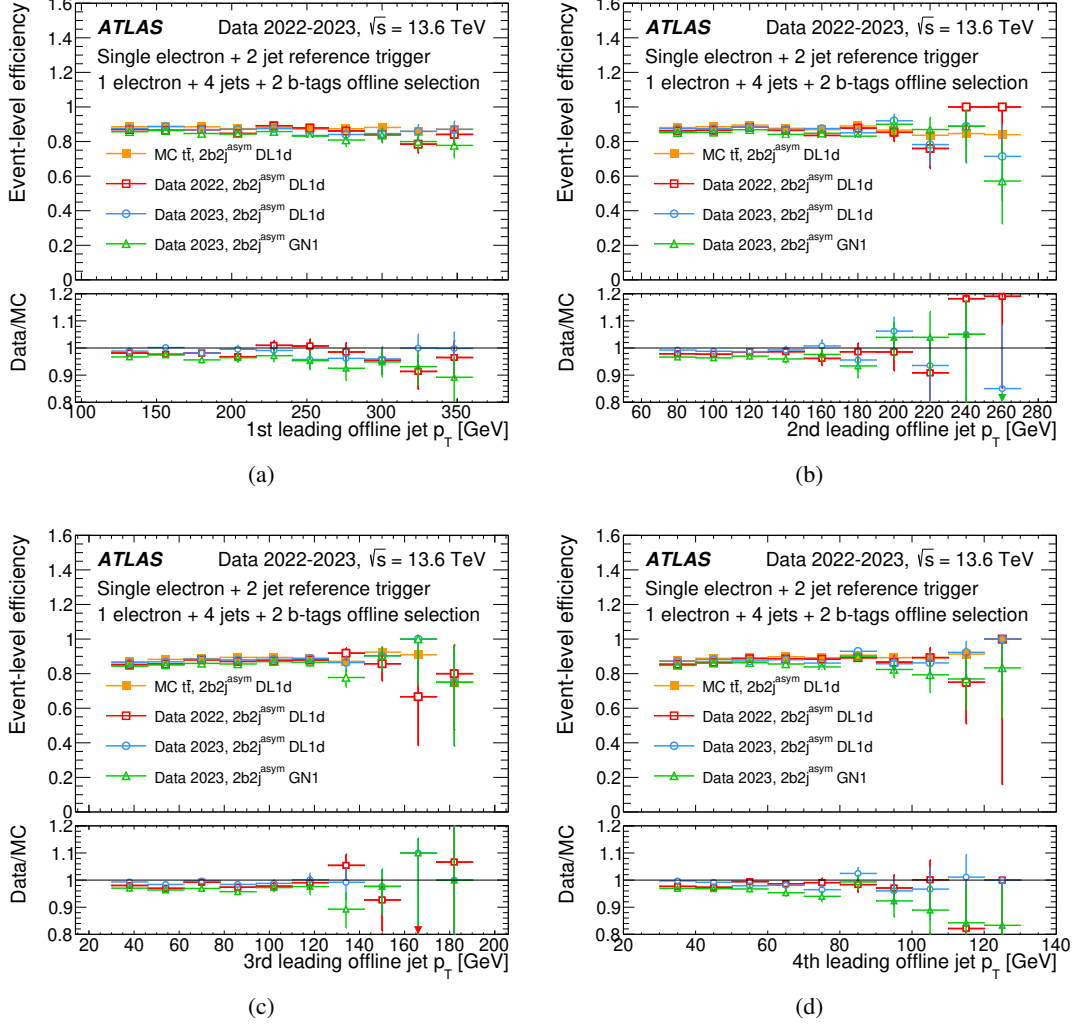


Figure 5: Trigger efficiencies in data and simulation for a $2b2j^{asym}$ HLT selection after requiring an isolated-electron-plus-jet trigger and an offline selection requiring one electron, four jets and two b -tagged jets in the event. The efficiency of the $2b2j^{asym}$ trigger selection is shown relative to the p_T of the (a) leading, (b) subleading, (c) third leading and (d) fourth leading reconstructed offline jet. Efficiencies, shown above the plateau of the jet trigger turn-on, are sensitive to differences between b -jet performance in data and MC $t\bar{t}$ events. The lower panels show the ratio between data and the simulated $t\bar{t}$ events.

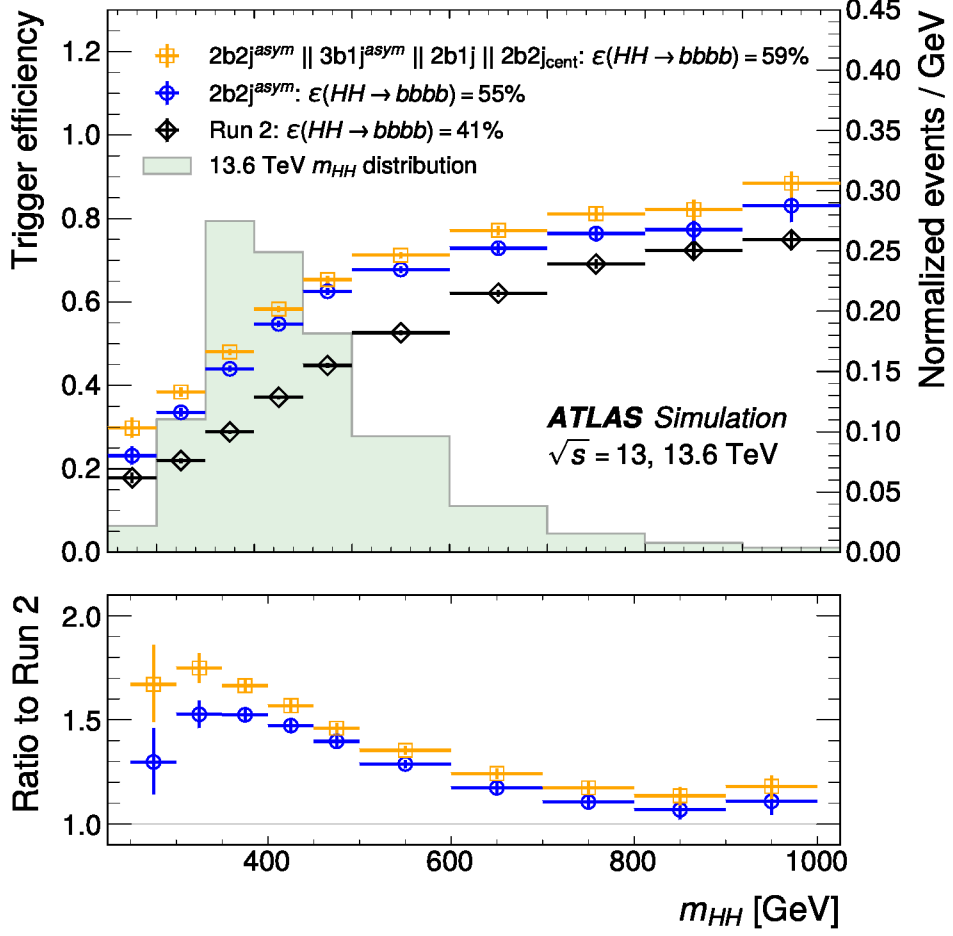


Figure 6: Performance of the b -jet trigger HLT selections in a simulated sample of $HH \rightarrow bbbb$ events. The trigger efficiency relative to inclusive $HH \rightarrow bbbb$ events is shown as a function of the true di-Higgs boson invariant mass, m_{HH} , for the $2b2j^{asym}$ selection and the union of $2b2j^{asym}$, $3b1j^{asym}$, $2b1j$, and $2b2j_{cent}$ triggers, as introduced in Tables 1 and 2, compared with the trigger selection employed in the Run 2 analysis [8]. The $2b2j^{asym}$ trigger has the highest efficiency of any single trigger chain in the Run 3 menu.

τ -leptons having the hadronic component of the transverse momentum ($p_T^{vis} > 20$ GeV, within the inner detector acceptance ($|\eta| < 2.5$)). The $2b2j^{asym}$ chain moreover achieves a large unique efficiency ($> 40\%$) with respect to a trigger strategy selecting events with pairs of τ -leptons in the HLT. This strategy was used by the ATLAS Collaboration in Run 2 searches for the $HH \rightarrow b\tau\tau$ process [69], where the leading- p_T (sub-leading- p_T) τ -lepton must have $p_T > 35$ GeV ($p_T > 25$ GeV). In Run 3, ATLAS deployed a similar trigger chain with looser τ -lepton p_T thresholds at 30 and 20 GeV. A comparison between the trigger efficiencies for these various $HH \rightarrow b\tau\tau$ trigger strategies is shown differentially in m_{HH} in Figure 7. To ensure the efficiencies are comparable and relevant for the ATLAS search for $HH \rightarrow b\tau\tau$ production, they are calculated relative to the $HH \rightarrow b\tau\tau$ fiducial selection.

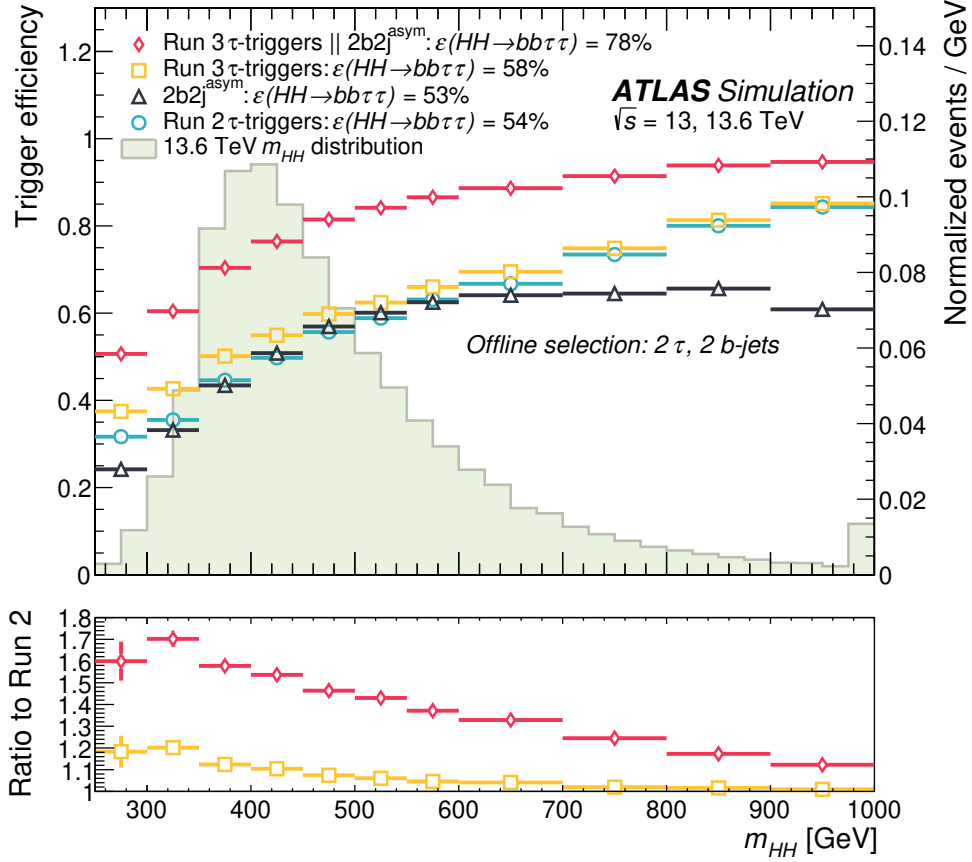


Figure 7: Performance of the b -jet trigger HLT selections in a simulated sample of $HH \rightarrow bb\tau\tau$ events: the trigger efficiency as a function of the true di-Higgs boson invariant mass, m_{HH} . The $2b2j^{asym}$ trigger selection compared with a trigger selection based purely on HLT τ -lepton identification is shown. To ensure efficiencies are comparable across trigger strategies, they are measured relative to events within the detector acceptance for the $HH \rightarrow bb\tau\tau$ analysis; these events must have two offline τ -lepton candidates matched to true hadronically decaying τ -leptons and two offline jets matched to b -hadrons. The τ -lepton based triggers shown follow the strategy used for the Run 2 $HH \rightarrow bb\tau\tau$ analysis [69] together with an additional di- τ -lepton trigger with lower p_T thresholds for Run 3, requiring at least one identified τ -lepton in the HLT system with $p_T > 30$ GeV and a second with $p_T > 20$ GeV. Efficiencies are calculated relative to a selection of two reconstructed b -jets ($p_T > 20$ GeV) and two reconstructed τ -leptons ($p_T^{vis} > 25, 20$ GeV) within the inner detector acceptance ($|\eta| < 2.5$).

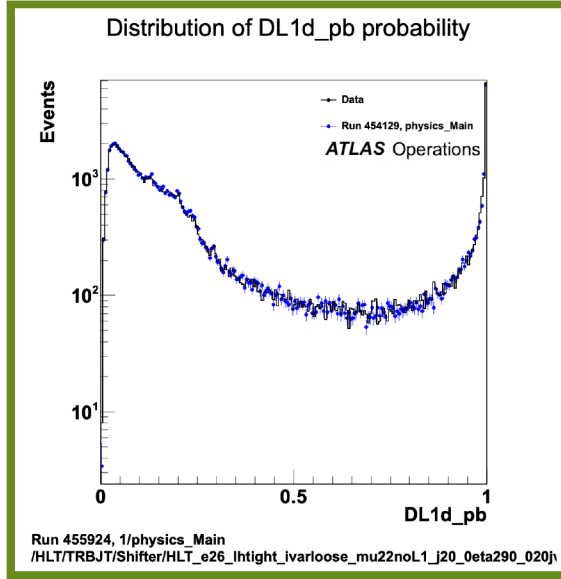
7 Offline and online b -jet trigger monitoring

As the trigger is the first step in the ATLAS event selection of LHC data, its behaviour must be understood at the deepest level since any failure during data-taking is unrecoverable. The quality of b -jet triggered data is continuously assessed, thanks to the trigger system monitoring infrastructure [70], which is part of the ATLAS Data Quality Monitoring system [71]. For the trigger, this consists of two parts: the online and the offline monitoring systems. The online monitoring system allows a real-time check of the quality of collected events during the data-taking, and provides quick detection of processing failures or reconstruction issues, ensuring that the ATLAS Trigger and Data Acquisition [4] operates properly and collects high

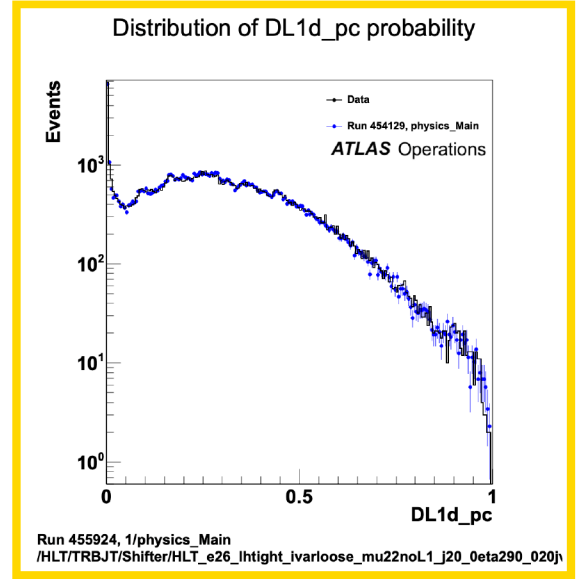
quality data. Using the Data Quality Monitoring Display (DQMD), shifters in the ATLAS control room can monitor distributions for b -tagging relevant quantities, such as track impact parameters, properties of secondary vertices and jet b -tagging weights, both inclusively, i.e. every time the algorithm is called, and separately for specific trigger chains. Inclusive quantities can provide high statistics distributions, available to the shifter as histograms, although these are more sensitive to changes in the trigger menu which could arise in the middle of the run from changes in the beam conditions. On the other hand, the exclusive monitoring of specific chains permits checking data behaviour in a stable environment, where each monitored trigger chain is chosen to have a different jet flavour composition, as an example multijet events are dominated by the light-jet component, while selecting data where muons are embedded in hadronic jets allows to enhance the b -jet component by taking advantage of the large semimuonic branching ratio of B -hadrons.

After the data are fully reconstructed, the offline monitoring allows a more detailed quality assessment. A set of automatic software routines run dedicated algorithms that first select events, based on the precise offline reconstructed physics objects, compare relevant trigger and offline distributions with the ones taken in a reference run and then make it available to the offline shifter, via a web-based display.

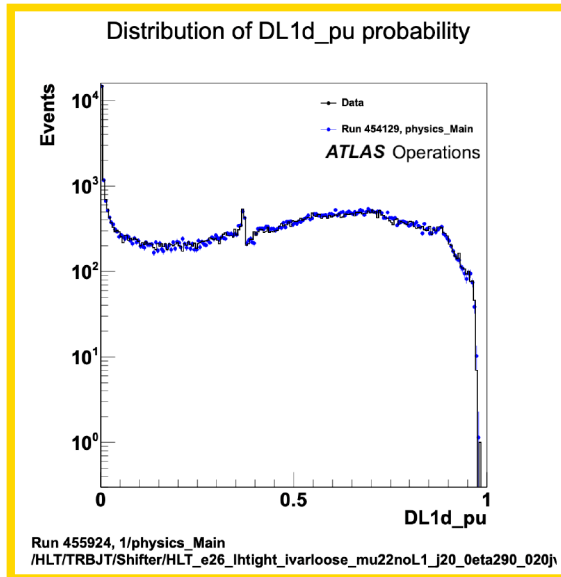
By using the DQMD in the ATLAS control room, and the web-based display, the tasks of both online and offline shifters are facilitated by a series of automatic tests, such as width and mean of the distribution comparison, or the Kolmogorov-Smirnov statistical test, which compares several parameters of a distribution to a reference histogram to evaluate data quality. Histograms then appear in different colours depending on to which degree the shown distributions satisfy these tests, for instance a χ^2 test, depending on the agreement, flags as green if the ratio of χ^2 over the number of degrees of freedom (χ^2/Ndof) is smaller than one, yellow if $1 < \chi^2/\text{Ndof} < 1.5$ and finally red if $\chi^2/\text{Ndof} > 1.5$. This is shown in Figure 8 where several b -tagging related quantities for a dilepton(one electron and one muon)-plus jets chain, naturally enhanced in $t\bar{t}$ events, for the run 455924, recorded in April 2023, are compared with a reference. Overall, mismatches can be due to actual problems such as differences in the run pile-up profile and instantaneous luminosity, slight differences in the beam position, LHC configuration changes, up to detector or reconstruction problems and are followed up and discussed in dedicated ATLAS forums.



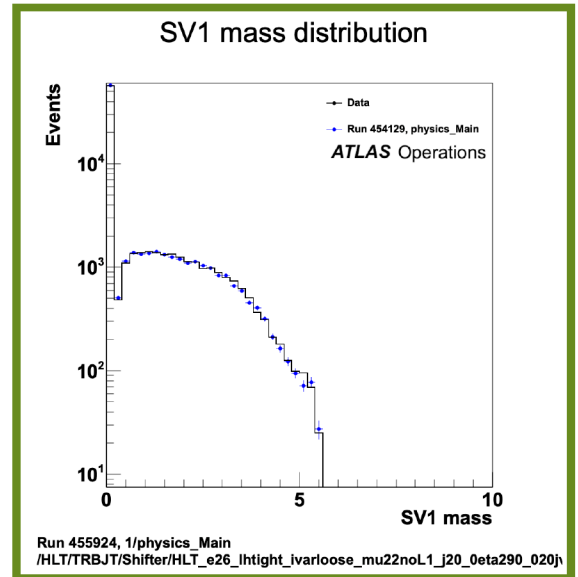
(a)



(b)



(c)



(d)

Figure 8: Examples of the monitored quantities present in the web display for the offline data quality assessment. Shown here are various plots for b -jet candidates as reconstructed in the HLT. The display shows b -tagging quantities for dedicated dilepton plus jets chains, enhanced in $t\bar{t}$ events, the DL1d probability for the (a) b -, (b) c -, (c) light-jet hypothesis and (d) the mass of the reconstructed Secondary Vertex (in GeV). The data for the relevant run (solid histogram) are compared with a reference (solid markers), and according to a χ^2 test, depending on the agreement, they are flagged as green ($\chi^2/\text{Ndof} < 1$), yellow ($1 < \chi^2/\text{Ndof} < 1.5$), or red ($\chi^2/\text{Ndof} > 1.5$). The reference run is updated periodically to reflect significant condition changes, such as updated trigger menus. This example shows run 455924, which was recorded in April 2023. Error bars include the statistical uncertainties only.

8 Conclusion

ATLAS restarted its data taking in 2022 deploying new state-of-the-art b -tagging algorithms constructed from neural networks. In the first year of the Run 3 data-taking the new DL1d algorithm led already to a sizeable increase in performance relative to Run 2. For the 2023 data-taking campaign the baseline tagger changed to the GN1 algorithm which added up to a factor two improvement in light-flavour rejection. These improvements are introduced together with a new two-step trigger strategy that mitigates the CPU demands by introducing a fast b -tagging preselection, running on calorimeter-based jets, which is scheduled before the HLT precision-tracking-based b -tagging. These ameliorations allow ATLAS to collect hadronic signatures such as $HH \rightarrow b\bar{b}\tau\tau$ with an increase in signal efficiency of up to a factor 1.7 relative to Run 2. Finally, to assess the quality of the simulation, conditional efficiencies are measured in data and compared with simulation in $t\bar{t}$ -enriched events, where an overall good agreement of the trigger efficiencies are observed.

Acknowledgements

We thank CERN for the very successful operation of the LHC and its injectors, as well as the support staff at CERN and at our institutions worldwide without whom ATLAS could not be operated efficiently.

The crucial computing support from all WLCG partners is acknowledged gratefully, in particular from CERN, the ATLAS Tier-1 facilities at TRIUMF/SFU (Canada), NDGF (Denmark, Norway, Sweden), CC-IN2P3 (France), KIT/GridKA (Germany), INFN-CNAF (Italy), NL-T1 (Netherlands), PIC (Spain), RAL (UK) and BNL (USA), the Tier-2 facilities worldwide and large non-WLCG resource providers. Major contributors of computing resources are listed in Ref. [72].

We gratefully acknowledge the support of ANPCyT, Argentina; YerPhI, Armenia; ARC, Australia; BMWFW and FWF, Austria; ANAS, Azerbaijan; CNPq and FAPESP, Brazil; NSERC, NRC and CFI, Canada; CERN; ANID, Chile; CAS, MOST and NSFC, China; Minciencias, Colombia; MEYS CR, Czech Republic; DNRF and DNSRC, Denmark; IN2P3-CNRS and CEA-DRF/IRFU, France; SRNSFG, Georgia; BMBF, HGF and MPG, Germany; GSRI, Greece; RGC and Hong Kong SAR, China; ICHEP and Academy of Sciences and Humanities, Israel; INFN, Italy; MEXT and JSPS, Japan; CNRST, Morocco; NWO, Netherlands; RCN, Norway; MNiSW, Poland; FCT, Portugal; MNE/IFA, Romania; MSTDI, Serbia; MSSR, Slovakia; ARIS and MVZI, Slovenia; DSI/NRF, South Africa; MICIU/AEI, Spain; SRC and Wallenberg Foundation, Sweden; SERI, SNSF and Cantons of Bern and Geneva, Switzerland; NSTC, Taipei; TENMAK, Türkiye; STFC/UKRI, United Kingdom; DOE and NSF, United States of America.

Individual groups and members have received support from BCKDF, CANARIE, CRC and DRAC, Canada; CERN-CZ, FORTE and PRIMUS, Czech Republic; COST, ERC, ERDF, Horizon 2020, ICSC-NextGenerationEU and Marie Skłodowska-Curie Actions, European Union; Investissements d’Avenir Labex, Investissements d’Avenir Idex and ANR, France; DFG and AvH Foundation, Germany; Herakleitos, Thales and Aristeia programmes co-financed by EU-ESF and the Greek NSRF, Greece; BSF-NSF and MINERVA, Israel; NCN and NAWA, Poland; La Caixa Banking Foundation, CERCA Programme Generalitat de Catalunya and PROMETEO and GenT Programmes Generalitat Valenciana, Spain; Göran Gustafssons Stiftelse, Sweden; The Royal Society and Leverhulme Trust, United Kingdom.

In addition, individual members wish to acknowledge support from Armenia: Yerevan Physics Institute (FAPERJ); CERN: European Organization for Nuclear Research (CERN DOCT); Chile: Agencia

Nacional de Investigación y Desarrollo (FONDECYT 1230812, FONDECYT 1230987, FONDECYT 1240864); China: Chinese Ministry of Science and Technology (MOST-2023YFA1605700, MOST-2023YFA1609300), National Natural Science Foundation of China (NSFC - 12175119, NSFC 12275265, NSFC-12075060); Czech Republic: Czech Science Foundation (GACR - 24-11373S), Ministry of Education Youth and Sports (FORTE CZ.02.01.01/00/22_008/0004632), PRIMUS Research Programme (PRIMUS/21/SCI/017); EU: H2020 European Research Council (ERC - 101002463); European Union: European Research Council (ERC - 948254, ERC 101089007, ERC, BARD, 101116429), European Union, Future Artificial Intelligence Research (FAIR-NextGenerationEU PE00000013), Italian Center for High Performance Computing, Big Data and Quantum Computing (ICSC, NextGenerationEU); France: Agence Nationale de la Recherche (ANR-20-CE31-0013, ANR-21-CE31-0013, ANR-21-CE31-0022, ANR-22-EDIR-0002); Germany: Baden-Württemberg Stiftung (BW Stiftung-Postdoc Eliteprogramme), Deutsche Forschungsgemeinschaft (DFG - 469666862, DFG - CR 312/5-2); Italy: Istituto Nazionale di Fisica Nucleare (ICSC, NextGenerationEU), Ministero dell'Università e della Ricerca (PRIN - 20223N7F8K - PNRR M4.C2.1.1); Japan: Japan Society for the Promotion of Science (JSPS KAKENHI JP22H01227, JSPS KAKENHI JP22H04944, JSPS KAKENHI JP22KK0227, JSPS KAKENHI JP23KK0245); Netherlands: Netherlands Organisation for Scientific Research (NWO Veni 2020 - VI.Veni.202.179); Norway: Research Council of Norway (RCN-314472); Poland: Ministry of Science and Higher Education (IDUB AGH, POB8, D4 no 9722), Polish National Agency for Academic Exchange (PPN/PPO/2020/1/00002/U/00001), Polish National Science Centre (NCN 2021/42/E/ST2/00350, NCN OPUS 2023/51/B/ST2/02507, NCN OPUS nr 2022/47/B/ST2/03059, NCN UMO-2019/34/E/ST2/00393, NCN & H2020 MSCA 945339, UMO-2020/37/B/ST2/01043, UMO-2021/40/C/ST2/00187, UMO-2022/47/O/ST2/00148, UMO-2023/49/B/ST2/04085, UMO-2023/51/B/ST2/00920); Slovenia: Slovenian Research Agency (ARIS grant J1-3010); Spain: Generalitat Valenciana (Artemisa, FEDER, ID-IFEDER/2018/048), Ministry of Science and Innovation (MCIN & NextGenEU PCI2022-135018-2, MICIN & FEDER PID2021-125273NB, RYC2019-028510-I, RYC2020-030254-I, RYC2021-031273-I, RYC2022-038164-I); Sweden: Carl Trygger Foundation (Carl Trygger Foundation CTS 22:2312), Swedish Research Council (Swedish Research Council 2023-04654, VR 2018-00482, VR 2022-03845, VR 2022-04683, VR 2023-03403, VR grant 2021-03651), Knut and Alice Wallenberg Foundation (KAW 2018.0458, KAW 2019.0447, KAW 2022.0358); Switzerland: Swiss National Science Foundation (SNSF - PCEFP2_194658); United Kingdom: Leverhulme Trust (Leverhulme Trust RPG-2020-004), Royal Society (NIF-R1-231091); United States of America: U.S. Department of Energy (ECA DE-AC02-76SF00515), Neubauer Family Foundation.

References

- [1] L. Evans and P. Bryant, *LHC Machine*, [JINST 3 \(2008\) S08001](#).
- [2] ATLAS Collaboration, *The ATLAS Experiment at the CERN Large Hadron Collider*, [JINST 3 \(2008\) S08003](#).
- [3] ATLAS Collaboration, *The ATLAS experiment at the CERN Large Hadron Collider: a description of the detector configuration for Run 3*, [JINST 19 \(2023\) P05063](#), [arXiv: 2305.16623 \[physics.ins-det\]](#).
- [4] ATLAS Collaboration, *The ATLAS trigger system for LHC Run 3 and trigger performance in 2022*, [JINST 19 \(2024\) P06029](#), [arXiv: 2401.06630 \[hep-ex\]](#).
- [5] ATLAS Collaboration, *ATLAS flavour-tagging algorithms for the LHC Run 2 pp collision dataset*, [Eur. Phys. J. C 83 \(2023\) 681](#), [arXiv: 2211.16345 \[physics.data-an\]](#).

- [6] ATLAS Collaboration, *Observation of $H \rightarrow b\bar{b}$ decays and VH production with the ATLAS detector*, [Phys. Lett. B **786** \(2018\) 59](#), arXiv: [1808.08238 \[hep-ex\]](#).
- [7] ATLAS Collaboration, *Observation of Higgs boson production in association with a top quark pair at the LHC with the ATLAS detector*, [Phys. Lett. B **784** \(2018\) 173](#), arXiv: [1806.00425 \[hep-ex\]](#).
- [8] ATLAS Collaboration, *Search for nonresonant pair production of Higgs bosons in the $b\bar{b}b\bar{b}$ final state in pp collisions at $\sqrt{s} = 13$ TeV with the ATLAS detector*, [Phys. Rev. D **108** \(2023\) 052003](#), arXiv: [2301.03212 \[hep-ex\]](#).
- [9] ATLAS Collaboration, *Measurement of the $t\bar{t}$ production cross-section and lepton differential distributions in $e\mu$ dilepton events from pp collisions at $\sqrt{s} = 13$ TeV with the ATLAS detector*, [Eur. Phys. J. C **80** \(2020\) 528](#), arXiv: [1910.08819 \[hep-ex\]](#).
- [10] ATLAS Collaboration, *Measurement of the top quark mass in the $t\bar{t} \rightarrow \text{lepton} + \text{jets}$ channel from $\sqrt{s} = 8$ TeV ATLAS data and combination with previous results*, [Eur. Phys. J. C **79** \(2019\) 290](#), arXiv: [1810.01772 \[hep-ex\]](#).
- [11] ATLAS Collaboration, *Search for heavy particles decaying into top-quark pairs using lepton-plus-jets events in proton–proton collisions at $\sqrt{s} = 13$ TeV with the ATLAS detector*, [Eur. Phys. J. C **78** \(2018\) 565](#), arXiv: [1804.10823 \[hep-ex\]](#).
- [12] ATLAS Collaboration, *Search for heavy particles in the b -tagged dijet mass distribution with additional b -tagged jets in proton–proton collisions at $\sqrt{s} = 13$ TeV with the ATLAS experiment*, [Phys. Rev. D **105** \(2022\) 012001](#), arXiv: [2108.07586 \[hep-ex\]](#).
- [13] ATLAS Collaboration, *Search for pair production of higgsinos in events with two Higgs bosons and missing transverse momentum in $\sqrt{s} = 13$ TeV pp collisions at the ATLAS experiment*, [Phys. Rev. D **109** \(2024\) 112011](#), arXiv: [2401.14922 \[hep-ex\]](#).
- [14] J. Bellm et al., *Jet Cross Sections at the LHC and the Quest for Higher Precision*, [Eur. Phys. J. C **80** \(2020\) 93](#), arXiv: [1903.12563 \[hep-ph\]](#).
- [15] ATLAS Collaboration, *Measurements of top-quark pair single- and double-differential cross-sections in the all-hadronic channel in pp collisions at $\sqrt{s} = 13$ TeV using the ATLAS detector*, [JHEP **01** \(2021\) 033](#), arXiv: [2006.09274 \[hep-ex\]](#).
- [16] ATLAS Collaboration, *Configuration and performance of the ATLAS b -jet triggers in Run 2*, [Eur. Phys. J. C **81** \(2021\) 1087](#), arXiv: [2106.03584 \[hep-ex\]](#).
- [17] ATLAS Collaboration, *Software and computing for Run 3 of the ATLAS experiment at the LHC*, (2024), arXiv: [2404.06335 \[hep-ex\]](#).
- [18] S. Frixione, G. Ridolfi, and P. Nason, *A positive-weight next-to-leading-order Monte Carlo for heavy flavour hadroproduction*, [JHEP **09** \(2007\) 126](#), arXiv: [0707.3088 \[hep-ph\]](#).
- [19] P. Nason, *A new method for combining NLO QCD with shower Monte Carlo algorithms*, [JHEP **11** \(2004\) 040](#), arXiv: [hep-ph/0409146](#).
- [20] S. Frixione, P. Nason, and C. Oleari, *Matching NLO QCD computations with parton shower simulations: the POWHEG method*, [JHEP **11** \(2007\) 070](#), arXiv: [0709.2092 \[hep-ph\]](#).

- [21] S. Alioli, P. Nason, C. Oleari, and E. Re, *A general framework for implementing NLO calculations in shower Monte Carlo programs: the POWHEG BOX*, **JHEP** **06** (2010) 043, arXiv: [1002.2581 \[hep-ph\]](#).
- [22] NNPDF Collaboration, R. D. Ball, et al., *Parton distributions for the LHC run II*, **JHEP** **04** (2015) 040, arXiv: [1410.8849 \[hep-ph\]](#).
- [23] ATLAS Collaboration, *Studies on top-quark Monte Carlo modelling for Top2016*, ATL-PHYS-PUB-2016-020, 2016, URL: <https://cds.cern.ch/record/2216168>.
- [24] T. Sjöstrand et al., *An introduction to PYTHIA 8.2*, **Comput. Phys. Commun.** **191** (2015) 159, arXiv: [1410.3012 \[hep-ph\]](#).
- [25] ATLAS Collaboration, *ATLAS Pythia 8 tunes to 7 TeV data*, ATL-PHYS-PUB-2014-021, 2014, URL: <https://cds.cern.ch/record/1966419>.
- [26] NNPDF Collaboration, R. D. Ball, et al., *Parton distributions with LHC data*, **Nucl. Phys. B** **867** (2013) 244, arXiv: [1207.1303 \[hep-ph\]](#).
- [27] ATLAS Collaboration, *ATLAS b-jet identification performance and efficiency measurement with $t\bar{t}$ events in pp collisions at $\sqrt{s} = 13$ TeV*, **Eur. Phys. J. C** **79** (2019) 970, arXiv: [1907.05120 \[hep-ex\]](#).
- [28] ATLAS Collaboration, *Measurements of jet observables sensitive to b-quark fragmentation in $t\bar{t}$ events at the LHC with the ATLAS detector*, **Phys. Rev. D** **106** (2022) 032008, arXiv: [2202.13901 \[hep-ex\]](#).
- [29] J. Butterworth et al., *PDF4LHC recommendations for LHC Run II*, **J. Phys. G** **43** (2016) 023001, arXiv: [1510.03865 \[hep-ph\]](#).
- [30] D. J. Lange, *The EvtGen particle decay simulation package*, **Nucl. Instrum. Meth. A** **462** (2001) 152.
- [31] T. Sjöstrand, S. Mrenna, and P. Skands, *A brief introduction to PYTHIA 8.1*, **Comput. Phys. Commun.** **178** (2008) 852, arXiv: [0710.3820 \[hep-ph\]](#).
- [32] ATLAS Collaboration, *The Pythia 8 A3 tune description of ATLAS minimum bias and inelastic measurements incorporating the Donnachie–Landshoff diffractive model*, ATL-PHYS-PUB-2016-017, 2016, URL: <https://cds.cern.ch/record/2206965>.
- [33] ATLAS Collaboration, *The ATLAS Simulation Infrastructure*, **Eur. Phys. J. C** **70** (2010) 823, arXiv: [1005.4568 \[physics.ins-det\]](#).
- [34] S. Agostinelli et al., *GEANT4 – a simulation toolkit*, **Nucl. Instrum. Meth. A** **506** (2003) 250.
- [35] ATLAS Collaboration, *Performance of the ATLAS muon triggers in Run 2*, **JINST** **15** (2020) P09015, arXiv: [2004.13447 \[physics.ins-det\]](#).
- [36] A. Armbruster et al., *The ATLAS Muon to Central Trigger Processor Interface Upgrade for the Run 3 of the LHC*, **2017 IEEE Nuclear Science Symposium and Medical Imaging Conference (NSS/MIC)** (2017) 1.
- [37] ATLAS Collaboration, *Search for Low-Mass Dijet Resonances Using Trigger-Level Jets with the ATLAS Detector in pp Collisions at $\sqrt{s} = 13$ TeV*, **Phys. Rev. Lett.** **121** (2018) 081801, arXiv: [1804.03496 \[hep-ex\]](#).
- [38] ATLAS Collaboration, *Performance of the ATLAS trigger system in 2015*, **Eur. Phys. J. C** **77** (2017) 317, arXiv: [1611.09661 \[hep-ex\]](#).

- [39] Particle Data Group, P. Zyla, et al., *Review of Particle Physics*, *Prog. Theor. Exp. Phys.* **2020** (2020) 083C01.
- [40] ATLAS Collaboration, *Early Inner Detector Tracking Performance in the 2015 Data at $\sqrt{s} = 13$ TeV*, ATL-PHYS-PUB-2015-051, 2015, URL: <https://cds.cern.ch/record/2110140>.
- [41] ATLAS Collaboration, *The ATLAS Inner Detector Trigger performance in pp collisions at 900 GeV and 13.6 TeV for LHC Run 3 operation during 2022*, ATL-DAQ-PUB-2023-002, 2023, URL: <https://cds.cern.ch/record/2881679>.
- [42] ATLAS Collaboration, *Software Performance of the ATLAS Track Reconstruction for LHC Run 3*, *Comput. Softw. Big Sci.* **8** (2024) 9, arXiv: 2308.09471 [hep-ex].
- [43] ATLAS Collaboration, *Development of ATLAS Primary Vertex Reconstruction for LHC Run 3*, ATL-PHYS-PUB-2019-015, 2019, URL: <https://cds.cern.ch/record/2670380>.
- [44] ATLAS Collaboration, *Jet energy scale and resolution measured in proton–proton collisions at $\sqrt{s} = 13$ TeV with the ATLAS detector*, *Eur. Phys. J. C* **81** (2021) 689, arXiv: 2007.02645 [hep-ex].
- [45] ATLAS Collaboration, *Jet reconstruction and performance using particle flow with the ATLAS Detector*, *Eur. Phys. J. C* **77** (2017) 466, arXiv: 1703.10485 [hep-ex].
- [46] M. Cacciari, G. P. Salam, and G. Soyez, *The anti- k_t jet clustering algorithm*, *JHEP* **04** (2008) 063, arXiv: 0802.1189 [hep-ph].
- [47] M. Cacciari, G. P. Salam, and G. Soyez, *FastJet user manual*, *Eur. Phys. J. C* **72** (2012) 1896, arXiv: 1111.6097 [hep-ph].
- [48] ATLAS Collaboration, *The performance of the jet trigger for the ATLAS detector during 2011 data taking*, *Eur. Phys. J. C* **76** (2016) 526, arXiv: 1606.07759 [hep-ex].
- [49] ATLAS Collaboration, *Performance of pile-up mitigation techniques for jets in pp collisions at $\sqrt{s} = 8$ TeV using the ATLAS detector*, *Eur. Phys. J. C* **76** (2016) 581, arXiv: 1510.03823 [hep-ex].
- [50] ATLAS Collaboration, *Performance of b -jet identification in the ATLAS experiment*, *JINST* **11** (2016) P04008, arXiv: 1512.01094 [hep-ex].
- [51] ATLAS Collaboration, *Secondary vertex finding for jet flavour identification with the ATLAS detector*, ATL-PHYS-PUB-2017-011, 2017, URL: <https://cds.cern.ch/record/2270366>.
- [52] ATLAS Collaboration, *Topological b -hadron decay reconstruction and identification of b -jets with the JetFitter package in the ATLAS experiment at the LHC*, ATL-PHYS-PUB-2018-025, 2018, URL: <https://cds.cern.ch/record/2645405>.
- [53] M. Zaheer et al., *Deep Sets*, NIPS (2017), arXiv: 1703.06114 [cs.LG].
- [54] ATLAS Collaboration, *Deep Sets based Neural Networks for Impact Parameter Flavour Tagging in ATLAS*, ATL-PHYS-PUB-2020-014, 2020, URL: <https://cds.cern.ch/record/2718948>.

- [55] ATLAS Collaboration, *Fast b -tagging at the high-level trigger of the ATLAS experiment in LHC Run 3*, *JINST* **18** (2023) P11006, arXiv: [2306.09738 \[hep-ex\]](#).
- [56] P. Ramachandran et al., *Searching for Activation Functions*, 2017, arXiv: [1710.05941 \[cs.NE\]](#).
- [57] ATLAS Collaboration, *Graph Neural Network Jet Flavour Tagging with the ATLAS Detector*, ATL-PHYS-PUB-2022-027, 2022, URL: <https://cds.cern.ch/record/2811135>.
- [58] ATLAS Collaboration, *Identification of Jets Containing b -Hadrons with Recurrent Neural Networks at the ATLAS Experiment*, ATL-PHYS-PUB-2017-003, 2017, URL: <https://cds.cern.ch/record/2255226>.
- [59] D. P. Kingma and J. Ba, *Adam: A Method for Stochastic Optimization*, 2017, arXiv: [1412.6980 \[cs.LG\]](#).
- [60] F. Chollet et al., *Keras*, 2015, URL: <https://keras.io>.
- [61] M. Zaheer et al., *Automatic differentiation in PyTorch*, NIPS (2017), URL: <https://openreview.net/forum?id=BJJsrmfCZ>.
- [62] ATLAS Collaboration, *Trigger monitoring and rate predictions using Enhanced Bias data from the ATLAS Detector at the LHC*, ATL-DAQ-PUB-2016-002, 2016, URL: <https://cds.cern.ch/record/2223498>.
- [63] ATLAS Collaboration, *Performance of the upgraded PreProcessor of the ATLAS Level-1 Calorimeter Trigger*, *JINST* **15** (2020) P11016, arXiv: [2005.04179 \[physics.ins-det\]](#).
- [64] P. D. Group, *Review of particle physics*, *Phys. Rev. D* **110** (2024) 030001.
- [65] ATLAS Collaboration, *Performance of the ATLAS track reconstruction algorithms in dense environments in LHC Run 2*, *Eur. Phys. J. C* **77** (2017) 673, arXiv: [1704.07983 \[hep-ex\]](#).
- [66] ATLAS Collaboration, *Electron and photon performance measurements with the ATLAS detector using the 2015–2017 LHC proton–proton collision data*, *JINST* **14** (2019) P12006, arXiv: [1908.00005 \[hep-ex\]](#).
- [67] ATLAS Collaboration, *Measurement of differential cross-sections in $t\bar{t}$ and $t\bar{t}$ +jets production in the lepton+jets final state in pp collisions at $\sqrt{s} = 13$ TeV using 140fb^{-1} of ATLAS data*, *JHEP* **08** (2024) 182, arXiv: [2406.19701 \[hep-ex\]](#).
- [68] M. Gouzevitch and A. Carvalho, *A review of Higgs boson pair production*, *Reviews in Physics* **5** (2020) 100039.
- [69] ATLAS Collaboration, *Search for the non-resonant production of Higgs boson pairs via gluon fusion and vector-boson fusion in the $b\bar{b}\tau^+\tau^-$ final state in proton–proton collisions at $\sqrt{s} = 13$ TeV with the ATLAS detector*, *Phys. Rev. D* **110** (2024) 032012, arXiv: [2404.12660 \[hep-ex\]](#).
- [70] ATLAS Collaboration, *Operation of the ATLAS trigger system in Run 2*, *JINST* **15** (2020) P10004, arXiv: [2007.12539 \[hep-ex\]](#).
- [71] ATLAS Collaboration, *ATLAS data quality operations and performance for 2015–2018 data-taking*, *JINST* **15** (2020) P04003, arXiv: [1911.04632 \[physics.ins-det\]](#).
- [72] ATLAS Collaboration, *ATLAS Computing Acknowledgements*, ATL-SOFT-PUB-2023-001, 2023, URL: <https://cds.cern.ch/record/2869272>.

The ATLAS Collaboration

G. Aad ¹⁰⁴, E. Aakvaag ¹⁷, B. Abbott ¹²³, S. Abdelhameed ^{119a}, K. Abeling ⁵⁶, N.J. Abicht ⁵⁰, S.H. Abidi ³⁰, M. Aboelela ⁴⁶, A. Aboulhorma ^{36e}, H. Abramowicz ¹⁵⁵, Y. Abulaiti ¹²⁰, B.S. Acharya ^{70a,70b,m}, A. Ackermann ^{64a}, C. Adam Bourdarios ⁴, L. Adamczyk ^{87a}, S.V. Addepalli ¹⁴⁷, M.J. Addison ¹⁰³, J. Adelman ¹¹⁸, A. Adiguzel ^{22c}, T. Adye ¹³⁷, A.A. Affolder ¹³⁹, Y. Afik ⁴¹, M.N. Agaras ¹³, A. Aggarwal ¹⁰², C. Agheorghiesei ^{28c}, F. Ahmadov ^{40,ac}, S. Ahuja ⁹⁷, X. Ai ^{63e}, G. Aielli ^{77a,77b}, A. Aikot ¹⁶⁷, M. Ait Tamlihat ^{36e}, B. Aitbenkikh ^{36a}, M. Akbiyik ¹⁰², T.P.A. Åkesson ¹⁰⁰, A.V. Akimov ¹⁴⁹, D. Akiyama ¹⁷², N.N. Akolkar ²⁵, S. Aktas ^{22a}, G.L. Alberghi ^{24b}, J. Albert ¹⁶⁹, P. Albicocco ⁵⁴, G.L. Albouy ⁶¹, S. Alderweireldt ⁵³, Z.L. Alegria ¹²⁴, M. Aleksa ³⁷, I.N. Aleksandrov ⁴⁰, C. Alexa ^{28b}, T. Alexopoulos ¹⁰, F. Alfonsi ^{24b}, M. Algren ⁵⁷, M. Alhroob ¹⁷¹, B. Ali ¹³⁵, H.M.J. Ali ^{93,v}, S. Ali ³², S.W. Alibocus ⁹⁴, M. Aliev ^{34c}, G. Alimonti ^{72a}, W. Alkakh ⁵⁶, C. Allaire ⁶⁷, B.M.M. Allbrooke ¹⁵⁰, J.S. Allen ¹⁰³, J.F. Allen ⁵³, C.A. Allendes Flores ^{140f}, P.P. Allport ²¹, A. Aloisio ^{73a,73b}, F. Alonso ⁹², C. Alpigiani ¹⁴², Z.M.K. Alsolami ⁹³, A. Alvarez Fernandez ¹⁰², M. Alves Cardoso ⁵⁷, M.G. Alviggi ^{73a,73b}, M. Aly ¹⁰³, Y. Amaral Coutinho ^{84b}, A. Ambler ¹⁰⁶, C. Amelung ³⁷, M. Amerl ¹⁰³, C.G. Ames ¹¹¹, D. Amidei ¹⁰⁸, B. Amini ⁵⁵, K.J. Amirie ¹⁵⁸, A. Amirkhanov ³⁹, S.P. Amor Dos Santos ^{133a}, K.R. Amos ¹⁶⁷, D. Amperiadou ¹⁵⁶, S. An ⁸⁵, V. Ananiev ¹²⁸, C. Anastopoulos ¹⁴³, T. Andeen ¹¹, J.K. Anders ³⁷, A.C. Anderson ⁶⁰, A. Andreazza ^{72a,72b}, S. Angelidakis ⁹, A. Angerami ⁴³, A.V. Anisenkov ³⁹, A. Annovi ^{75a}, C. Antel ⁵⁷, E. Antipov ¹⁴⁹, M. Antonelli ⁵⁴, F. Anulli ^{76a}, M. Aoki ⁸⁵, T. Aoki ¹⁵⁷, M.A. Aparo ¹⁵⁰, L. Aperio Bella ⁴⁹, C. Appelt ¹⁵⁵, A. Apyan ²⁷, S.J. Arbiol Val ⁸⁸, C. Arcangeletti ⁵⁴, A.T.H. Arce ⁵², J-F. Arguin ¹¹⁰, S. Argyropoulos ¹⁵⁶, J.-H. Arling ⁴⁹, O. Arnaez ⁴, H. Arnold ¹⁴⁹, G. Artoni ^{76a,76b}, H. Asada ¹¹³, K. Asai ¹²¹, S. Asai ¹⁵⁷, N.A. Asbah ³⁷, R.A. Ashby Pickering ¹⁷¹, A.M. Aslam ⁹⁷, K. Assamagan ³⁰, R. Astalos ^{29a}, K.S.V. Astrand ¹⁰⁰, S. Atashi ¹⁶², R.J. Atkin ^{34a}, H. Atmani ^{36f}, P.A. Atlasiddha ¹³¹, K. Augsten ¹³⁵, A.D. Auriol ⁴², V.A. Austrup ¹⁰³, G. Avolio ³⁷, K. Axiotis ⁵⁷, G. Azuelos ^{110,ag}, D. Babal ^{29b}, H. Bachacou ¹³⁸, K. Bachas ^{156,q}, A. Bachi ³⁵, E. Bachmann ⁵¹, A. Badea ⁴¹, T.M. Baer ¹⁰⁸, P. Bagnaia ^{76a,76b}, M. Bahmani ¹⁹, D. Bahner ⁵⁵, K. Bai ¹²⁶, J.T. Baines ¹³⁷, L. Baines ⁹⁶, O.K. Baker ¹⁷⁶, E. Bakos ¹⁶, D. Bakshi Gupta ⁸, L.E. Balabram Filho ^{84b}, V. Balakrishnan ¹²³, R. Balasubramanian ⁴, E.M. Baldin ³⁹, P. Balek ^{87a}, E. Ballabene ^{24b,24a}, F. Balli ¹³⁸, L.M. Baltes ^{64a}, W.K. Balunas ³³, J. Balz ¹⁰², I. Bamwidhi ^{119b}, E. Banas ⁸⁸, M. Bandieramonte ¹³², A. Bandyopadhyay ²⁵, S. Bansal ²⁵, L. Barak ¹⁵⁵, M. Barakat ⁴⁹, E.L. Barberio ¹⁰⁷, D. Barberis ^{58b,58a}, M. Barbero ¹⁰⁴, M.Z. Barel ¹¹⁷, T. Barillari ¹¹², M-S. Barisits ³⁷, T. Barklow ¹⁴⁷, P. Baron ¹²⁵, D.A. Baron Moreno ¹⁰³, A. Baroncelli ^{63a}, A.J. Barr ¹²⁹, J.D. Barr ⁹⁸, F. Barreiro ¹⁰¹, J. Barreiro Guimarães da Costa ¹⁴, M.G. Barros Teixeira ^{133a}, S. Barsov ³⁹, F. Bartels ^{64a}, R. Bartoldus ¹⁴⁷, A.E. Barton ⁹³, P. Bartos ^{29a}, A. Basan ¹⁰², M. Baselga ⁵⁰, S. Bashiri ⁸⁸, A. Bassalat ^{67,b}, M.J. Basso ^{159a}, S. Bataju ⁴⁶, R. Bate ¹⁶⁸, R.L. Bates ⁶⁰, S. Batlamous ¹⁰¹, M. Battaglia ¹³⁹, D. Battulga ¹⁹, M. Bauge ^{76a,76b}, M. Bauer ⁸⁰, P. Bauer ²⁵, L.T. Bazzano Hurrell ³¹, J.B. Beacham ⁵², T. Beau ¹³⁰, J.Y. Beaucamp ⁹², P.H. Beauchemin ¹⁶¹, P. Bechtel ²⁵, H.P. Beck ^{20,p}, K. Becker ¹⁷¹, A.J. Beddall ⁸³, V.A. Bednyakov ⁴⁰, C.P. Bee ¹⁴⁹, L.J. Beemster ¹⁶, M. Begalli ^{84d}, M. Begel ³⁰, J.K. Behr ⁴⁹, J.F. Beirer ³⁷, F. Beisiegel ²⁵, M. Belfkir ^{119b}, G. Bella ¹⁵⁵, L. Bellagamba ^{24b}, A. Bellerive ³⁵, P. Bellos ²¹, K. Beloborodov ³⁹, D. Benckekroun ^{36a}, F. Bendebba ^{36a}, Y. Benhammou ¹⁵⁵, K.C. Benkendorfer ⁶², L. Beresford ⁴⁹, M. Beretta ⁵⁴, E. Bergeas Kuutmann ¹⁶⁵, N. Berger ⁴, B. Bergmann ¹³⁵, J. Beringer ^{18a},

G. Bernardi ^{id5}, C. Bernius ^{id147}, F.U. Bernlochner ^{id25}, F. Bernon ^{id37}, A. Berrocal Guardia ^{id13}, T. Berry ^{id97}, P. Berta ^{id136}, A. Berthold ^{id51}, S. Bethke ^{id112}, A. Betti ^{id76a,76b}, A.J. Bevan ^{id96}, N.K. Bhalla ^{id55}, S. Bharthuar ^{id112}, S. Bhatta ^{id149}, D.S. Bhattacharya ^{id170}, P. Bhattacharai ^{id147}, Z.M. Bhatti ^{id120}, K.D. Bhide ^{id55}, V.S. Bhopatkar ^{id124}, R.M. Bianchi ^{id132}, G. Bianco ^{id24b,24a}, O. Biebel ^{id111}, M. Biglietti ^{id78a}, C.S. Billingsley ^{id46}, Y. Bingdi ^{id36f}, M. Bindi ^{id56}, A. Bingham ^{id175}, A. Bingul ^{id22b}, C. Bini ^{id76a,76b}, G.A. Bird ^{id33}, M. Birman ^{id173}, M. Biros ^{id136}, S. Biryukov ^{id150}, T. Bisanz ^{id50}, E. Bisceglie ^{id45b,45a}, J.P. Biswal ^{id137}, D. Biswas ^{id145}, I. Bloch ^{id49}, A. Blue ^{id60}, U. Blumenschein ^{id96}, J. Blumenthal ^{id102}, V.S. Bobrovnikov ^{id39}, M. Boehler ^{id55}, B. Boehm ^{id170}, D. Bogavac ^{id37}, A.G. Bogdanchikov ^{id39}, L.S. Boggia ^{id130}, V. Boisvert ^{id97}, P. Bokan ^{id37}, T. Bold ^{id87a}, M. Bomben ^{id5}, M. Bona ^{id96}, M. Boonekamp ^{id138}, A.G. Borbély ^{id60}, I.S. Bordulev ^{id39}, G. Borissov ^{id93}, D. Bortoletto ^{id129}, D. Boscherini ^{id24b}, M. Bosman ^{id13}, K. Bouaouda ^{id36a}, N. Bouchhar ^{id167}, L. Boudet ^{id4}, J. Boudreau ^{id132}, E.V. Bouhova-Thacker ^{id93}, D. Boumediene ^{id42}, R. Bouquet ^{id58b,58a}, A. Boveia ^{id122}, J. Boyd ^{id37}, D. Boye ^{id30}, I.R. Boyko ^{id40}, L. Bozianu ^{id57}, J. Bracinik ^{id21}, N. Brahimi ^{id4}, G. Brandt ^{id175}, O. Brandt ^{id33}, B. Brau ^{id105}, J.E. Brau ^{id126}, R. Brenner ^{id173}, L. Brenner ^{id117}, R. Brenner ^{id165}, S. Bressler ^{id173}, G. Brianti ^{id79a,79b}, D. Britton ^{id60}, D. Britzger ^{id112}, I. Brock ^{id25}, R. Brock ^{id109}, G. Brooijmans ^{id43}, A.J. Brooks ^{id69}, E.M. Brooks ^{id159b}, E. Brost ^{id30}, L.M. Brown ^{id169}, L.E. Bruce ^{id62}, T.L. Bruckler ^{id129}, P.A. Bruckman de Renstrom ^{id88}, B. Brüers ^{id49}, A. Bruni ^{id24b}, G. Bruni ^{id24b}, D. Brunner ^{id48a,48b}, M. Bruschi ^{id24b}, N. Bruscino ^{id76a,76b}, T. Buanes ^{id17}, Q. Buat ^{id142}, D. Buchin ^{id112}, A.G. Buckley ^{id60}, O. Bulekov ^{id39}, B.A. Bullard ^{id147}, S. Burdin ^{id94}, C.D. Burgard ^{id50}, A.M. Burger ^{id37}, B. Burghgrave ^{id8}, O. Burlayenko ^{id55}, J. Burleson ^{id166}, J.T.P. Burr ^{id33}, J.C. Burzynski ^{id146}, E.L. Busch ^{id43}, V. Büscher ^{id102}, P.J. Bussey ^{id60}, J.M. Butler ^{id26}, C.M. Buttar ^{id60}, J.M. Butterworth ^{id98}, W. Buttinger ^{id137}, C.J. Buxo Vazquez ^{id109}, A.R. Buzykaev ^{id39}, S. Cabrera Urbán ^{id167}, L. Cadamuro ^{id67}, D. Caforio ^{id59}, H. Cai ^{id132}, Y. Cai ^{id24b,114c,24a}, Y. Cai ^{id114a}, V.M.M. Cairo ^{id37}, O. Cakir ^{id3a}, N. Calace ^{id37}, P. Calafiura ^{id18a}, G. Calderini ^{id130}, P. Calfayan ^{id35}, G. Callea ^{id60}, L.P. Caloba ^{id84b}, D. Calvet ^{id42}, S. Calvet ^{id42}, R. Camacho Toro ^{id130}, S. Camarda ^{id37}, D. Camarero Munoz ^{id27}, P. Camarri ^{id77a,77b}, M.T. Camerlingo ^{id73a,73b}, D. Cameron ^{id37}, C. Camincher ^{id169}, M. Campanelli ^{id98}, A. Camplani ^{id44}, V. Canale ^{id73a,73b}, A.C. Canbay ^{id3a}, E. Canonero ^{id97}, J. Cantero ^{id167}, Y. Cao ^{id166}, F. Capocasa ^{id27}, M. Capua ^{id45b,45a}, A. Carbone ^{id72a,72b}, R. Cardarelli ^{id77a}, J.C.J. Cardenas ^{id8}, M.P. Cardiff ^{id27}, G. Carducci ^{id45b,45a}, T. Carli ^{id37}, G. Carlino ^{id73a}, J.I. Carlotta ^{id13}, B.T. Carlson ^{id132,r}, E.M. Carlson ^{id169}, J. Carmignani ^{id94}, L. Carminati ^{id72a,72b}, A. Carnelli ^{id138}, M. Carnesale ^{id37}, S. Caron ^{id116}, E. Carquin ^{id140f}, I.B. Carr ^{id107}, S. Carrá ^{id72a}, G. Carratta ^{id24b,24a}, A.M. Carroll ^{id126}, M.P. Casado ^{id13,i}, M. Caspar ^{id49}, F.L. Castillo ^{id4}, L. Castillo Garcia ^{id13}, V. Castillo Gimenez ^{id167}, N.F. Castro ^{id133a,133e}, A. Catinaccio ^{id37}, J.R. Catmore ^{id128}, T. Cavaliere ^{id4}, V. Cavaliere ^{id30}, L.J. Caviedes Betancourt ^{id23b}, Y.C. Cekmecelioglu ^{id49}, E. Celebi ^{id83}, S. Cella ^{id37}, V. Cepaitis ^{id57}, K. Cerny ^{id125}, A.S. Cerqueira ^{id84a}, A. Cerri ^{id150}, L. Cerrito ^{id77a,77b}, F. Cerutti ^{id18a}, B. Cervato ^{id145}, A. Cervelli ^{id24b}, G. Cesarini ^{id54}, S.A. Cetin ^{id83}, P.M. Chabrilat ^{id130}, J. Chan ^{id18a}, W.Y. Chan ^{id157}, J.D. Chapman ^{id33}, E. Chapon ^{id138}, B. Chargeishvili ^{id153b}, D.G. Charlton ^{id21}, C. Chauhan ^{id136}, Y. Che ^{id114a}, S. Chekanov ^{id6}, S.V. Chekulaev ^{id159a}, G.A. Chelkov ^{id40,a}, B. Chen ^{id155}, B. Chen ^{id169}, H. Chen ^{id114a}, H. Chen ^{id30}, J. Chen ^{id63c}, J. Chen ^{id146}, M. Chen ^{id129}, S. Chen ^{id89}, S.J. Chen ^{id114a}, X. Chen ^{id63c}, X. Chen ^{id15,af}, Y. Chen ^{id63a}, C.L. Cheng ^{id174}, H.C. Cheng ^{id65a}, S. Cheong ^{id147}, A. Cheplakov ^{id40}, E. Cheremushkina ^{id49}, E. Cherepanova ^{id117}, R. Cherkaoui El Moursli ^{id36e}, E. Cheu ^{id7}, K. Cheung ^{id66}, L. Chevalier ^{id138}, V. Chiarella ^{id54}, G. Chiarelli ^{id75a}, N. Chiedde ^{id104}, G. Chiodini ^{id71a}, A.S. Chisholm ^{id21}, A. Chitan ^{id28b}, M. Chitishvili ^{id167}, M.V. Chizhov ^{id40,s}, K. Choi ^{id11}, Y. Chou ^{id142}, E.Y.S. Chow ^{id116}, K.L. Chu ^{id173}, M.C. Chu ^{id65a}, X. Chu ^{id14,114c}, Z. Chubinidze ^{id54}, J. Chudoba ^{id134}, J.J. Chwastowski ^{id88}, D. Cieri ^{id112}, K.M. Ciesla ^{id87a}, V. Cindro ^{id95}, A. Ciocio ^{id18a}, F. Ciotto ^{id73a,73b}, Z.H. Citron ^{id173}, M. Citterio ^{id72a}, D.A. Ciubotaru ^{id28b},

A. Clark ⁵⁷, P.J. Clark ⁵³, N. Clarke Hall ⁹⁸, C. Clarry ¹⁵⁸, S.E. Clawson ⁴⁹, C. Clement ^{48a,48b},
 Y. Coadou ¹⁰⁴, M. Cobal ^{70a,70c}, A. Coccaro ^{58b}, R.F. Coelho Barrue ^{133a},
 R. Coelho Lopes De Sa ¹⁰⁵, S. Coelli ^{72a}, L.S. Colangeli ¹⁵⁸, B. Cole ⁴³, J. Collot ⁶¹,
 P. Conde Muiño ^{133a,133g}, M.P. Connell ^{34c}, S.H. Connell ^{34c}, E.I. Conroy ¹²⁹, F. Conventi ^{73a,ah},
 H.G. Cooke ²¹, A.M. Cooper-Sarkar ¹²⁹, F.A. Corchia ^{24b,24a}, A. Cordeiro Oudot Choi ¹³⁰,
 L.D. Corpe ⁴², M. Corradi ^{76a,76b}, F. Corriveau ^{106,aa}, A. Cortes-Gonzalez ¹⁹, M.J. Costa ¹⁶⁷,
 F. Costanza ⁴, D. Costanzo ¹⁴³, B.M. Cote ¹²², J. Couthures ⁴, G. Cowan ⁹⁷, K. Cranmer ¹⁷⁴,
 L. Cremer ⁵⁰, D. Cremonini ^{24b,24a}, S. Crépé-Renaudin ⁶¹, F. Crescioli ¹³⁰, M. Cristinziani ¹⁴⁵,
 M. Cristoforetti ^{79a,79b}, V. Croft ¹¹⁷, J.E. Crosby ¹²⁴, G. Crosetti ^{45b,45a}, A. Cueto ¹⁰¹, H. Cui ⁹⁸,
 Z. Cui ⁷, W.R. Cunningham ⁶⁰, F. Curcio ¹⁶⁷, J.R. Curran ⁵³, P. Czodrowski ³⁷,
 M.J. Da Cunha Sargedas De Sousa ^{58b,58a}, J.V. Da Fonseca Pinto ^{84b}, C. Da Via ¹⁰³,
 W. Dabrowski ^{87a}, T. Dado ³⁷, S. Dahbi ¹⁵², T. Dai ¹⁰⁸, D. Dal Santo ²⁰, C. Dallapiccola ¹⁰⁵,
 M. Dam ⁴⁴, G. D'amen ³⁰, V. D'Amico ¹¹¹, J. Damp ¹⁰², J.R. Dandoy ³⁵, D. Dannheim ³⁷,
 M. Danninger ¹⁴⁶, V. Dao ¹⁴⁹, G. Darbo ^{58b}, S.J. Das ³⁰, F. Dattola ⁴⁹, S. D'Auria ^{72a,72b},
 A. D'Avanzo ^{73a,73b}, T. Davidek ¹³⁶, I. Dawson ⁹⁶, H.A. Day-hall ¹³⁵, K. De ⁸,
 C. De Almeida Rossi ¹⁵⁸, R. De Asmundis ^{73a}, N. De Biase ⁴⁹, S. De Castro ^{24b,24a},
 N. De Groot ¹¹⁶, P. de Jong ¹¹⁷, H. De la Torre ¹¹⁸, A. De Maria ^{114a}, A. De Salvo ^{76a},
 U. De Sanctis ^{77a,77b}, F. De Santis ^{71a,71b}, A. De Santo ¹⁵⁰, J.B. De Vivie De Regie ⁶¹,
 J. Debevc ⁹⁵, D.V. Dedovich ⁴⁰, J. Degens ⁹⁴, A.M. Deiana ⁴⁶, J. Del Peso ¹⁰¹, L. Delagrangé ¹³⁰,
 F. Deliot ¹³⁸, C.M. Delitzsch ⁵⁰, M. Della Pietra ^{73a,73b}, D. Della Volpe ⁵⁷, A. Dell'Acqua ³⁷,
 L. Dell'Asta ^{72a,72b}, M. Delmastro ⁴, C.C. Delogu ¹⁰², P.A. Delsart ⁶¹, S. Demers ¹⁷⁶,
 M. Demichev ⁴⁰, S.P. Denisov ³⁹, H. Denizli ^{22a}, L. D'Eramo ⁴², D. Derendarz ⁸⁸, F. Derue ¹³⁰,
 P. Dervan ⁹⁴, K. Desch ²⁵, C. Deutsch ²⁵, F.A. Di Bello ^{58b,58a}, A. Di Ciaccio ^{77a,77b},
 L. Di Ciaccio ⁴, A. Di Domenico ^{76a,76b}, C. Di Donato ^{73a,73b}, A. Di Girolamo ³⁷,
 G. Di Gregorio ³⁷, A. Di Luca ^{79a,79b}, B. Di Micco ^{78a,78b}, R. Di Nardo ^{78a,78b}, K.F. Di Petrillo ⁴¹,
 M. Diamantopoulou ³⁵, F.A. Dias ¹¹⁷, T. Dias Do Vale ¹⁴⁶, M.A. Diaz ^{140a,140b}, A.R. Didenko ⁴⁰,
 M. Didenko ¹⁶⁷, E.B. Diehl ¹⁰⁸, S. Díez Cornell ⁴⁹, C. Díez Pardos ¹⁴⁵, C. Dimitriadi ¹⁴⁸,
 A. Dimitrievska ²¹, J. Dingfelder ²⁵, T. Dingley ¹²⁹, I-M. Dinu ^{28b}, S.J. Dittmeier ^{64b},
 F. Dittus ³⁷, M. Divisek ¹³⁶, B. Dixit ⁹⁴, F. Djama ¹⁰⁴, T. Djobava ^{153b}, C. Doglioni ^{103,100},
 A. Dohnalova ^{29a}, Z. Dolezal ¹³⁶, K. Domijan ^{87a}, K.M. Dona ⁴¹, M. Donadelli ^{84d},
 B. Dong ¹⁰⁹, J. Donini ⁴², A. D'Onofrio ^{73a,73b}, M. D'Onofrio ⁹⁴, J. Dopke ¹³⁷, A. Doria ^{73a},
 N. Dos Santos Fernandes ^{133a}, P. Dougan ¹⁰³, M.T. Dova ⁹², A.T. Doyle ⁶⁰, M.A. Draguet ¹²⁹,
 M.P. Drescher ⁵⁶, E. Dreyer ¹⁷³, I. Drivas-koulouris ¹⁰, M. Drnevich ¹²⁰, M. Drozdova ⁵⁷,
 D. Du ^{63a}, T.A. du Pree ¹¹⁷, F. Dubinin ³⁹, M. Dubovsky ^{29a}, E. Duchovni ¹⁷³, G. Duckeck ¹¹¹,
 O.A. Ducu ^{28b}, D. Duda ⁵³, A. Dudarev ³⁷, E.R. Duden ²⁷, M. D'uffizi ¹⁰³, L. Duflot ⁶⁷,
 M. Dührssen ³⁷, I. Duminica ^{28g}, A.E. Dumitriu ^{28b}, M. Dunford ^{64a}, S. Dungs ⁵⁰,
 K. Dunne ^{48a,48b}, A. Duperrin ¹⁰⁴, H. Duran Yildiz ^{3a}, M. Düren ⁵⁹, A. Durglishvili ^{153b},
 D. Duvnjak ³⁵, B.L. Dwyer ¹¹⁸, G.I. Dyckes ^{18a}, M. Dyndal ^{87a}, B.S. Dziedzic ³⁷,
 Z.O. Earnshaw ¹⁵⁰, G.H. Eberwein ¹²⁹, B. Eckerova ^{29a}, S. Eggebrecht ⁵⁶,
 E. Egidio Purcino De Souza ^{84e}, L.F. Ehrke ⁵⁷, G. Eigen ¹⁷, K. Einsweiler ^{18a}, T. Ekelof ¹⁶⁵,
 P.A. Ekman ¹⁰⁰, S. El Farkh ^{36b}, Y. El Ghazali ^{63a}, H. El Jarrari ³⁷, A. El Moussaouy ^{36a},
 V. Ellajosyula ¹⁶⁵, M. Ellert ¹⁶⁵, F. Ellinghaus ¹⁷⁵, N. Ellis ³⁷, J. Elmsheuser ³⁰, M. Elsayy ^{119a},
 M. Elsing ³⁷, D. Emeliyanov ¹³⁷, Y. Enari ⁸⁵, I. Ene ^{18a}, S. Epari ¹³, P.A. Erland ⁸⁸,
 D. Ernani Martins Neto ⁸⁸, M. Errenst ¹⁷⁵, M. Escalier ⁶⁷, C. Escobar ¹⁶⁷, E. Etzion ¹⁵⁵,
 G. Evans ^{133a,133b}, H. Evans ⁶⁹, L.S. Evans ⁹⁷, A. Ezhilov ³⁹, S. Ezzarqtouni ^{36a},
 F. Fabbri ^{24b,24a}, L. Fabbri ^{24b,24a}, G. Facini ⁹⁸, V. Fadeyev ¹³⁹, R.M. Fakhrutdinov ³⁹,
 D. Fakoudis ¹⁰², S. Falciano ^{76a}, L.F. Falda Ulhoa Coelho ^{133a}, F. Fallavollita ¹¹²,

G. Falsetti ^{45b,45a}, J. Faltova ¹³⁶, C. Fan ¹⁶⁶, K.Y. Fan ^{65b}, Y. Fan ¹⁴, Y. Fang ^{14,114c}, M. Fanti ^{72a,72b}, M. Faraj ^{70a,70b}, Z. Farazpay ⁹⁹, A. Farbin ⁸, A. Farilla ^{78a}, T. Farooque ¹⁰⁹, J.N. Farr ¹⁷⁶, S.M. Farrington ^{137,53}, F. Fassi ^{36e}, D. Fassouliotis ⁹, M. Faucci Giannelli ^{77a,77b}, W.J. Fawcett ³³, L. Fayard ⁶⁷, P. Federic ¹³⁶, P. Federicova ¹³⁴, O.L. Fedin ^{39,a}, M. Feickert ¹⁷⁴, L. Feligioni ¹⁰⁴, D.E. Fellers ¹²⁶, C. Feng ^{63b}, Z. Feng ¹¹⁷, M.J. Fenton ¹⁶², L. Ferencz ⁴⁹, R.A.M. Ferguson ⁹³, P. Fernandez Martinez ⁴⁸, M.J.V. Fernoux ¹⁰⁴, J. Ferrando ⁹³, A. Ferrari ¹⁶⁵, P. Ferrari ^{117,116}, R. Ferrari ^{74a}, D. Ferrere ⁵⁷, C. Ferretti ¹⁰⁸, M.P. Fewell ¹, D. Fiacco ^{76a,76b}, F. Fiedler ¹⁰², P. Fiedler ¹³⁵, S. Filimonov ³⁹, A. Filipčič ⁹⁵, E.K. Filmer ^{159a}, F. Filthaut ¹¹⁶, M.C.N. Fiolhais ^{133a,133c,c}, L. Fiorini ¹⁶⁷, W.C. Fisher ¹⁰⁹, T. Fitschen ¹⁰³, P.M. Fitzhugh ¹³⁸, I. Fleck ¹⁴⁵, P. Fleischmann ¹⁰⁸, T. Flick ¹⁷⁵, M. Flores ^{34d,ad}, L.R. Flores Castillo ^{65a}, L. Flores Sanz De Acedo ³⁷, F.M. Follega ^{79a,79b}, N. Fomin ³³, J.H. Foo ¹⁵⁸, A. Formica ¹³⁸, A.C. Forti ¹⁰³, E. Fortin ³⁷, A.W. Fortman ^{18a}, L. Fountas ^{9j}, D. Fournier ⁶⁷, H. Fox ⁹³, P. Francavilla ^{75a,75b}, S. Francescato ⁶², S. Franchellucci ⁵⁷, M. Franchini ^{24b,24a}, S. Franchino ^{64a}, D. Francis ³⁷, L. Franco ¹¹⁶, V. Franco Lima ³⁷, L. Franconi ⁴⁹, M. Franklin ⁶², G. Frattari ²⁷, Y.Y. Frid ¹⁵⁵, J. Friend ⁶⁰, N. Fritzsche ³⁷, A. Froch ⁵⁷, D. Froidevaux ³⁷, J.A. Frost ¹²⁹, Y. Fu ¹⁰⁹, S. Fuenzalida Garrido ^{140f}, M. Fujimoto ¹⁰⁴, K.Y. Fung ^{65a}, E. Furtado De Simas Filho ^{84e}, M. Furukawa ¹⁵⁷, J. Fuster ¹⁶⁷, A. Gaa ⁵⁶, A. Gabrielli ^{24b,24a}, A. Gabrielli ¹⁵⁸, P. Gadow ³⁷, G. Gagliardi ^{58b,58a}, L.G. Gagnon ^{18a}, S. Gaid ¹⁶⁴, S. Galantzan ¹⁵⁵, J. Gallagher ¹, E.J. Gallas ¹²⁹, A.L. Gallen ¹⁶⁵, B.J. Gallop ¹³⁷, K.K. Gan ¹²², S. Ganguly ¹⁵⁷, Y. Gao ⁵³, A. Garabaglu ¹⁴², F.M. Garay Walls ^{140a,140b}, B. Garcia ³⁰, C. García ¹⁶⁷, A. Garcia Alonso ¹¹⁷, A.G. Garcia Caffaro ¹⁷⁶, J.E. García Navarro ¹⁶⁷, M. Garcia-Sciveres ^{18a}, G.L. Gardner ¹³¹, R.W. Gardner ⁴¹, N. Garelli ¹⁶¹, R.B. Garg ¹⁴⁷, J.M. Gargan ⁵³, C.A. Garner ¹⁵⁸, C.M. Garvey ^{34a}, V.K. Gassmann ¹⁶¹, G. Gaudio ^{74a}, V. Gautam ¹³, P. Gauzzi ^{76a,76b}, J. Gavranovic ⁹⁵, I.L. Gavrilenko ³⁹, A. Gavrilyuk ³⁹, C. Gay ¹⁶⁸, G. Gaycken ¹²⁶, E.N. Gazis ¹⁰, A. Gekow ¹²², C. Gemme ^{58b}, M.H. Genest ⁶¹, A.D. Gentry ¹¹⁵, S. George ⁹⁷, W.F. George ²¹, T. Geralis ⁴⁷, A.A. Gerwin ¹²³, P. Gessinger-Befurt ³⁷, M.E. Geyik ¹⁷⁵, M. Ghani ¹⁷¹, K. Ghorbanian ⁹⁶, A. Ghosal ¹⁴⁵, A. Ghosh ¹⁶², A. Ghosh ⁷, B. Giacobbe ^{24b}, S. Giagu ^{76a,76b}, T. Giani ¹¹⁷, A. Giannini ^{63a}, S.M. Gibson ⁹⁷, M. Gignac ¹³⁹, D.T. Gil ^{87b}, A.K. Gilbert ^{87a}, B.J. Gilbert ⁴³, D. Gillberg ³⁵, G. Gilles ¹¹⁷, L. Ginabat ¹³⁰, D.M. Gingrich ^{2,ag}, M.P. Giordani ^{70a,70c}, P.F. Giraud ¹³⁸, G. Giugliarelli ^{70a,70c}, D. Giugni ^{72a}, F. Giuli ^{77a,77b}, I. Gkialas ^{9j}, L.K. Gladilin ³⁹, C. Glasman ¹⁰¹, G. Glemža ⁴⁹, M. Glisic ¹²⁶, I. Gnesi ^{45b}, Y. Go ³⁰, M. Goblirsch-Kolb ³⁷, B. Gocke ⁵⁰, D. Godin ¹¹⁰, B. Gokturk ^{22a}, S. Goldfarb ¹⁰⁷, T. Golling ⁵⁷, M.G.D. Gololo ^{34c}, D. Golubkov ³⁹, J.P. Gombas ¹⁰⁹, A. Gomes ^{133a,133b}, G. Gomes Da Silva ¹⁴⁵, A.J. Gomez Delegido ¹⁶⁷, R. Gonçalo ^{133a}, L. Gonella ²¹, A. Gongadze ^{153c}, F. Gonnella ²¹, J.L. Gonski ¹⁴⁷, R.Y. González Andana ⁵³, S. González de la Hoz ¹⁶⁷, R. Gonzalez Lopez ⁹⁴, C. Gonzalez Renteria ^{18a}, M.V. Gonzalez Rodrigues ⁴⁹, R. Gonzalez Suarez ¹⁶⁵, S. Gonzalez-Sevilla ⁵⁷, L. Goossens ³⁷, B. Gorini ³⁷, E. Gorini ^{71a,71b}, A. Gorišek ⁹⁵, T.C. Gosart ¹³¹, A.T. Goshaw ⁵², M.I. Gostkin ⁴⁰, S. Goswami ¹²⁴, C.A. Gottardo ³⁷, S.A. Gotz ¹¹¹, M. Goughri ^{36b}, A.G. Goussiou ¹⁴², N. Govender ^{34c}, R.P. Grabarczyk ¹²⁹, I. Grabowska-Bold ^{87a}, K. Graham ³⁵, E. Gramstad ¹²⁸, S. Grancagnolo ^{71a,71b}, C.M. Grant ^{1,138}, P.M. Gravila ^{28f}, F.G. Gravili ^{71a,71b}, H.M. Gray ^{18a}, M. Greco ¹¹², M.J. Green ¹, C. Grefe ²⁵, A.S. Grefsrud ¹⁷, I.M. Gregor ⁴⁹, K.T. Greif ¹⁶², P. Grenier ¹⁴⁷, S.G. Grewe ¹¹², A.A. Grillo ¹³⁹, K. Grimm ³², S. Grinstein ^{13,w}, J.-F. Grivaz ⁶⁷, E. Gross ¹⁷³, J. Grosse-Knetter ⁵⁶, L. Guan ¹⁰⁸, J.G.R. Guerrero Rojas ¹⁶⁷, G. Guerrieri ³⁷, D. Guest ¹⁹, R. Gugel ¹⁰², J.A.M. Guhit ¹⁰⁸, A. Guida ¹⁹, E. Guilloton ¹⁷¹, S. Guindon ³⁷, F. Guo ^{14,114c}, J. Guo ^{63c}, L. Guo ⁴⁹, L. Guo ^{114b,u}, Y. Guo ¹⁰⁸, A. Gupta ⁵⁰, R. Gupta ¹³², S. Gurbuz ²⁵, S.S. Gurdasani ⁴⁹, G. Gustavino ^{76a,76b}, P. Gutierrez ¹²³,

L.F. Gutierrez Zagazeta ¹³¹, M. Gutsche ⁵¹, C. Gutsche ⁹⁸, C. Gwenlan ¹²⁹, C.B. Gwilliam ⁹⁴,
 E.S. Haaland ¹²⁸, A. Haas ¹²⁰, M. Habedank ⁶⁰, C. Haber ^{18a}, H.K. Hadavand ⁸, A. Hadeif ⁵¹,
 A.I. Hagan ⁹³, J.J. Hahn ¹⁴⁵, E.H. Haines ⁹⁸, M. Haleem ¹⁷⁰, J. Haley ¹²⁴, G.D. Hallowell ¹⁰⁴,
 L. Halser ²⁰, K. Hamano ¹⁶⁹, M. Hamer ²⁵, E.J. Hampshire ⁹⁷, J. Han ^{63b}, L. Han ^{114a},
 L. Han ^{63a}, S. Han ^{18a}, K. Hanagaki ⁸⁵, M. Hance ¹³⁹, D.A. Hangal ⁴³, H. Hanif ¹⁴⁶,
 M.D. Hank ¹³¹, J.B. Hansen ⁴⁴, P.H. Hansen ⁴⁴, D. Harada ⁵⁷, T. Harenberg ¹⁷⁵,
 S. Harkusha ¹⁷⁷, M.L. Harris ¹⁰⁵, Y.T. Harris ²⁵, J. Harrison ¹³, N.M. Harrison ¹²²,
 P.F. Harrison ¹⁷¹, N.M. Hartman ¹¹², N.M. Hartmann ¹¹¹, R.Z. Hasan ^{97,137}, Y. Hasegawa ¹⁴⁴,
 F. Haslbeck ¹²⁹, S. Hassan ¹⁷, R. Hauser ¹⁰⁹, C.M. Hawkes ²¹, R.J. Hawkings ³⁷,
 Y. Hayashi ¹⁵⁷, D. Hayden ¹⁰⁹, C. Hayes ¹⁰⁸, R.L. Hayes ¹¹⁷, C.P. Hays ¹²⁹, J.M. Hays ⁹⁶,
 H.S. Hayward ⁹⁴, F. He ^{63a}, M. He ^{14,114c}, Y. He ⁴⁹, Y. He ⁹⁸, N.B. Heatley ⁹⁶, V. Hedberg ¹⁰⁰,
 A.L. Heggelund ¹²⁸, C. Heidegger ⁵⁵, K.K. Heidegger ⁵⁵, J. Heilman ³⁵, S. Heim ⁴⁹,
 T. Heim ^{18a}, J.G. Heinlein ¹³¹, J.J. Heinrich ¹²⁶, L. Heinrich ^{112,ae}, J. Hejbal ¹³⁴, A. Held ¹⁷⁴,
 S. Hellesund ¹⁷, C.M. Helling ¹⁶⁸, S. Hellman ^{48a,48b}, R.C.W. Henderson ⁹³, L. Henkelmann ³³,
 A.M. Henriques Correia ³⁷, H. Herde ¹⁰⁰, Y. Hernández Jiménez ¹⁴⁹, L.M. Herrmann ²⁵,
 T. Herrmann ⁵¹, G. Herten ⁵⁵, R. Hertenberger ¹¹¹, L. Hervas ³⁷, M.E. Hespings ¹⁰²,
 N.P. Hessey ^{159a}, J. Hessler ¹¹², M. Hidaoui ^{36b}, N. Hidic ¹³⁶, E. Hill ¹⁵⁸, S.J. Hillier ²¹,
 J.R. Hinds ¹⁰⁹, F. Hinterkeuser ²⁵, M. Hirose ¹²⁷, S. Hirose ¹⁶⁰, D. Hirschbuehl ¹⁷⁵,
 T.G. Hitchings ¹⁰³, B. Hiti ⁹⁵, J. Hobbs ¹⁴⁹, R. Hobincu ^{28e}, N. Hod ¹⁷³, M.C. Hodgkinson ¹⁴³,
 B.H. Hodgkinson ¹²⁹, A. Hoecker ³⁷, D.D. Hofer ¹⁰⁸, J. Hofer ¹⁶⁷, M. Holzbock ³⁷,
 L.B.A.H. Hommels ³³, B.P. Honan ¹⁰³, J.J. Hong ⁶⁹, J. Hong ^{63c}, T.M. Hong ¹³²,
 B.H. Hooberman ¹⁶⁶, W.H. Hopkins ⁶, M.C. Hoppesch ¹⁶⁶, Y. Horii ¹¹³, M.E. Horstmann ¹¹²,
 S. Hou ¹⁵², M.R. Housenga ¹⁶⁶, A.S. Howard ⁹⁵, J. Howarth ⁶⁰, J. Hoya ⁶, M. Hrabovsky ¹²⁵,
 T. Hryn'ova ⁴, P.J. Hsu ⁶⁶, S.-C. Hsu ¹⁴², T. Hsu ⁶⁷, M. Hu ^{18a}, Q. Hu ^{63a}, S. Huang ³³,
 X. Huang ^{14,114c}, Y. Huang ¹⁴³, Y. Huang ^{114b}, Y. Huang ¹⁰², Y. Huang ¹⁴, Z. Huang ¹⁰³,
 Z. Hubacek ¹³⁵, M. Huebner ²⁵, F. Huegging ²⁵, T.B. Huffman ¹²⁹,
 M. Hufnagel Maranha De Faria ^{84a}, C.A. Hugli ⁴⁹, M. Huhtinen ³⁷, S.K. Huiberts ¹⁷,
 R. Hulsken ¹⁰⁶, C.E. Hultquist ^{18a}, N. Huseynov ^{12,g}, J. Huston ¹⁰⁹, J. Huth ⁶², R. Hyneman ⁷,
 G. Iacobucci ⁵⁷, G. Iakovidis ³⁰, L. Iconomidou-Fayard ⁶⁷, J.P. Iddon ³⁷, P. Iengo ^{73a,73b},
 R. Iguchi ¹⁵⁷, Y. Iiyama ¹⁵⁷, T. Iizawa ¹²⁹, Y. Ikegami ⁸⁵, D. Iliadis ¹⁵⁶, N. Ilic ¹⁵⁸,
 H. Imam ^{84c}, G. Inacio Goncalves ^{84d}, S.A. Infante Cabanas ^{140c}, T. Ingebretsen Carlson ^{48a,48b},
 J.M. Inglis ⁹⁶, G. Introzzi ^{74a,74b}, M. Iodice ^{78a}, V. Ippolito ^{76a,76b}, R.K. Irwin ⁹⁴, M. Ishino ¹⁵⁷,
 W. Islam ¹⁷⁴, C. Issever ¹⁹, S. Istin ^{22a,al}, H. Ito ¹⁷², R. Iuppa ^{79a,79b}, A. Ivina ¹⁷³, V. Izzo ^{73a},
 P. Jacka ¹³⁴, P. Jackson ¹, C.S. Jagfeld ¹¹¹, G. Jain ^{159a}, P. Jain ⁴⁹, K. Jakobs ⁵⁵,
 T. Jakoubek ¹⁷³, J. Jamieson ⁶⁰, W. Jang ¹⁵⁷, M. Javurkova ¹⁰⁵, P. Jawahar ¹⁰³, L. Jeanty ¹²⁶,
 J. Jejelava ^{153a}, P. Jenni ^{55,f}, C.E. Jessiman ³⁵, C. Jia ^{63b}, H. Jia ¹⁶⁸, J. Jia ¹⁴⁹, X. Jia ^{14,114c},
 Z. Jia ^{114a}, C. Jiang ⁵³, Q. Jiang ^{65b}, S. Jiggins ⁴⁹, J. Jimenez Pena ¹³, S. Jin ^{114a},
 A. Jinaru ^{28b}, O. Jinnouchi ¹⁴¹, P. Johansson ¹⁴³, K.A. Johns ⁷, J.W. Johnson ¹³⁹, F.A. Jolly ⁴⁹,
 D.M. Jones ¹⁵⁰, E. Jones ⁴⁹, K.S. Jones ⁸, P. Jones ³³, R.W.L. Jones ⁹³, T.J. Jones ⁹⁴,
 H.L. Joos ^{56,37}, R. Joshi ¹²², J. Jovicevic ¹⁶, X. Ju ^{18a}, J.J. Junggeburth ³⁷, T. Junkermann ^{64a},
 A. Juste Rozas ^{13,w}, M.K. Juzek ⁸⁸, S. Kabana ^{140e}, A. Kaczmarzka ⁸⁸, M. Kado ¹¹²,
 H. Kagan ¹²², M. Kagan ¹⁴⁷, A. Kahn ¹³¹, C. Kahra ¹⁰², T. Kaji ¹⁵⁷, E. Kajomovitz ¹⁵⁴,
 N. Kakati ¹⁷³, I. Kalaitzidou ⁵⁵, N.J. Kang ¹³⁹, D. Kar ^{34g}, K. Karava ¹²⁹, E. Karentzos ²⁵,
 O. Karkout ¹¹⁷, S.N. Karpov ⁴⁰, Z.M. Karpova ⁴⁰, V. Kartvelishvili ⁹³, A.N. Karyukhin ³⁹,
 E. Kasimi ¹⁵⁶, J. Katzy ⁴⁹, S. Kaur ³⁵, K. Kawade ¹⁴⁴, M.P. Kawale ¹²³, C. Kawamoto ⁸⁹,
 T. Kawamoto ^{63a}, E.F. Kay ³⁷, F.I. Kaya ¹⁶¹, S. Kazakos ¹⁰⁹, V.F. Kazanin ³⁹, Y. Ke ¹⁴⁹,
 J.M. Keaveney ^{34a}, R. Keeler ¹⁶⁹, G.V. Kehris ⁶², J.S. Keller ³⁵, J.J. Kempster ¹⁵⁰, O. Kepka ¹³⁴,

J. Kerr ^{159b}, B.P. Kerridge ¹³⁷, B.P. Kerševan ⁹⁵, L. Keszeghova ^{29a}, R.A. Khan ¹³², A. Khanov ¹²⁴, A.G. Kharlamov ³⁹, T. Kharlamova ³⁹, E.E. Khoda ¹⁴², M. Kholodenko ^{133a}, T.J. Khoo ¹⁹, G. Khorialuli ¹⁷⁰, J. Khubua ^{153b,*}, Y.A.R. Khwaira ¹³⁰, B. Kibirige ^{34g}, D. Kim ⁶, D.W. Kim ^{48a,48b}, Y.K. Kim ⁴¹, N. Kimura ⁹⁸, M.K. Kingston ⁵⁶, A. Kirchhoff ⁵⁶, C. Kirfel ²⁵, F. Kirfel ²⁵, J. Kirk ¹³⁷, A.E. Kiryunin ¹¹², S. Kita ¹⁶⁰, C. Kitsaki ¹⁰, O. Kivernyk ²⁵, M. Klassen ¹⁶¹, C. Klein ³⁵, L. Klein ¹⁷⁰, M.H. Klein ⁴⁶, S.B. Klein ⁵⁷, U. Klein ⁹⁴, A. Klimentov ³⁰, T. Klioutchnikova ³⁷, P. Kluit ¹¹⁷, S. Kluth ¹¹², E. Kneringer ⁸⁰, T.M. Knight ¹⁵⁸, A. Knue ⁵⁰, D. Kobylanskii ¹⁷³, S.F. Koch ¹²⁹, M. Kocian ¹⁴⁷, P. Kodyš ¹³⁶, D.M. Koeck ¹²⁶, P.T. Koenig ²⁵, T. Koffas ³⁵, O. Kolay ⁵¹, I. Koletsou ⁴, T. Komarek ⁸⁸, K. Köneke ⁵⁶, A.X.Y. Kong ¹, T. Kono ¹²¹, N. Konstantinidis ⁹⁸, P. Kontaxakis ⁵⁷, B. Konya ¹⁰⁰, R. Kopeliansky ⁴³, S. Koperny ^{87a}, K. Korcyl ⁸⁸, K. Kordas ^{156,e}, A. Korn ⁹⁸, S. Korn ⁵⁶, I. Korolkov ¹³, N. Korotkova ³⁹, B. Kortman ¹¹⁷, O. Kortner ¹¹², S. Kortner ¹¹², W.H. Kostecka ¹¹⁸, V.V. Kostyukhin ¹⁴⁵, A. Kotsokechagia ³⁷, A. Kotwal ⁵², A. Koulouris ³⁷, A. Kourkoumeli-Charalampidi ^{74a,74b}, C. Kourkoumelis ⁹, E. Kourlitis ¹¹², O. Kovanda ¹²⁶, R. Kowalewski ¹⁶⁹, W. Kozanecki ¹²⁶, A.S. Kozhin ³⁹, V.A. Kramarenko ³⁹, G. Kramberger ⁹⁵, P. Kramer ²⁵, M.W. Krasny ¹³⁰, A. Krasznahorkay ¹⁰⁵, A.C. Kraus ¹¹⁸, J.W. Kraus ¹⁷⁵, J.A. Kremer ⁴⁹, T. Kresse ⁵¹, L. Kretschmann ¹⁷⁵, J. Kretzschmar ⁹⁴, K. Kreul ¹⁹, P. Krieger ¹⁵⁸, K. Krizka ²¹, K. Kroeninger ⁵⁰, H. Kroha ¹¹², J. Kroll ¹³⁴, J. Kroll ¹³¹, K.S. Krowpman ¹⁰⁹, U. Kruchonak ⁴⁰, H. Krüger ²⁵, N. Krumnack ⁸², M.C. Kruse ⁵², O. Kuchinskaia ³⁹, S. Kuday ^{3a}, S. Kuehn ³⁷, R. Kuesters ⁵⁵, T. Kuhl ⁴⁹, V. Kukhtin ⁴⁰, Y. Kulchitsky ⁴⁰, S. Kuleshov ^{140d,140b}, M. Kumar ^{34g}, N. Kumari ⁴⁹, P. Kumari ^{159b}, A. Kupco ¹³⁴, T. Kupfer ⁵⁰, A. Kupich ³⁹, O. Kuprash ⁵⁵, H. Kurashige ⁸⁶, L.L. Kurchaninov ^{159a}, O. Kurdysh ⁶⁷, Y.A. Kurochkin ³⁸, A. Kurova ³⁹, M. Kuze ¹⁴¹, A.K. Kvam ¹⁰⁵, J. Kvita ¹²⁵, N.G. Kyriacou ¹⁰⁸, L.A.O. Laatu ¹⁰⁴, C. Lacasta ¹⁶⁷, F. Lacava ^{76a,76b}, H. Lacker ¹⁹, D. Lacour ¹³⁰, N.N. Lad ⁹⁸, E. Ladygin ⁴⁰, A. Lafarge ⁴², B. Laforge ¹³⁰, T. Lagouri ¹⁷⁶, F.Z. Lahbabi ^{36a}, S. Lai ⁵⁶, J.E. Lambert ¹⁶⁹, S. Lammers ⁶⁹, W. Lampl ⁷, C. Lampoudis ^{156,e}, G. Lamprinoudis ¹⁰², A.N. Lancaster ¹¹⁸, E. Lançon ³⁰, U. Landgraf ⁵⁵, M.P.J. Landon ⁹⁶, V.S. Lang ⁵⁵, O.K.B. Langrekken ¹²⁸, A.J. Lankford ¹⁶², F. Lanni ³⁷, K. Lantzsche ²⁵, A. Lanza ^{74a}, M. Lanzac Berrocal ¹⁶⁷, J.F. Laporte ¹³⁸, T. Lari ^{72a}, F. Lasagni Manghi ^{24b}, M. Lassnig ³⁷, V. Latonova ¹³⁴, S.D. Lawlor ¹⁴³, Z. Lawrence ¹⁰³, R. Lazaridou ¹⁷¹, M. Lazzaroni ^{72a,72b}, H.D.M. Le ¹⁰⁹, E.M. Le Boulicaut ¹⁷⁶, L.T. Le Pottier ^{18a}, B. Leban ^{24b,24a}, M. LeBlanc ¹⁰³, F. Ledroit-Guillon ⁶¹, S.C. Lee ¹⁵², T.F. Lee ⁹⁴, L.L. Leeuw ^{34c,aj}, M. Lefebvre ¹⁶⁹, C. Leggett ^{18a}, G. Lehmann Miotto ³⁷, M. Leigh ⁵⁷, W.A. Leight ¹⁰⁵, W. Leinonen ¹¹⁶, A. Leisos ^{156,t}, M.A.L. Leite ^{84c}, C.E. Leitgeb ¹⁹, R. Leitner ¹³⁶, K.J.C. Leney ⁴⁶, T. Lenz ²⁵, S. Leone ^{75a}, C. Leonidopoulos ⁵³, A. Leopold ¹⁴⁸, R. Les ¹⁰⁹, C.G. Lester ³³, M. Levchenko ³⁹, J. Levêque ⁴, L.J. Levinson ¹⁷³, G. Levriani ^{24b,24a}, M.P. Lewicki ⁸⁸, C. Lewis ¹⁴², D.J. Lewis ⁴, L. Lewitt ¹⁴³, A. Li ³⁰, B. Li ^{63b}, C. Li ¹⁰⁸, C-Q. Li ¹¹², H. Li ^{63a}, H. Li ^{63b}, H. Li ^{114a}, H. Li ¹⁵, H. Li ^{63b}, J. Li ^{63c}, K. Li ¹⁴, L. Li ^{63c}, R. Li ¹⁷⁶, S. Li ^{14,114c}, S. Li ^{63d,63c,d}, T. Li ⁵, X. Li ¹⁰⁶, Z. Li ¹⁵⁷, Z. Li ^{14,114c}, Z. Li ^{63a}, S. Liang ^{14,114c}, Z. Liang ¹⁴, M. Liberatore ¹³⁸, B. Liberti ^{77a}, K. Lie ^{65c}, J. Lieber Marin ^{84e}, H. Lien ⁶⁹, H. Lin ¹⁰⁸, L. Linden ¹¹¹, R.E. Lindley ⁷, J.H. Lindon ², J. Ling ⁶², E. Lipeles ¹³¹, A. Lipniacka ¹⁷, A. Lister ¹⁶⁸, J.D. Little ⁶⁹, B. Liu ¹⁴, B.X. Liu ^{114b}, D. Liu ^{63d,63c}, E.H.L. Liu ²¹, J.K.K. Liu ³³, K. Liu ^{63d}, K. Liu ^{63d,63c}, M. Liu ^{63a}, M.Y. Liu ^{63a}, P. Liu ¹⁴, Q. Liu ^{63d,142,63c}, X. Liu ^{63a}, X. Liu ^{63b}, Y. Liu ^{114b,114c}, Y.L. Liu ^{63b}, Y.W. Liu ^{63a}, S.L. Lloyd ⁹⁶, E.M. Lobodzinska ⁴⁹, P. Loch ⁷, E. Lodhi ¹⁵⁸, T. Lohse ¹⁹, K. Lohwasser ¹⁴³, E. Loiacono ⁴⁹, J.D. Lomas ²¹, J.D. Long ⁴³, I. Longarini ¹⁶², R. Longo ¹⁶⁶, A. Lopez Solis ⁴⁹, N.A. Lopez-canelas ⁷, N. Lorenzo Martinez ⁴, A.M. Lory ¹¹¹, M. Losada ^{119a},

G. Löschcke Centeno ^{id150}, O. Loseva ^{id39}, X. Lou ^{id48a,48b}, X. Lou ^{id14,114c}, A. Lounis ^{id67}, P.A. Love ^{id93}, G. Lu ^{id14,114c}, M. Lu ^{id67}, S. Lu ^{id131}, Y.J. Lu ^{id152}, H.J. Lubatti ^{id142}, C. Luci ^{id76a,76b}, F.L. Lucio Alves ^{id114a}, F. Luehring ^{id69}, O. Lukianchuk ^{id67}, B.S. Lunday ^{id131}, O. Lundberg ^{id148}, B. Lund-Jensen ^{id148,*}, N.A. Luongo ^{id6}, M.S. Lutz ^{id37}, A.B. Lux ^{id26}, D. Lynn ^{id30}, R. Lysak ^{id134}, E. Lytken ^{id100}, V. Lyubushkin ^{id40}, T. Lyubushkina ^{id40}, M.M. Lyukova ^{id149}, M.Firdaus M. Soberi ^{id53}, H. Ma ^{id30}, K. Ma ^{id63a}, L.L. Ma ^{id63b}, W. Ma ^{id63a}, Y. Ma ^{id124}, J.C. MacDonald ^{id102}, P.C. Machado De Abreu Farias ^{id84e}, R. Madar ^{id42}, T. Madula ^{id98}, J. Maeda ^{id86}, T. Maeno ^{id30}, P.T. Mafa ^{id34c,k}, H. Maguire ^{id143}, V. Maiboroda ^{id138}, A. Maio ^{id133a,133b,133d}, K. Maj ^{id87a}, O. Majersky ^{id49}, S. Majewski ^{id126}, R. Makhmanazarov ^{id39}, N. Makovec ^{id67}, V. Maksimovic ^{id16}, B. Malaescu ^{id130}, Pa. Malecki ^{id88}, V.P. Maleev ^{id39}, F. Malek ^{id61,o}, M. Mali ^{id95}, D. Malito ^{id97}, U. Mallik ^{id81,*}, S. Maltezos ^{id10}, S. Malyukov ^{id40}, J. Mamuzic ^{id13}, G. Mancini ^{id54}, M.N. Mancini ^{id27}, G. Manco ^{id74a,74b}, J.P. Mandalia ^{id96}, S.S. Mandarry ^{id150}, I. Mandić ^{id95}, L. Manhaes de Andrade Filho ^{id84a}, I.M. Maniatis ^{id173}, J. Manjarres Ramos ^{id91}, D.C. Mankad ^{id173}, A. Mann ^{id111}, S. Manzoni ^{id37}, L. Mao ^{id63c}, X. Mapekula ^{id34c}, A. Marantis ^{id156,t}, G. Marchiori ^{id5}, M. Marcisovsky ^{id134}, C. Marcon ^{id72a}, M. Marinescu ^{id21}, S. Marium ^{id49}, M. Marjanovic ^{id123}, A. Markhoos ^{id55}, M. Markovitch ^{id67}, M.K. Maroun ^{id105}, E.J. Marshall ^{id93}, Z. Marshall ^{id18a}, S. Marti-Garcia ^{id167}, J. Martin ^{id98}, T.A. Martin ^{id137}, V.J. Martin ^{id53}, B. Martin dit Latour ^{id17}, L. Martinelli ^{id76a,76b}, M. Martinez ^{id13,w}, P. Martinez Agullo ^{id167}, V.I. Martinez Outschoorn ^{id105}, P. Martinez Suarez ^{id13}, S. Martin-Haugh ^{id137}, G. Martinovicova ^{id136}, V.S. Martoiu ^{id28b}, A.C. Martyniuk ^{id98}, A. Marzin ^{id37}, D. Mascione ^{id79a,79b}, L. Masetti ^{id102}, J. Masik ^{id103}, A.L. Maslennikov ^{id39}, S.L. Mason ^{id43}, P. Massarotti ^{id73a,73b}, P. Mastrandrea ^{id75a,75b}, A. Mastroberardino ^{id45b,45a}, T. Masubuchi ^{id127}, T.T. Mathew ^{id126}, J. Matousek ^{id136}, D.M. Mattern ^{id50}, J. Maurer ^{id28b}, T. Maurin ^{id60}, A.J. Maury ^{id67}, B. Maček ^{id95}, D.A. Maximov ^{id39}, A.E. May ^{id103}, R. Mazini ^{id34g}, I. Maznas ^{id118}, M. Mazza ^{id109}, S.M. Mazza ^{id139}, E. Mazzeo ^{id72a,72b}, J.P. Mc Gowan ^{id169}, S.P. Mc Kee ^{id108}, C.A. Mc Lean ^{id6}, C.C. McCracken ^{id168}, E.F. McDonald ^{id107}, A.E. McDougall ^{id117}, L.F. Mcelhinney ^{id93}, J.A. Mcfayden ^{id150}, R.P. McGovern ^{id131}, R.P. McKenzie ^{id34g}, T.C. McLachlan ^{id49}, D.J. McLaughlin ^{id98}, S.J. McMahon ^{id137}, C.M. Mcpartland ^{id94}, R.A. McPherson ^{id169,aa}, S. Mehlhase ^{id111}, A. Mehta ^{id94}, D. Melini ^{id167}, B.R. Mellado Garcia ^{id34g}, A.H. Melo ^{id56}, F. Meloni ^{id49}, A.M. Mendes Jacques Da Costa ^{id103}, H.Y. Meng ^{id158}, L. Meng ^{id93}, S. Menke ^{id112}, M. Mentink ^{id37}, E. Meoni ^{id45b,45a}, G. Mercado ^{id118}, S. Merianos ^{id156}, C. Merlassino ^{id70a,70c}, C. Meroni ^{id72a,72b}, J. Metcalfe ^{id6}, A.S. Mete ^{id6}, E. Meuser ^{id102}, C. Meyer ^{id69}, J-P. Meyer ^{id138}, R.P. Middleton ^{id137}, L. Mijović ^{id53}, G. Mikenberg ^{id173}, M. Mikestikova ^{id134}, M. Mikuž ^{id95}, H. Mildner ^{id102}, A. Milic ^{id37}, D.W. Miller ^{id41}, E.H. Miller ^{id147}, L.S. Miller ^{id35}, A. Milov ^{id173}, D.A. Milstead ^{id48a,48b}, T. Min ^{id114a}, A.A. Minaenko ^{id39}, I.A. Minashvili ^{id153b}, A.I. Mincer ^{id120}, B. Mindur ^{id87a}, M. Mineev ^{id40}, Y. Mino ^{id89}, L.M. Mir ^{id13}, M. Miralles Lopez ^{id60}, M. Mironova ^{id18a}, M.C. Missio ^{id116}, A. Mitra ^{id171}, V.A. Mitsou ^{id167}, Y. Mitsumori ^{id113}, O. Miu ^{id158}, P.S. Miyagawa ^{id96}, T. Mkrtchyan ^{id64a}, M. Mlinarevic ^{id98}, T. Mlinarevic ^{id98}, M. Mlynarikova ^{id37}, S. Mobius ^{id20}, P. Mogg ^{id111}, M.H. Mohamed Farook ^{id115}, A.F. Mohammed ^{id14,114c}, S. Mohapatra ^{id43}, G. Mokgatitswane ^{id34g}, L. Moleri ^{id173}, B. Mondal ^{id145}, S. Mondal ^{id135}, K. Mönig ^{id49}, E. Monnier ^{id104}, L. Monsonis Romero ^{id167}, J. Montejo Berlingen ^{id13}, A. Montella ^{id48a,48b}, M. Montella ^{id122}, F. Montekali ^{id78a,78b}, F. Monticelli ^{id92}, S. Monzani ^{id70a,70c}, A. Morancho Tarda ^{id44}, N. Morange ^{id67}, A.L. Moreira De Carvalho ^{id49}, M. Moreno Llácer ^{id167}, C. Moreno Martinez ^{id57}, J.M. Moreno Perez ^{id23b}, P. Morettini ^{id58b}, S. Morgenstern ^{id37}, M. Morii ^{id62}, M. Morinaga ^{id157}, M. Moritsu ^{id90}, F. Morodei ^{id76a,76b}, P. Moschovakos ^{id37}, B. Moser ^{id129}, M. Mosidze ^{id153b}, T. Moskalets ^{id46}, P. Moskvitina ^{id116}, J. Moss ^{id32,1}, P. Moszkowicz ^{id87a}, A. Moussa ^{id36d}, Y. Moyal ^{id173}, E.J.W. Moyse ^{id105}, O. Mtintsilana ^{id34g}, S. Muanza ^{id104}, J. Mueller ^{id132}, D. Muenstermann ^{id93},

R. Müller ³⁷, G.A. Mullier ¹⁶⁵, A.J. Mullin³³, J.J. Mullin¹³¹, A.E. Mulski ⁶², D.P. Mungo ¹⁵⁸, D. Munoz Perez ¹⁶⁷, F.J. Munoz Sanchez ¹⁰³, M. Murin ¹⁰³, W.J. Murray ^{171,137}, M. Muškinja ⁹⁵, C. Mwewa ³⁰, A.G. Myagkov ^{39,a}, A.J. Myers ⁸, G. Myers ¹⁰⁸, M. Myska ¹³⁵, B.P. Nachman ^{18a}, K. Nagai ¹²⁹, K. Nagano ⁸⁵, R. Nagasaka¹⁵⁷, J.L. Nagle ^{30,ai}, E. Nagy ¹⁰⁴, A.M. Nairz ³⁷, Y. Nakahama ⁸⁵, K. Nakamura ⁸⁵, K. Nakkalil ⁵, H. Nanjo ¹²⁷, E.A. Narayanan ⁴⁶, Y. Narukawa ¹⁵⁷, I. Naryshkin ³⁹, L. Nasella ^{72a,72b}, S. Nasri ^{119b}, C. Nass ²⁵, G. Navarro ^{23a}, J. Navarro-Gonzalez ¹⁶⁷, A. Nayaz ¹⁹, P.Y. Nechaeva ³⁹, S. Nechaeva ^{24b,24a}, F. Nechansky ¹³⁴, L. Nedic ¹²⁹, T.J. Neep ²¹, A. Negri ^{74a,74b}, M. Negrini ^{24b}, C. Nellist ¹¹⁷, C. Nelson ¹⁰⁶, K. Nelson ¹⁰⁸, S. Nemecek ¹³⁴, M. Nessi ^{37,h}, M.S. Neubauer ¹⁶⁶, F. Neuhaus ¹⁰², J. Newell ⁹⁴, P.R. Newman ²¹, Y.W.Y. Ng ¹⁶⁶, B. Ngair ^{119a}, H.D.N. Nguyen ¹¹⁰, R.B. Nickerson ¹²⁹, R. Nicolaidou ¹³⁸, J. Nielsen ¹³⁹, M. Niemeyer ⁵⁶, J. Niermann ³⁷, N. Nikiforou ³⁷, V. Nikolaenko ^{39,a}, I. Nikolic-Audit ¹³⁰, P. Nilsson ³⁰, I. Ninca ⁴⁹, G. Ninio ¹⁵⁵, A. Nisati ^{76a}, N. Nishu ², R. Nisius ¹¹², N. Nitika ^{70a,70c}, J-E. Nitschke ⁵¹, E.K. Nkadimeng ^{34g}, T. Nobe ¹⁵⁷, T. Nommensen ¹⁵¹, M.B. Norfolk ¹⁴³, B.J. Norman ³⁵, M. Noury ^{36a}, J. Novak ⁹⁵, T. Novak ⁹⁵, R. Novotny ¹¹⁵, L. Nozka ¹²⁵, K. Ntekas ¹⁶², N.M.J. Nunes De Moura Junior ^{84b}, J. Ocariz ¹³⁰, A. Ochi ⁸⁶, I. Ochoa ^{133a}, S. Oerdek ^{49,x}, J.T. Offermann ⁴¹, A. Ogrodnik ¹³⁶, A. Oh ¹⁰³, C.C. Ohm ¹⁴⁸, H. Oide ⁸⁵, R. Oishi ¹⁵⁷, M.L. Ojeda ³⁷, Y. Okumura ¹⁵⁷, L.F. Oleiro Seabra ^{133a}, I. Oleksiyuk ⁵⁷, S.A. Olivares Pino ^{140d}, G. Oliveira Correa ¹³, D. Oliveira Damazio ³⁰, J.L. Oliver ¹⁶², Ö.O. Öncel ⁵⁵, A.P. O'Neill ²⁰, A. Onofre ^{133a,133e}, P.U.E. Onyisi ¹¹, M.J. Oreglia ⁴¹, D. Orestano ^{78a,78b}, R.S. Orr ¹⁵⁸, L.M. Osojnak ¹³¹, Y. Osumi ¹¹³, G. Otero y Garzon ³¹, H. Otono ⁹⁰, P.S. Ott ^{64a}, G.J. Ottino ^{18a}, M. Ouchrif ^{36d}, F. Ould-Saada ¹²⁸, T. Ovsianikova ¹⁴², M. Owen ⁶⁰, R.E. Owen ¹³⁷, V.E. Ozcan ^{22a}, F. Ozturk ⁸⁸, N. Ozturk ⁸, S. Ozturk ⁸³, H.A. Pacey ¹²⁹, A. Pacheco Pages ¹³, C. Padilla Aranda ¹³, G. Padovano ^{76a,76b}, S. Pagan Griso ^{18a}, G. Palacino ⁶⁹, A. Palazzo ^{71a,71b}, J. Pampel ²⁵, J. Pan ¹⁷⁶, T. Pan ^{65a}, D.K. Panchal ¹¹, C.E. Pandini ¹¹⁷, J.G. Panduro Vazquez ¹³⁷, H.D. Pandya ¹, H. Pang ¹³⁸, P. Pani ⁴⁹, G. Panizzo ^{70a,70c}, L. Panwar ¹³⁰, L. Paolozzi ⁵⁷, S. Parajuli ¹⁶⁶, A. Paramonov ⁶, C. Paraskevopoulos ⁵⁴, D. Paredes Hernandez ^{65b}, A. Pareti ^{74a,74b}, K.R. Park ⁴³, T.H. Park ¹¹², F. Parodi ^{58b,58a}, J.A. Parsons ⁴³, U. Parzefall ⁵⁵, B. Pascual Dias ¹¹⁰, L. Pascual Dominguez ¹⁰¹, E. Pasqualucci ^{76a}, S. Passaggio ^{58b}, F. Pastore ⁹⁷, P. Patel ⁸⁸, U.M. Patel ⁵², J.R. Pater ¹⁰³, T. Pauly ³⁷, F. Pauwels ¹³⁶, C.I. Pazos ¹⁶¹, M. Pedersen ¹²⁸, R. Pedro ^{133a}, S.V. Peleganchuk ³⁹, O. Penc ³⁷, E.A. Pender ⁵³, S. Peng ¹⁵, G.D. Penn ¹⁷⁶, K.E. Penski ¹¹¹, M. Penzin ³⁹, B.S. Peralva ^{84d}, A.P. Pereira Peixoto ¹⁴², L. Pereira Sanchez ¹⁴⁷, D.V. Perepelitsa ^{30,ai}, G. Perera ¹⁰⁵, E. Perez Codina ^{159a}, M. Perganti ¹⁰, H. Pernegger ³⁷, S. Perrella ^{76a,76b}, O. Perrin ⁴², K. Peters ⁴⁹, R.F.Y. Peters ¹⁰³, B.A. Petersen ³⁷, T.C. Petersen ⁴⁴, E. Petit ¹⁰⁴, V. Petousis ¹³⁵, C. Petridou ^{156,e}, T. Petru ¹³⁶, A. Petrukhin ¹⁴⁵, M. Pettee ^{18a}, A. Petukhov ⁸³, K. Petukhova ³⁷, R. Pezoa ^{140f}, L. Pezzotti ³⁷, G. Pezzullo ¹⁷⁶, A.J. Pfleger ³⁷, T.M. Pham ¹⁷⁴, T. Pham ¹⁰⁷, P.W. Phillips ¹³⁷, G. Piacquadio ¹⁴⁹, E. Pianori ^{18a}, F. Piazza ¹²⁶, R. Piegaia ³¹, D. Pietreanu ^{28b}, A.D. Pilkington ¹⁰³, M. Pinamonti ^{70a,70c}, J.L. Pinfeld ², B.C. Pinheiro Pereira ^{133a}, J. Pinol Bel ¹³, A.E. Pinto Pinoargote ^{138,138}, L. Pintucci ^{70a,70c}, K.M. Piper ¹⁵⁰, A. Pirttikoski ⁵⁷, D.A. Pizzi ³⁵, L. Pizzimento ^{65b}, M.-A. Pleier ³⁰, V. Pleskot ¹³⁶, E. Plotnikova ⁴⁰, G. Poddar ⁹⁶, R. Poettgen ¹⁰⁰, L. Poggioli ¹³⁰, S. Polacek ¹³⁶, G. Polesello ^{74a}, A. Poley ^{146,159a}, A. Polini ^{24b}, C.S. Pollard ¹⁷¹, Z.B. Pollock ¹²², E. Pompa Pacchi ¹²³, N.I. Pond ⁹⁸, D. Ponomarenko ⁶⁹, L. Pontecorvo ³⁷, S. Popa ^{28a}, G.A. Popeneciu ^{28d}, A. Poreba ³⁷, D.M. Portillo Quintero ^{159a}, S. Pospisil ¹³⁵, M.A. Postill ¹⁴³, P. Postolache ^{28c}, K. Potamianos ¹⁷¹, P.A. Potepa ^{87a}, I.N. Potrap ⁴⁰, C.J. Potter ³³, H. Potti ¹⁵¹, J. Poveda ¹⁶⁷, M.E. Pozo Astigarraga ³⁷, A. Prades Ibanez ^{77a,77b}, J. Pretel ¹⁶⁹, D. Price ¹⁰³,

M. Primavera ^{71a}, L. Primomo ^{70a,70c}, M.A. Principe Martin ¹⁰¹, R. Privara ¹²⁵, T. Procter ⁶⁰,
M.L. Proffitt ¹⁴², N. Proklova ¹³¹, K. Prokofiev ^{65c}, G. Proto ¹¹², J. Proudfoot ⁶,
M. Przybycien ^{87a}, W.W. Przygoda ^{87b}, A. Psallidas ⁴⁷, J.E. Puddefoot ¹⁴³, D. Pudzha ⁵⁵,
D. Pyatiizbyantseva ³⁹, J. Qian ¹⁰⁸, R. Qian ¹⁰⁹, D. Qichen ¹⁰³, Y. Qin ¹³, T. Qiu ⁵³,
A. Quadt ⁵⁶, M. Queitsch-Maitland ¹⁰³, G. Quetant ⁵⁷, R.P. Quinn ¹⁶⁸, G. Rabanal Bolanos ⁶²,
D. Rafanoharana ⁵⁵, F. Raffaeli ^{77a,77b}, F. Ragusa ^{72a,72b}, J.L. Rainbolt ⁴¹, J.A. Raine ⁵⁷,
S. Rajagopalan ³⁰, E. Ramakoti ³⁹, L. Rambelli ^{58b,58a}, I.A. Ramirez-Berend ³⁵, K. Ran ^{49,114c},
D.S. Rankin ¹³¹, N.P. Rapheeha ^{34g}, H. Rasheed ^{28b}, V. Raskina ¹³⁰, D.F. Rassloff ^{64a},
A. Rastogi ^{18a}, S. Rave ¹⁰², S. Ravera ^{58b,58a}, B. Ravina ³⁷, I. Ravinovich ¹⁷³, M. Raymond ³⁷,
A.L. Read ¹²⁸, N.P. Readioff ¹⁴³, D.M. Rebuzzi ^{74a,74b}, A.S. Reed ¹¹², K. Reeves ²⁷,
J.A. Reidelsturz ¹⁷⁵, D. Reikher ¹²⁶, A. Rej ⁵⁰, C. Rembser ³⁷, H. Ren ^{63a}, M. Renda ^{28b},
F. Renner ⁴⁹, A.G. Rennie ¹⁶², A.L. Rescia ⁴⁹, S. Resconi ^{72a}, M. Ressegotti ^{58b,58a}, S. Rettie ³⁷,
W.F. Rettie ³⁵, J.G. Reyes Rivera ¹⁰⁹, E. Reynolds ^{18a}, O.L. Rezanova ³⁹, P. Reznicek ¹³⁶,
H. Riani ^{36d}, N. Ribaric ⁵², E. Ricci ^{79a,79b}, R. Richter ¹¹², S. Richter ^{48a,48b}, E. Richter-Was ^{87b},
M. Ridel ¹³⁰, S. Ridouani ^{36d}, P. Rieck ¹²⁰, P. Riedler ³⁷, E.M. Riefel ^{48a,48b}, J.O. Rieger ¹¹⁷,
M. Rijssenbeek ¹⁴⁹, M. Rimoldi ³⁷, L. Rinaldi ^{24b,24a}, P. Rincke ^{56,165}, M.P. Rinnagel ¹¹¹,
G. Ripellino ¹⁶⁵, I. Riu ¹³, J.C. Rivera Vergara ¹⁶⁹, F. Rizatdinova ¹²⁴, E. Rizvi ⁹⁶,
B.R. Roberts ^{18a}, S.S. Roberts ¹³⁹, D. Robinson ³³, M. Robles Manzano ¹⁰², A. Robson ⁶⁰,
A. Rocchi ^{77a,77b}, C. Roda ^{75a,75b}, S. Rodriguez Bosca ³⁷, Y. Rodriguez Garcia ^{23a},
A.M. Rodríguez Vera ¹¹⁸, S. Roe ³⁷, J.T. Roemer ³⁷, O. Røhne ¹²⁸, R.A. Rojas ³⁷,
C.P.A. Roland ¹³⁰, J. Roloff ³⁰, A. Romaniouk ⁸⁰, E. Romano ^{74a,74b}, M. Romano ^{24b},
A.C. Romero Hernandez ¹⁶⁶, N. Rompotis ⁹⁴, L. Roos ¹³⁰, S. Rosati ^{76a}, B.J. Rosser ⁴¹,
E. Rossi ¹²⁹, E. Rossi ^{73a,73b}, L.P. Rossi ⁶², L. Rossini ⁵⁵, R. Rosten ¹²², M. Rotaru ^{28b},
B. Rottler ⁵⁵, C. Rougier ⁹¹, D. Rousseau ⁶⁷, D. Rousso ⁴⁹, S. Roy-Garand ¹⁵⁸, A. Rozanov ¹⁰⁴,
Z.M.A. Rozario ⁶⁰, Y. Rozen ¹⁵⁴, A. Rubio Jimenez ¹⁶⁷, V.H. Ruelas Rivera ¹⁹, T.A. Ruggeri ¹,
A. Ruggiero ¹²⁹, A. Ruiz-Martinez ¹⁶⁷, A. Rummler ³⁷, G.B. Rupnik Boero ³⁷, Z. Rurikova ⁵⁵,
N.A. Rusakovich ⁴⁰, H.L. Russell ¹⁶⁹, G. Russo ^{76a,76b}, J.P. Rutherford ⁷,
S. Rutherford Colmenares ³³, M. Rybar ¹³⁶, E.B. Rye ¹²⁸, A. Ryzhov ⁴⁶, J.A. Sabater Iglesias ⁵⁷,
H.F.W. Sadrozinski ¹³⁹, F. Safai Tehrani ^{76a}, S. Saha ¹, M. Sahinsoy ⁸³, A. Saibel ¹⁶⁷,
M. Saimpert ¹³⁸, M. Saito ¹⁵⁷, T. Saito ¹⁵⁷, A. Sala ^{72a,72b}, D. Salamani ³⁷, A. Salnikov ¹⁴⁷,
J. Salt ¹⁶⁷, A. Salvador Salas ¹⁵⁵, D. Salvatore ^{45b,45a}, F. Salvatore ¹⁵⁰, A. Salzburger ³⁷,
D. Sammel ⁵⁵, E. Sampson ⁹³, D. Sampsonidis ^{156,e}, D. Sampsonidou ¹²⁶, J. Sánchez ¹⁶⁷,
V. Sanchez Sebastian ¹⁶⁷, H. Sandaker ¹²⁸, C.O. Sander ⁴⁹, J.A. Sandesara ¹⁰⁵, M. Sandhoff ¹⁷⁵,
C. Sandoval ^{23b}, L. Sanfilippo ^{64a}, D.P.C. Sankey ¹³⁷, T. Sano ⁸⁹, A. Sansoni ⁵⁴, L. Santi ^{37,76b},
C. Santoni ⁴², H. Santos ^{133a,133b}, A. Santra ¹⁷³, E. Sanzani ^{24b,24a}, K.A. Saoucha ¹⁶⁴,
J.G. Saraiva ^{133a,133d}, J. Sardain ⁷, O. Sasaki ⁸⁵, K. Sato ¹⁶⁰, C. Sauer ³⁷, E. Sauvan ⁴,
P. Savard ^{158,ag}, R. Sawada ¹⁵⁷, C. Sawyer ¹³⁷, L. Sawyer ⁹⁹, C. Sbarra ^{24b}, A. Sbrizzi ^{24b,24a},
T. Scanlon ⁹⁸, J. Schaarschmidt ¹⁴², U. Schäfer ¹⁰², A.C. Schaffer ^{67,46}, D. Schaile ¹¹¹,
R.D. Schamberger ¹⁴⁹, C. Scharf ¹⁹, M.M. Schefer ²⁰, V.A. Schegelsky ³⁹, D. Scheirich ¹³⁶,
M. Schernau ^{140e}, C. Scheulen ⁵⁷, C. Schiavi ^{58b,58a}, M. Schioppa ^{45b,45a}, B. Schlag ¹⁴⁷,
S. Schlenker ³⁷, J. Schmeing ¹⁷⁵, M.A. Schmidt ¹⁷⁵, K. Schmieden ¹⁰², C. Schmitt ¹⁰²,
N. Schmitt ¹⁰², S. Schmitt ⁴⁹, L. Schoeffel ¹³⁸, A. Schoening ^{64b}, P.G. Scholer ³⁵, E. Schopf ¹²⁹,
M. Schott ²⁵, J. Schovancova ³⁷, S. Schramm ⁵⁷, T. Schroer ⁵⁷, H-C. Schultz-Coulon ^{64a},
M. Schumacher ⁵⁵, B.A. Schumm ¹³⁹, Ph. Schune ¹³⁸, H.R. Schwartz ¹³⁹, A. Schwartzman ¹⁴⁷,
T.A. Schwarz ¹⁰⁸, Ph. Schwemling ¹³⁸, R. Schwienhorst ¹⁰⁹, F.G. Sciacca ²⁰, A. Sciandra ³⁰,
G. Sciolla ²⁷, F. Scuri ^{75a}, C.D. Sebastiani ⁹⁴, K. Sedlaczek ¹¹⁸, S.C. Seidel ¹¹⁵, A. Seiden ¹³⁹,
B.D. Seidlitz ⁴³, C. Seitz ⁴⁹, J.M. Seixas ^{84b}, G. Sekhniaidze ^{73a}, L. Selem ⁶¹,

N. Semprini-Cesari ^{24b,24a}, A. Semushin ^{177,39}, D. Sengupta ⁵⁷, V. Senthilkumar ¹⁶⁷, L. Serin ⁶⁷,
 M. Sessa ^{77a,77b}, H. Severini ¹²³, F. Sforza ^{58b,58a}, A. Sfyrila ⁵⁷, Q. Sha ¹⁴, E. Shabalina ⁵⁶,
 H. Shaddix ¹¹⁸, A.H. Shah ³³, R. Shaheen ¹⁴⁸, J.D. Shahinian ¹³¹, D. Shaked Renous ¹⁷³,
 L.Y. Shan ¹⁴, M. Shapiro ^{18a}, A. Sharma ³⁷, A.S. Sharma ¹⁶⁸, P. Sharma ³⁰, P.B. Shatalov ³⁹,
 K. Shaw ¹⁵⁰, S.M. Shaw ¹⁰³, Q. Shen ^{63c}, D.J. Sheppard ¹⁴⁶, P. Sherwood ⁹⁸, L. Shi ⁹⁸,
 X. Shi ¹⁴, S. Shimizu ⁸⁵, C.O. Shimmin ¹⁷⁶, I.P.J. Shipsey ^{129,*}, S. Shirabe ⁹⁰,
 M. Shiyakova ^{40,y}, M.J. Shochet ⁴¹, D.R. Shope ¹²⁸, B. Shrestha ¹²³, S. Shrestha ^{122,ak},
 I. Shreyber ³⁹, M.J. Shroff ¹⁶⁹, P. Sicho ¹³⁴, A.M. Sickles ¹⁶⁶, E. Sideras Haddad ^{34g,163},
 A.C. Sidley ¹¹⁷, A. Sidoti ^{24b}, F. Siegert ⁵¹, Dj. Sijacki ¹⁶, F. Sili ⁹², J.M. Silva ⁵³,
 I. Silva Ferreira ^{84b}, M.V. Silva Oliveira ³⁰, S.B. Silverstein ^{48a}, S. Simion ⁶⁷, R. Simoniello ³⁷,
 E.L. Simpson ¹⁰³, H. Simpson ¹⁵⁰, L.R. Simpson ¹⁰⁸, S. Simsek ⁸³, S. Sindhu ⁵⁶, P. Sinervo ¹⁵⁸,
 S.N. Singh ²⁷, S. Singh ³⁰, S. Sinha ⁴⁹, S. Sinha ¹⁰³, M. Sioli ^{24b,24a}, I. Siral ³⁷,
 E. Sitnikova ⁴⁹, J. Sjölin ^{48a,48b}, A. Skaf ⁵⁶, E. Skorda ²¹, P. Skubic ¹²³, M. Slawinska ⁸⁸,
 I. Slazyk ¹⁷, V. Smakhtin ¹⁷³, B.H. Smart ¹³⁷, S.Yu. Smirnov ³⁹, Y. Smirnov ³⁹,
 L.N. Smirnova ^{39,a}, O. Smirnova ¹⁰⁰, A.C. Smith ⁴³, D.R. Smith ¹⁶², E.A. Smith ⁴¹, J.L. Smith ¹⁰³,
 M.B. Smith ³⁵, R. Smith ¹⁴⁷, H. Smitmanns ¹⁰², M. Smizanska ⁹³, K. Smolek ¹³⁵,
 A.A. Snesarev ³⁹, H.L. Snoek ¹¹⁷, S. Snyder ³⁰, R. Sobie ^{169,aa}, A. Soffer ¹⁵⁵,
 C.A. Solans Sanchez ³⁷, E.Yu. Soldatov ³⁹, U. Soldevila ¹⁶⁷, A.A. Solodkov ³⁹, S. Solomon ²⁷,
 A. Soloshenko ⁴⁰, K. Solovieva ⁵⁵, O.V. Solovyanov ⁴², P. Sommer ⁵¹, A. Sonay ¹³,
 W.Y. Song ^{159b}, A. Sopczak ¹³⁵, A.L. Sopio ⁵³, F. Sopkova ^{29b}, J.D. Sorenson ¹¹⁵,
 I.R. Sotarriva Alvarez ¹⁴¹, V. Sothilingam ^{64a}, O.J. Soto Sandoval ^{140c,140b}, S. Sottocornola ⁶⁹,
 R. Soualah ¹⁶⁴, Z. Soumami ^{36e}, D. South ⁴⁹, N. Soybelman ¹⁷³, S. Spagnolo ^{71a,71b},
 M. Spalla ¹¹², D. Sperlich ⁵⁵, B. Spisso ^{73a,73b}, D.P. Spiteri ⁶⁰, M. Spousta ¹³⁶, E.J. Staats ³⁵,
 R. Stamen ^{64a}, E. Stanecka ⁸⁸, W. Stanek-Maslouska ⁴⁹, M.V. Stange ⁵¹, B. Stanislaus ^{18a},
 M.M. Stanitzki ⁴⁹, B. Stapf ⁴⁹, E.A. Starchenko ³⁹, G.H. Stark ¹³⁹, J. Stark ⁹¹, P. Staroba ¹³⁴,
 P. Starovoitov ¹⁶⁴, R. Staszewski ⁸⁸, G. Stavropoulos ⁴⁷, A. Stefl ³⁷, P. Steinberg ³⁰,
 B. Stelzer ^{146,159a}, H.J. Stelzer ¹³², O. Stelzer-Chilton ^{159a}, H. Stenzel ⁵⁹, T.J. Stevenson ¹⁵⁰,
 G.A. Stewart ³⁷, J.R. Stewart ¹²⁴, M.C. Stockton ³⁷, G. Stoicea ^{28b}, M. Stolarski ^{133a},
 S. Stonjek ¹¹², A. Straessner ⁵¹, J. Strandberg ¹⁴⁸, S. Strandberg ^{48a,48b}, M. Stratmann ¹⁷⁵,
 M. Strauss ¹²³, T. Streblor ¹⁰⁴, P. Strizenec ^{29b}, R. Ströhmer ¹⁷⁰, D.M. Strom ¹²⁶,
 R. Stroynowski ⁴⁶, A. Strubig ^{48a,48b}, S.A. Stucci ³⁰, B. Stugu ¹⁷, J. Stupak ¹²³, N.A. Styles ⁴⁹,
 D. Su ¹⁴⁷, S. Su ^{63a}, W. Su ^{63d}, X. Su ^{63a}, D. Suchy ^{29a}, K. Sugizaki ¹⁵⁷, V.V. Sulin ³⁹,
 M.J. Sullivan ⁹⁴, D.M.S. Sultan ¹²⁹, L. Sultanaliev ³⁹, S. Sultansoy ^{3b}, S. Sun ¹⁷⁴, W. Sun ¹⁴,
 O. Sunneborn Gudnadottir ¹⁶⁵, N. Sur ¹⁰⁴, M.R. Sutton ¹⁵⁰, H. Suzuki ¹⁶⁰, M. Svatos ¹³⁴,
 M. Swiatlowski ^{159a}, T. Swirski ¹⁷⁰, I. Sykora ^{29a}, M. Sykora ¹³⁶, T. Sykora ¹³⁶, D. Ta ¹⁰²,
 K. Tackmann ^{49,x}, A. Taffard ¹⁶², R. Tafirout ^{159a}, J.S. Tafoya Vargas ⁶⁷, Y. Takubo ⁸⁵,
 M. Talby ¹⁰⁴, A.A. Talyshiev ³⁹, K.C. Tam ^{65b}, N.M. Tamir ¹⁵⁵, A. Tanaka ¹⁵⁷, J. Tanaka ¹⁵⁷,
 R. Tanaka ⁶⁷, M. Tanasini ¹⁴⁹, Z. Tao ¹⁶⁸, S. Tapia Araya ^{140f}, S. Tapprogge ¹⁰²,
 A. Tarek Abouelfadl Mohamed ¹⁰⁹, S. Tarem ¹⁵⁴, K. Tariq ¹⁴, G. Tarna ^{28b}, G.F. Tartarelli ^{72a},
 M.J. Tartarin ⁹¹, P. Tas ¹³⁶, M. Tasevsky ¹³⁴, E. Tassi ^{45b,45a}, A.C. Tate ¹⁶⁶, G. Tateno ¹⁵⁷,
 Y. Tayalati ^{36e,z}, G.N. Taylor ¹⁰⁷, W. Taylor ^{159b}, P. Teixeira-Dias ⁹⁷, J.J. Teoh ¹⁵⁸,
 K. Terashi ¹⁵⁷, J. Terron ¹⁰¹, S. Terzo ¹³, M. Testa ⁵⁴, R.J. Teuscher ^{158,aa}, A. Thaler ⁸⁰,
 O. Theiner ⁵⁷, T. Thevenaux-Pelzer ¹⁰⁴, O. Thielmann ¹⁷⁵, D.W. Thomas ⁹⁷, J.P. Thomas ²¹,
 E.A. Thompson ^{18a}, P.D. Thompson ²¹, E. Thomson ¹³¹, R.E. Thornberry ⁴⁶, C. Tian ^{63a},
 Y. Tian ⁵⁷, V. Tikhomirov ^{39,a}, Yu.A. Tikhonov ³⁹, S. Timoshenko ³⁹, D. Timoshyn ¹³⁶,
 E.X.L. Ting ¹, P. Tipton ¹⁷⁶, A. Tishelman-Charny ³⁰, S.H. Tlou ^{34g}, K. Todome ¹⁴¹,
 S. Todorova-Nova ¹³⁶, S. Todt ⁵¹, L. Toffolin ^{70a,70c}, M. Togawa ⁸⁵, J. Tojo ⁹⁰, S. Tokár ^{29a},

O. Toldaiev ⁶⁹, G. Tolkachev ¹⁰⁴, M. Tomoto ^{85,113}, L. Tompkins ^{147,n}, E. Torrence ¹²⁶, H. Torres ⁹¹, E. Torró Pastor ¹⁶⁷, M. Toscani ³¹, C. Tosciri ⁴¹, M. Tost ¹¹, D.R. Tovey ¹⁴³, T. Trefzger ¹⁷⁰, A. Tricoli ³⁰, I.M. Trigger ^{159a}, S. Trincas-Duvoid ¹³⁰, D.A. Trischuk ²⁷, A. Tropina ⁴⁰, L. Truong ^{34c}, M. Trzebinski ⁸⁸, A. Trzupke ⁸⁸, F. Tsai ¹⁴⁹, M. Tsai ¹⁰⁸, A. Tsiamis ¹⁵⁶, P.V. Tsiareshka ⁴⁰, S. Tsigaridas ^{159a}, A. Tsirigotis ^{156,t}, V. Tsiskaridze ¹⁵⁸, E.G. Tskhadadze ^{153a}, M. Tsopoulou ¹⁵⁶, Y. Tsujikawa ⁸⁹, I.I. Tsukerman ³⁹, V. Tsulaia ^{18a}, S. Tsuno ⁸⁵, K. Tsuru ¹²¹, D. Tsybychev ¹⁴⁹, Y. Tu ^{65b}, A. Tudorache ^{28b}, V. Tudorache ^{28b}, S. Turchikhin ^{58b,58a}, I. Turk Cakir ^{3a}, R. Turra ^{72a}, T. Turtuvshin ^{40,ab}, P.M. Tuts ⁴³, S. Tzamarias ^{156,e}, E. Tzovara ¹⁰², F. Ukegawa ¹⁶⁰, P.A. Ulloa Poblete ^{140c,140b}, E.N. Umaka ³⁰, G. Unal ³⁷, A. Undrus ³⁰, G. Unel ¹⁶², J. Urban ^{29b}, P. Urrejola ^{140a}, G. Usai ⁸, R. Ushioda ¹⁴¹, M. Usman ¹¹⁰, F. Ustuner ⁵³, Z. Uysal ⁸³, V. Vacek ¹³⁵, B. Vachon ¹⁰⁶, T. Vafeiadis ³⁷, A. Vaitkus ⁹⁸, C. Valderanis ¹¹¹, E. Valdes Santurio ^{48a,48b}, M. Valente ^{159a}, S. Valentinetti ^{24b,24a}, A. Valero ¹⁶⁷, E. Valiente Moreno ¹⁶⁷, A. Vallier ⁹¹, J.A. Valls Ferrer ¹⁶⁷, D.R. Van Arneeman ¹¹⁷, T.R. Van Daalen ¹⁴², A. Van Der Graaf ⁵⁰, P. Van Gemmeren ⁶, M. Van Rijnbach ³⁷, S. Van Stroud ⁹⁸, I. Van Vulpen ¹¹⁷, P. Vana ¹³⁶, M. Vanadia ^{77a,77b}, U.M. Vande Voorde ¹⁴⁸, W. Vandelli ³⁷, E.R. Vandewall ¹²⁴, D. Vannicola ¹⁵⁵, L. Vannoli ⁵⁴, R. Vari ^{76a}, E.W. Varnes ⁷, C. Varni ^{18b}, D. Varouchas ⁶⁷, L. Varriale ¹⁶⁷, K.E. Varvell ¹⁵¹, M.E. Vasile ^{28b}, L. Vaslin ⁸⁵, A. Vasyukov ⁴⁰, L.M. Vaughan ¹²⁴, R. Vavricka ¹⁰², T. Vazquez Schroeder ¹³, J. Veatch ³², V. Vecchio ¹⁰³, M.J. Veen ¹⁰⁵, I. Veliscek ³⁰, L.M. Veloce ¹⁵⁸, F. Veloso ^{133a,133c}, S. Veneziano ^{76a}, A. Ventura ^{71a,71b}, S. Ventura Gonzalez ¹³⁸, A. Verbytskyi ¹¹², M. Verducci ^{75a,75b}, C. Vergis ⁹⁶, M. Verissimo De Araujo ^{84b}, W. Verkerke ¹¹⁷, J.C. Vermeulen ¹¹⁷, C. Vernieri ¹⁴⁷, M. Vessella ¹⁶², M.C. Vetterli ^{146,ag}, A. Vgenopoulos ¹⁰², N. Viaux Maira ^{140f}, T. Vickey ¹⁴³, O.E. Vickey Boeriu ¹⁴³, G.H.A. Viehhauser ¹²⁹, L. Vigani ^{64b}, M. Vigl ¹¹², M. Villa ^{24b,24a}, M. Villaplana Perez ¹⁶⁷, E.M. Villhauer ⁵³, E. Vilucchi ⁵⁴, M.G. Vincet ³⁵, A. Visibile ¹¹⁷, C. Vittori ³⁷, I. Vivarelli ^{24b,24a}, E. Voevodina ¹¹², F. Vogel ¹¹¹, J.C. Voigt ⁵¹, P. Vokac ¹³⁵, Yu. Volkotrub ^{87b}, E. Von Toerne ²⁵, B. Vormwald ³⁷, K. Vorobev ³⁹, M. Vos ¹⁶⁷, K. Voss ¹⁴⁵, M. Vozak ¹¹⁷, L. Vozdecky ¹²³, N. Vranjes ¹⁶, M. Vranjes Milosavljevic ¹⁶, M. Vreeswijk ¹¹⁷, N.K. Vu ^{63d,63c}, R. Vuillermet ³⁷, O. Vujinovic ¹⁰², I. Vukotic ⁴¹, I.K. Vyas ³⁵, S. Wada ¹⁶⁰, C. Wagner ¹⁴⁷, J.M. Wagner ^{18a}, W. Wagner ¹⁷⁵, S. Wahdan ¹⁷⁵, H. Wahlberg ⁹², C.H. Waits ¹²³, J. Walder ¹³⁷, R. Walker ¹¹¹, W. Walkowiak ¹⁴⁵, A. Wall ¹³¹, E.J. Wallin ¹⁰⁰, T. Wamorkar ^{18a}, A.Z. Wang ¹³⁹, C. Wang ¹⁰², C. Wang ¹¹, H. Wang ^{18a}, J. Wang ^{65c}, P. Wang ¹⁰³, P. Wang ⁹⁸, R. Wang ⁶², R. Wang ⁶, S.M. Wang ¹⁵², S. Wang ¹⁴, T. Wang ^{63a}, W.T. Wang ⁸¹, W. Wang ¹⁴, X. Wang ¹⁶⁶, X. Wang ^{63c}, Y. Wang ^{114a}, Y. Wang ^{63a}, Z. Wang ¹⁰⁸, Z. Wang ^{63d,52,63c}, Z. Wang ¹⁰⁸, C. Wanotayaroj ⁸⁵, A. Warburton ¹⁰⁶, R.J. Ward ²¹, A.L. Warnerbring ¹⁴⁵, N. Warrack ⁶⁰, S. Waterhouse ⁹⁷, A.T. Watson ²¹, H. Watson ⁵³, M.F. Watson ²¹, E. Watton ^{60,137}, G. Watts ¹⁴², B.M. Waugh ⁹⁸, J.M. Webb ⁵⁵, C. Weber ³⁰, H.A. Weber ¹⁹, M.S. Weber ²⁰, S.M. Weber ^{64a}, C. Wei ^{63a}, Y. Wei ⁵⁵, A.R. Weidberg ¹²⁹, E.J. Weik ¹²⁰, J. Weingarten ⁵⁰, C. Weiser ⁵⁵, C.J. Wells ⁴⁹, T. Wenaus ³⁰, B. Wendland ⁵⁰, T. Wengler ³⁷, N.S. Wenke ¹¹², N. Wermes ²⁵, M. Wessels ^{64a}, A.M. Wharton ⁹³, A.S. White ⁶², A. White ⁸, M.J. White ¹, D. Whiteson ¹⁶², L. Wickremasinghe ¹²⁷, W. Wiedenmann ¹⁷⁴, M. Wielers ¹³⁷, C. Wiglesworth ⁴⁴, D.J. Wilbern ¹²³, H.G. Wilkens ³⁷, J.J.H. Wilkinson ³³, D.M. Williams ⁴³, H.H. Williams ¹³¹, S. Williams ³³, S. Willocq ¹⁰⁵, B.J. Wilson ¹⁰³, D.J. Wilson ¹⁰³, P.J. Windischhofer ⁴¹, F.I. Winkel ³¹, F. Winklmeier ¹²⁶, B.T. Winter ⁵⁵, M. Wittgen ¹⁴⁷, M. Wobisch ⁹⁹, T. Wojtkowski ⁶¹, Z. Wolffs ¹¹⁷, J. Wollrath ³⁷, M.W. Wolter ⁸⁸, H. Wolters ^{133a,133c}, M.C. Wong ¹³⁹, E.L. Woodward ⁴³, S.D. Worm ⁴⁹, B.K. Wosiek ⁸⁸, K.W. Woźniak ⁸⁸, S. Wozniowski ⁵⁶, K. Wraight ⁶⁰, C. Wu ²¹, M. Wu ^{114b}, M. Wu ¹¹⁶, S.L. Wu ¹⁷⁴, X. Wu ⁵⁷,

X. Wu , Y. Wu , Z. Wu , J. Wuerzinger , T.R. Wyatt , B.M. Wynne , S. Xella , L. Xia , M. Xia , M. Xie , A. Xiong , J. Xiong , D. Xu , H. Xu , L. Xu , R. Xu , T. Xu , Y. Xu , Z. Xu , Z. Xu , B. Yabsley , S. Yacoob , Y. Yamaguchi , E. Yamashita , H. Yamauchi , T. Yamazaki , Y. Yamazaki , S. Yan , Z. Yan , H.J. Yang , H.T. Yang , S. Yang , T. Yang , X. Yang , X. Yang , Y. Yang , Y. Yang , W.-M. Yao , H. Ye , J. Ye , S. Ye , X. Ye , Y. Yeh , I. Yeletsikh , B. Yeo , M.R. Yexley , T.P. Yildirim , P. Yin , K. Yorita , S. Younas , C.J.S. Young , C. Young , N.D. Young , C. Yu , Y. Yu , J. Yuan , M. Yuan , R. Yuan , L. Yue , M. Zaazoua , B. Zabinski , I. Zahir , Z.K. Zak , T. Zakareishvili , S. Zambito , J.A. Zamora Saa , J. Zang , D. Zanzi , R. Zanzottera , O. Zaplatilek , C. Zeitnitz , H. Zeng , J.C. Zeng , D.T. Zenger Jr , O. Zenin , T. Ženiš , S. Zenz , S. Zerradi , D. Zerwas , M. Zhai , D.F. Zhang , J. Zhang , J. Zhang , K. Zhang , L. Zhang , L. Zhang , P. Zhang , R. Zhang , S. Zhang , T. Zhang , X. Zhang , Y. Zhang , Y. Zhang , Y. Zhang , Z. Zhang , Z. Zhang , Z. Zhang , H. Zhao , T. Zhao , Y. Zhao , Z. Zhao , Z. Zhao , A. Zhemchugov , J. Zheng , K. Zheng , X. Zheng , Z. Zheng , D. Zhong , B. Zhou , H. Zhou , N. Zhou , Y. Zhou , Y. Zhou , Y. Zhou , C.G. Zhu , J. Zhu , X. Zhu , Y. Zhu , Y. Zhu , X. Zhuang , K. Zhukov , N.I. Zimine , J. Zinsser , M. Ziolkowski , L. Živković , A. Zoccoli , K. Zoch , T.G. Zorbas , O. Zormpa , W. Zou , L. Zwalinski .

¹Department of Physics, University of Adelaide, Adelaide; Australia.

²Department of Physics, University of Alberta, Edmonton AB; Canada.

^{3(a)}Department of Physics, Ankara University, Ankara; ^(b)Division of Physics, TOBB University of Economics and Technology, Ankara; Türkiye.

⁴LAPP, Université Savoie Mont Blanc, CNRS/IN2P3, Annecy; France.

⁵APC, Université Paris Cité, CNRS/IN2P3, Paris; France.

⁶High Energy Physics Division, Argonne National Laboratory, Argonne IL; United States of America.

⁷Department of Physics, University of Arizona, Tucson AZ; United States of America.

⁸Department of Physics, University of Texas at Arlington, Arlington TX; United States of America.

⁹Physics Department, National and Kapodistrian University of Athens, Athens; Greece.

¹⁰Physics Department, National Technical University of Athens, Zografou; Greece.

¹¹Department of Physics, University of Texas at Austin, Austin TX; United States of America.

¹²Institute of Physics, Azerbaijan Academy of Sciences, Baku; Azerbaijan.

¹³Institut de Física d'Altes Energies (IFAE), Barcelona Institute of Science and Technology, Barcelona; Spain.

¹⁴Institute of High Energy Physics, Chinese Academy of Sciences, Beijing; China.

¹⁵Physics Department, Tsinghua University, Beijing; China.

¹⁶Institute of Physics, University of Belgrade, Belgrade; Serbia.

¹⁷Department for Physics and Technology, University of Bergen, Bergen; Norway.

^{18(a)}Physics Division, Lawrence Berkeley National Laboratory, Berkeley CA; ^(b)University of California, Berkeley CA; United States of America.

¹⁹Institut für Physik, Humboldt Universität zu Berlin, Berlin; Germany.

²⁰Albert Einstein Center for Fundamental Physics and Laboratory for High Energy Physics, University of Bern, Bern; Switzerland.

²¹School of Physics and Astronomy, University of Birmingham, Birmingham; United Kingdom.

- ^{22(a)}Department of Physics, Bogazici University, Istanbul; ^(b)Department of Physics Engineering, Gaziantep University, Gaziantep; ^(c)Department of Physics, Istanbul University, Istanbul; Türkiye.
- ^{23(a)}Facultad de Ciencias y Centro de Investigaciones, Universidad Antonio Nariño, Bogotá; ^(b)Departamento de Física, Universidad Nacional de Colombia, Bogotá; Colombia.
- ^{24(a)}Dipartimento di Fisica e Astronomia A. Righi, Università di Bologna, Bologna; ^(b)INFN Sezione di Bologna; Italy.
- ²⁵Physikalisches Institut, Universität Bonn, Bonn; Germany.
- ²⁶Department of Physics, Boston University, Boston MA; United States of America.
- ²⁷Department of Physics, Brandeis University, Waltham MA; United States of America.
- ^{28(a)}Transilvania University of Brasov, Brasov; ^(b)Horia Hulubei National Institute of Physics and Nuclear Engineering, Bucharest; ^(c)Department of Physics, Alexandru Ioan Cuza University of Iasi, Iasi; ^(d)National Institute for Research and Development of Isotopic and Molecular Technologies, Physics Department, Cluj-Napoca; ^(e)National University of Science and Technology Politehnica, Bucharest; ^(f)West University in Timisoara, Timisoara; ^(g)Faculty of Physics, University of Bucharest, Bucharest; Romania.
- ^{29(a)}Faculty of Mathematics, Physics and Informatics, Comenius University, Bratislava; ^(b)Department of Subnuclear Physics, Institute of Experimental Physics of the Slovak Academy of Sciences, Kosice; Slovak Republic.
- ³⁰Physics Department, Brookhaven National Laboratory, Upton NY; United States of America.
- ³¹Universidad de Buenos Aires, Facultad de Ciencias Exactas y Naturales, Departamento de Física, y CONICET, Instituto de Física de Buenos Aires (IFIBA), Buenos Aires; Argentina.
- ³²California State University, CA; United States of America.
- ³³Cavendish Laboratory, University of Cambridge, Cambridge; United Kingdom.
- ^{34(a)}Department of Physics, University of Cape Town, Cape Town; ^(b)iThemba Labs, Western Cape; ^(c)Department of Mechanical Engineering Science, University of Johannesburg, Johannesburg; ^(d)National Institute of Physics, University of the Philippines Diliman (Philippines); ^(e)University of South Africa, Department of Physics, Pretoria; ^(f)University of Zululand, KwaDlangezwa; ^(g)School of Physics, University of the Witwatersrand, Johannesburg; South Africa.
- ³⁵Department of Physics, Carleton University, Ottawa ON; Canada.
- ^{36(a)}Faculté des Sciences Ain Chock, Université Hassan II de Casablanca; ^(b)Faculté des Sciences, Université Ibn-Tofail, Kénitra; ^(c)Faculté des Sciences Semailia, Université Cadi Ayyad, LPHEA-Marrakech; ^(d)LPMR, Faculté des Sciences, Université Mohamed Premier, Oujda; ^(e)Faculté des sciences, Université Mohammed V, Rabat; ^(f)Institute of Applied Physics, Mohammed VI Polytechnic University, Ben Guerir; Morocco.
- ³⁷CERN, Geneva; Switzerland.
- ³⁸Affiliated with an institute formerly covered by a cooperation agreement with CERN.
- ³⁹Affiliated with an institute covered by a cooperation agreement with CERN.
- ⁴⁰Affiliated with an international laboratory covered by a cooperation agreement with CERN.
- ⁴¹Enrico Fermi Institute, University of Chicago, Chicago IL; United States of America.
- ⁴²LPC, Université Clermont Auvergne, CNRS/IN2P3, Clermont-Ferrand; France.
- ⁴³Nevis Laboratory, Columbia University, Irvington NY; United States of America.
- ⁴⁴Niels Bohr Institute, University of Copenhagen, Copenhagen; Denmark.
- ^{45(a)}Dipartimento di Fisica, Università della Calabria, Rende; ^(b)INFN Gruppo Collegato di Cosenza, Laboratori Nazionali di Frascati; Italy.
- ⁴⁶Physics Department, Southern Methodist University, Dallas TX; United States of America.
- ⁴⁷National Centre for Scientific Research "Demokritos", Agia Paraskevi; Greece.
- ^{48(a)}Department of Physics, Stockholm University; ^(b)Oskar Klein Centre, Stockholm; Sweden.
- ⁴⁹Deutsches Elektronen-Synchrotron DESY, Hamburg and Zeuthen; Germany.

- ⁵⁰Fakultät Physik , Technische Universität Dortmund, Dortmund; Germany.
- ⁵¹Institut für Kern- und Teilchenphysik, Technische Universität Dresden, Dresden; Germany.
- ⁵²Department of Physics, Duke University, Durham NC; United States of America.
- ⁵³SUPA - School of Physics and Astronomy, University of Edinburgh, Edinburgh; United Kingdom.
- ⁵⁴INFN e Laboratori Nazionali di Frascati, Frascati; Italy.
- ⁵⁵Physikalisches Institut, Albert-Ludwigs-Universität Freiburg, Freiburg; Germany.
- ⁵⁶II. Physikalisches Institut, Georg-August-Universität Göttingen, Göttingen; Germany.
- ⁵⁷Département de Physique Nucléaire et Corpusculaire, Université de Genève, Genève; Switzerland.
- ⁵⁸(^a)Dipartimento di Fisica, Università di Genova, Genova;(^b)INFN Sezione di Genova; Italy.
- ⁵⁹II. Physikalisches Institut, Justus-Liebig-Universität Giessen, Giessen; Germany.
- ⁶⁰SUPA - School of Physics and Astronomy, University of Glasgow, Glasgow; United Kingdom.
- ⁶¹LPSC, Université Grenoble Alpes, CNRS/IN2P3, Grenoble INP, Grenoble; France.
- ⁶²Laboratory for Particle Physics and Cosmology, Harvard University, Cambridge MA; United States of America.
- ⁶³(^a)Department of Modern Physics and State Key Laboratory of Particle Detection and Electronics, University of Science and Technology of China, Hefei;(^b)Institute of Frontier and Interdisciplinary Science and Key Laboratory of Particle Physics and Particle Irradiation (MOE), Shandong University, Qingdao;(^c)School of Physics and Astronomy, Shanghai Jiao Tong University, Key Laboratory for Particle Astrophysics and Cosmology (MOE), SKLPPC, Shanghai;(^d)Tsung-Dao Lee Institute, Shanghai;(^e)School of Physics, Zhengzhou University; China.
- ⁶⁴(^a)Kirchhoff-Institut für Physik, Ruprecht-Karls-Universität Heidelberg, Heidelberg;(^b)Physikalisches Institut, Ruprecht-Karls-Universität Heidelberg, Heidelberg; Germany.
- ⁶⁵(^a)Department of Physics, Chinese University of Hong Kong, Shatin, N.T., Hong Kong;(^b)Department of Physics, University of Hong Kong, Hong Kong;(^c)Department of Physics and Institute for Advanced Study, Hong Kong University of Science and Technology, Clear Water Bay, Kowloon, Hong Kong; China.
- ⁶⁶Department of Physics, National Tsing Hua University, Hsinchu; Taiwan.
- ⁶⁷IJCLab, Université Paris-Saclay, CNRS/IN2P3, 91405, Orsay; France.
- ⁶⁸Centro Nacional de Microelectrónica (IMB-CNM-CSIC), Barcelona; Spain.
- ⁶⁹Department of Physics, Indiana University, Bloomington IN; United States of America.
- ⁷⁰(^a)INFN Gruppo Collegato di Udine, Sezione di Trieste, Udine;(^b)ICTP, Trieste;(^c)Dipartimento Politecnico di Ingegneria e Architettura, Università di Udine, Udine; Italy.
- ⁷¹(^a)INFN Sezione di Lecce;(^b)Dipartimento di Matematica e Fisica, Università del Salento, Lecce; Italy.
- ⁷²(^a)INFN Sezione di Milano;(^b)Dipartimento di Fisica, Università di Milano, Milano; Italy.
- ⁷³(^a)INFN Sezione di Napoli;(^b)Dipartimento di Fisica, Università di Napoli, Napoli; Italy.
- ⁷⁴(^a)INFN Sezione di Pavia;(^b)Dipartimento di Fisica, Università di Pavia, Pavia; Italy.
- ⁷⁵(^a)INFN Sezione di Pisa;(^b)Dipartimento di Fisica E. Fermi, Università di Pisa, Pisa; Italy.
- ⁷⁶(^a)INFN Sezione di Roma;(^b)Dipartimento di Fisica, Sapienza Università di Roma, Roma; Italy.
- ⁷⁷(^a)INFN Sezione di Roma Tor Vergata;(^b)Dipartimento di Fisica, Università di Roma Tor Vergata, Roma; Italy.
- ⁷⁸(^a)INFN Sezione di Roma Tre;(^b)Dipartimento di Matematica e Fisica, Università Roma Tre, Roma; Italy.
- ⁷⁹(^a)INFN-TIFPA;(^b)Università degli Studi di Trento, Trento; Italy.
- ⁸⁰Universität Innsbruck, Department of Astro and Particle Physics, Innsbruck; Austria.
- ⁸¹University of Iowa, Iowa City IA; United States of America.
- ⁸²Department of Physics and Astronomy, Iowa State University, Ames IA; United States of America.
- ⁸³Istinye University, Sariyer, Istanbul; Türkiye.
- ⁸⁴(^a)Departamento de Engenharia Elétrica, Universidade Federal de Juiz de Fora (UFJF), Juiz de

Fora;^(b)Universidade Federal do Rio De Janeiro COPPE/EE/IF, Rio de Janeiro;^(c)Instituto de Física, Universidade de São Paulo, São Paulo;^(d)Rio de Janeiro State University, Rio de Janeiro;^(e)Federal University of Bahia, Bahia; Brazil.

⁸⁵KEK, High Energy Accelerator Research Organization, Tsukuba; Japan.

⁸⁶Graduate School of Science, Kobe University, Kobe; Japan.

⁸⁷(^a) AGH University of Krakow, Faculty of Physics and Applied Computer Science, Krakow;^(b)Marian Smoluchowski Institute of Physics, Jagiellonian University, Krakow; Poland.

⁸⁸Institute of Nuclear Physics Polish Academy of Sciences, Krakow; Poland.

⁸⁹Faculty of Science, Kyoto University, Kyoto; Japan.

⁹⁰Research Center for Advanced Particle Physics and Department of Physics, Kyushu University, Fukuoka ; Japan.

⁹¹L2IT, Université de Toulouse, CNRS/IN2P3, UPS, Toulouse; France.

⁹²Instituto de Física La Plata, Universidad Nacional de La Plata and CONICET, La Plata; Argentina.

⁹³Physics Department, Lancaster University, Lancaster; United Kingdom.

⁹⁴Oliver Lodge Laboratory, University of Liverpool, Liverpool; United Kingdom.

⁹⁵Department of Experimental Particle Physics, Jožef Stefan Institute and Department of Physics, University of Ljubljana, Ljubljana; Slovenia.

⁹⁶School of Physics and Astronomy, Queen Mary University of London, London; United Kingdom.

⁹⁷Department of Physics, Royal Holloway University of London, Egham; United Kingdom.

⁹⁸Department of Physics and Astronomy, University College London, London; United Kingdom.

⁹⁹Louisiana Tech University, Ruston LA; United States of America.

¹⁰⁰Fysiska institutionen, Lunds universitet, Lund; Sweden.

¹⁰¹Departamento de Física Teórica C-15 and CIAFF, Universidad Autónoma de Madrid, Madrid; Spain.

¹⁰²Institut für Physik, Universität Mainz, Mainz; Germany.

¹⁰³School of Physics and Astronomy, University of Manchester, Manchester; United Kingdom.

¹⁰⁴CPPM, Aix-Marseille Université, CNRS/IN2P3, Marseille; France.

¹⁰⁵Department of Physics, University of Massachusetts, Amherst MA; United States of America.

¹⁰⁶Department of Physics, McGill University, Montreal QC; Canada.

¹⁰⁷School of Physics, University of Melbourne, Victoria; Australia.

¹⁰⁸Department of Physics, University of Michigan, Ann Arbor MI; United States of America.

¹⁰⁹Department of Physics and Astronomy, Michigan State University, East Lansing MI; United States of America.

¹¹⁰Group of Particle Physics, University of Montreal, Montreal QC; Canada.

¹¹¹Fakultät für Physik, Ludwig-Maximilians-Universität München, München; Germany.

¹¹²Max-Planck-Institut für Physik (Werner-Heisenberg-Institut), München; Germany.

¹¹³Graduate School of Science and Kobayashi-Maskawa Institute, Nagoya University, Nagoya; Japan.

¹¹⁴(^a) Department of Physics, Nanjing University, Nanjing;^(b)School of Science, Shenzhen Campus of Sun Yat-sen University;^(c)University of Chinese Academy of Science (UCAS), Beijing; China.

¹¹⁵Department of Physics and Astronomy, University of New Mexico, Albuquerque NM; United States of America.

¹¹⁶Institute for Mathematics, Astrophysics and Particle Physics, Radboud University/Nikhef, Nijmegen; Netherlands.

¹¹⁷Nikhef National Institute for Subatomic Physics and University of Amsterdam, Amsterdam; Netherlands.

¹¹⁸Department of Physics, Northern Illinois University, DeKalb IL; United States of America.

¹¹⁹(^a) New York University Abu Dhabi, Abu Dhabi;^(b)United Arab Emirates University, Al Ain; United Arab Emirates.

- ¹²⁰Department of Physics, New York University, New York NY; United States of America.
- ¹²¹Ochanomizu University, Otsuka, Bunkyo-ku, Tokyo; Japan.
- ¹²²Ohio State University, Columbus OH; United States of America.
- ¹²³Homer L. Dodge Department of Physics and Astronomy, University of Oklahoma, Norman OK; United States of America.
- ¹²⁴Department of Physics, Oklahoma State University, Stillwater OK; United States of America.
- ¹²⁵Palacký University, Joint Laboratory of Optics, Olomouc; Czech Republic.
- ¹²⁶Institute for Fundamental Science, University of Oregon, Eugene, OR; United States of America.
- ¹²⁷Graduate School of Science, Osaka University, Osaka; Japan.
- ¹²⁸Department of Physics, University of Oslo, Oslo; Norway.
- ¹²⁹Department of Physics, Oxford University, Oxford; United Kingdom.
- ¹³⁰LPNHE, Sorbonne Université, Université Paris Cité, CNRS/IN2P3, Paris; France.
- ¹³¹Department of Physics, University of Pennsylvania, Philadelphia PA; United States of America.
- ¹³²Department of Physics and Astronomy, University of Pittsburgh, Pittsburgh PA; United States of America.
- ¹³³(^a) Laboratório de Instrumentação e Física Experimental de Partículas - LIP, Lisboa; (^b) Departamento de Física, Faculdade de Ciências, Universidade de Lisboa, Lisboa; (^c) Departamento de Física, Universidade de Coimbra, Coimbra; (^d) Centro de Física Nuclear da Universidade de Lisboa, Lisboa; (^e) Departamento de Física, Universidade do Minho, Braga; (^f) Departamento de Física Teórica y del Cosmos, Universidad de Granada, Granada (Spain); (^g) Departamento de Física, Instituto Superior Técnico, Universidade de Lisboa, Lisboa; Portugal.
- ¹³⁴Institute of Physics of the Czech Academy of Sciences, Prague; Czech Republic.
- ¹³⁵Czech Technical University in Prague, Prague; Czech Republic.
- ¹³⁶Charles University, Faculty of Mathematics and Physics, Prague; Czech Republic.
- ¹³⁷Particle Physics Department, Rutherford Appleton Laboratory, Didcot; United Kingdom.
- ¹³⁸IRFU, CEA, Université Paris-Saclay, Gif-sur-Yvette; France.
- ¹³⁹Santa Cruz Institute for Particle Physics, University of California Santa Cruz, Santa Cruz CA; United States of America.
- ¹⁴⁰(^a) Departamento de Física, Pontificia Universidad Católica de Chile, Santiago; (^b) Millennium Institute for Subatomic physics at high energy frontier (SAPHIR), Santiago; (^c) Instituto de Investigación Multidisciplinario en Ciencia y Tecnología, y Departamento de Física, Universidad de La Serena; (^d) Universidad Andres Bello, Department of Physics, Santiago; (^e) Instituto de Alta Investigación, Universidad de Tarapacá, Arica; (^f) Departamento de Física, Universidad Técnica Federico Santa María, Valparaíso; Chile.
- ¹⁴¹Department of Physics, Institute of Science, Tokyo; Japan.
- ¹⁴²Department of Physics, University of Washington, Seattle WA; United States of America.
- ¹⁴³Department of Physics and Astronomy, University of Sheffield, Sheffield; United Kingdom.
- ¹⁴⁴Department of Physics, Shinshu University, Nagano; Japan.
- ¹⁴⁵Department Physik, Universität Siegen, Siegen; Germany.
- ¹⁴⁶Department of Physics, Simon Fraser University, Burnaby BC; Canada.
- ¹⁴⁷SLAC National Accelerator Laboratory, Stanford CA; United States of America.
- ¹⁴⁸Department of Physics, Royal Institute of Technology, Stockholm; Sweden.
- ¹⁴⁹Departments of Physics and Astronomy, Stony Brook University, Stony Brook NY; United States of America.
- ¹⁵⁰Department of Physics and Astronomy, University of Sussex, Brighton; United Kingdom.
- ¹⁵¹School of Physics, University of Sydney, Sydney; Australia.
- ¹⁵²Institute of Physics, Academia Sinica, Taipei; Taiwan.

- ¹⁵³(^a) E. Andronikashvili Institute of Physics, Iv. Javakhishvili Tbilisi State University, Tbilisi; (^b) High Energy Physics Institute, Tbilisi State University, Tbilisi; (^c) University of Georgia, Tbilisi; Georgia.
- ¹⁵⁴ Department of Physics, Technion, Israel Institute of Technology, Haifa; Israel.
- ¹⁵⁵ Raymond and Beverly Sackler School of Physics and Astronomy, Tel Aviv University, Tel Aviv; Israel.
- ¹⁵⁶ Department of Physics, Aristotle University of Thessaloniki, Thessaloniki; Greece.
- ¹⁵⁷ International Center for Elementary Particle Physics and Department of Physics, University of Tokyo, Tokyo; Japan.
- ¹⁵⁸ Department of Physics, University of Toronto, Toronto ON; Canada.
- ¹⁵⁹(^a) TRIUMF, Vancouver BC; (^b) Department of Physics and Astronomy, York University, Toronto ON; Canada.
- ¹⁶⁰ Division of Physics and Tomonaga Center for the History of the Universe, Faculty of Pure and Applied Sciences, University of Tsukuba, Tsukuba; Japan.
- ¹⁶¹ Department of Physics and Astronomy, Tufts University, Medford MA; United States of America.
- ¹⁶² Department of Physics and Astronomy, University of California Irvine, Irvine CA; United States of America.
- ¹⁶³ University of West Attica, Athens; Greece.
- ¹⁶⁴ University of Sharjah, Sharjah; United Arab Emirates.
- ¹⁶⁵ Department of Physics and Astronomy, University of Uppsala, Uppsala; Sweden.
- ¹⁶⁶ Department of Physics, University of Illinois, Urbana IL; United States of America.
- ¹⁶⁷ Instituto de Física Corpuscular (IFIC), Centro Mixto Universidad de Valencia - CSIC, Valencia; Spain.
- ¹⁶⁸ Department of Physics, University of British Columbia, Vancouver BC; Canada.
- ¹⁶⁹ Department of Physics and Astronomy, University of Victoria, Victoria BC; Canada.
- ¹⁷⁰ Fakultät für Physik und Astronomie, Julius-Maximilians-Universität Würzburg, Würzburg; Germany.
- ¹⁷¹ Department of Physics, University of Warwick, Coventry; United Kingdom.
- ¹⁷² Waseda University, Tokyo; Japan.
- ¹⁷³ Department of Particle Physics and Astrophysics, Weizmann Institute of Science, Rehovot; Israel.
- ¹⁷⁴ Department of Physics, University of Wisconsin, Madison WI; United States of America.
- ¹⁷⁵ Fakultät für Mathematik und Naturwissenschaften, Fachgruppe Physik, Bergische Universität Wuppertal, Wuppertal; Germany.
- ¹⁷⁶ Department of Physics, Yale University, New Haven CT; United States of America.
- ¹⁷⁷ Yerevan Physics Institute, Yerevan; Armenia.
- ^a Also Affiliated with an institute covered by a cooperation agreement with CERN.
- ^b Also at An-Najah National University, Nablus; Palestine.
- ^c Also at Borough of Manhattan Community College, City University of New York, New York NY; United States of America.
- ^d Also at Center for High Energy Physics, Peking University; China.
- ^e Also at Center for Interdisciplinary Research and Innovation (CIRI-AUTH), Thessaloniki; Greece.
- ^f Also at CERN, Geneva; Switzerland.
- ^g Also at CMD-AC UNEC Research Center, Azerbaijan State University of Economics (UNEC); Azerbaijan.
- ^h Also at Département de Physique Nucléaire et Corpusculaire, Université de Genève, Genève; Switzerland.
- ⁱ Also at Departament de Física de la Universitat Autònoma de Barcelona, Barcelona; Spain.
- ^j Also at Department of Financial and Management Engineering, University of the Aegean, Chios; Greece.
- ^k Also at Department of Mathematical Sciences, University of South Africa, Johannesburg; South Africa.
- ^l Also at Department of Physics, California State University, Sacramento; United States of America.
- ^m Also at Department of Physics, King's College London, London; United Kingdom.

- ⁿ Also at Department of Physics, Stanford University, Stanford CA; United States of America.
- ^o Also at Department of Physics, Stellenbosch University; South Africa.
- ^p Also at Department of Physics, University of Fribourg, Fribourg; Switzerland.
- ^q Also at Department of Physics, University of Thessaly; Greece.
- ^r Also at Department of Physics, Westmont College, Santa Barbara; United States of America.
- ^s Also at Faculty of Physics, Sofia University, 'St. Kliment Ohridski', Sofia; Bulgaria.
- ^t Also at Hellenic Open University, Patras; Greece.
- ^u Also at Henan University; China.
- ^v Also at Imam Mohammad Ibn Saud Islamic University; Saudi Arabia.
- ^w Also at Institutio Catalana de Recerca i Estudis Avancats, ICREA, Barcelona; Spain.
- ^x Also at Institut für Experimentalphysik, Universität Hamburg, Hamburg; Germany.
- ^y Also at Institute for Nuclear Research and Nuclear Energy (INRNE) of the Bulgarian Academy of Sciences, Sofia; Bulgaria.
- ^z Also at Institute of Applied Physics, Mohammed VI Polytechnic University, Ben Guerir; Morocco.
- ^{aa} Also at Institute of Particle Physics (IPP); Canada.
- ^{ab} Also at Institute of Physics and Technology, Mongolian Academy of Sciences, Ulaanbaatar; Mongolia.
- ^{ac} Also at Institute of Physics, Azerbaijan Academy of Sciences, Baku; Azerbaijan.
- ^{ad} Also at National Institute of Physics, University of the Philippines Diliman (Philippines); Philippines.
- ^{ae} Also at Technical University of Munich, Munich; Germany.
- ^{af} Also at The Collaborative Innovation Center of Quantum Matter (CICQM), Beijing; China.
- ^{ag} Also at TRIUMF, Vancouver BC; Canada.
- ^{ah} Also at Università di Napoli Parthenope, Napoli; Italy.
- ^{ai} Also at University of Colorado Boulder, Department of Physics, Colorado; United States of America.
- ^{aj} Also at University of the Western Cape; South Africa.
- ^{ak} Also at Washington College, Chestertown, MD; United States of America.
- ^{al} Also at Yeditepe University, Physics Department, Istanbul; Türkiye.
- * Deceased